EXPERIMENTAL EVALUATION OF THERMAL RESPONSE TESTS PERFORMED ON BOREHOLE STRINGS

EXPERIMENTAL EVALUATION OF THERMAL RESPONSE TESTS PERFORMED ON BOREHOLE STRINGS

By CHANTEL MILLAR, B.Eng.

A Thesis Submitted to the School of Graduate Studies in Partial Fulfilment of the Requirements for the Degree Master of Applied Science

Master of Applied Science 2020 McMaster University

(Mechanical Engineering) Hamilton, Ontario, Canada

TITLE: Experimental Evaluation of Thermal Response Tests Performed on Borehole Strings

AUTHOR: Chantel Millar

B.Eng. (Mechanical Engineering)

McMaster University, Hamilton, Ontario, Canada

SUPERVISORS: Dr. James Cotton and Dr. Marilyn Lightstone

NUMBER OF PAGES: 116

Abstract

This thesis investigates the validity of the standard thermal response test (TRT) results when performed on a series of boreholes (string). The typical TRT consists of subjecting a single borehole to a constant heat injection rate to obtain the temperature response in the ground which can then be used to determine the ground thermal conductivity. When completed on a single borehole, the results may be analyzed with the line source theory, since the assumption of a single line heat source is valid. For multiple boreholes, the assumption of a single line source becomes invalid if the spacing between the boreholes is small enough for borehole thermal interaction to occur. Moreover, for boreholes that are charged in series, heat transfer from the horizontal pipes that connect the vertical boreholes may also influence the ground thermal response. This thesis takes an in-depth look at the different factors that affect the results of TRTs performed on borehole strings. Different analysis methods are implemented to determine areas of improvement for determining the thermal conductivity of the soil surrounding the borehole string.

For the analysis, the infinite line source (ILS) model and a model developed using TRNSYS 18 were used to determine the effective thermal conductivity. The results show that TRNSYS is unable to accurately model a TRT performed on a borehole string. The horizontal pipe model within TRNSYS proved to have significant fundamental issues, as the effective thermal conductivity is greatly underestimated with values of 1.2±0.1W/mK and the results of increasing the horizontal length both increased and decreased the effective thermal conductivities. The results from the ILS demonstrate that an effective thermal conductivity of 1.7±0.2W/mK is an appropriate estimate of the soil at the BTES field tested, as the borehole string with the furthest spacing between boreholes gave an effective thermal conductivity of 1.7W/mK.

Performing multiple thermal response tests within the same BTES field also provided evidence of the need to implement multiple TRTs as common practise. The testing presented shows that the effective thermal conductivity can vary within ±0.2W/mK within the same relative location. With better knowledge of the thermal properties within the BTES field location comes the opportunity for improved planning of operation and control of thermal distribution within the field. This would be especially beneficial when dealing with seasonal BTES fields.

Acknowledgments

I would like to thank my supervisors Dr. Jim Cotton and Dr. Marilyn Lightstone for their guidance and effort towards my research. I have been very fortunate to have the both of them offer their intelligence and support and for that I am very grateful.

I would also like to thank Dr. Yasser Abdelsalam for his guidance and mentorship. Without his efforts this experience would have been very different. Your patience and mentorship has been essential to the thermal storage group and I look forward to where your teaching career leads you.

To my friend, Brendan Sullivan, I would like to say thank-you for the good times and memories. I am very glad that we started our Masters' degrees together. I wish you all the best as you move forward with your career. Again, thank-you for making the last few years more enjoyable.

I am very grateful for the whole ICE-Harvest team. I am thankful that I have the opportunity to meet so many intelligent people and learn about the different aspects of the project. I look forward to continue learning with all of you under the guidance of Dr. Cotton. Many thanks to Dr. Stan Reitsma at GeoSource for providing equipment and knowledge towards thermal response tests and borehole thermal energy storage. I look forward to continue to collaborate with you.

Finally, I would like to thank my parents, Charles Millar and Dr. Marilyn Ott, and my brothers, CJ and Mac. Their encouragement and support was incredibly essential for me over the last few years. Thank-you to all my friends and colleagues who have been so patient during my educational journey.

Table of Contents

Notations & Abbreviations

Nomenclature

k	Thermal Conductivity [W/mK]
α	Thermal Diffusivity [m^2/s]
t	time [sec]
m	slope
ṁ	Mass flow rate [kg/s]
r	radius [m]
R	Thermal Resistance [K/W]
T	Temperature [K]
q	Heat Injection Rate [W/m]
ε	Error
c	Specific Heat Capacity [m]
r	Density [kg/m^3]
V	Volume [m^3]
L	Length [m]

Abbreviations

ATES	Aquifer Thermal Energy Storage
CTES	Rock Cavern Thermal Energy Storage
TTES	Tank Thermal Energy Storage
PTES	Pit Thermal Energy Storage
BTES	Borehole Thermal Energy Storage
GSHP	Ground Source Heat Pump
BHE	Borehole Heat Exchanger
GHG	Green House Gases
DLSC	Drake Landing Solar Community
TRT	Thermal Response Test

HDPE	High Density Polyethylene
SBTES	Soil-Borehole Thermal Energy Storage
TRNSYS	Transient System Simulation Tool
DTS	Duct Ground Heat Storage
MIR	Multi-Injection Rate
MFR	Multi-Flow Rate
DTRT	Distributed Thermal Response Test
MLS	Moving Line Source
GW	Ground Water
GHB	Gerald Hatch Building
ILS	Infinite Line Source
GLD	Ground Loop Design
DOE	Design of Experiments
RMSE	Root Mean Square Error
STD	Standard Deviation
MAX	Maximum
LFA	Laser Flash Apparatus

List of Tables

List of Figures

1 Introduction

1.1 Background

Renewable energy sources provide 17% of the primary energy supply in Canada [1]. Resources such as wind or solar can be utilized when available without contributing to greenhouse gas (GHG) emissions. Renewable energy sources such as wind and solar are dependent on time-variable weather which can result in a mismatch between the supply and demand for energy. This misalignment results in a need for sources that can meet peak demand such as gas power plants which contributes to GHG emissions. The same misalignment of demand and availability occurs with thermal energy in Ontario. During the summer, air conditioners work to remove heat from homes, resulting in thermal energy being exhausted into the atmosphere. During the winter, the outdoor temperature is much lower, and typically furnaces or boilers are turned on to provide heat. The availability of excess heat and the demand for heat occurs at two different seasons within a year. The equipment from both the summer and winter seasons require the consumption of electrical power or fossil fuels such as natural gas or oil, resulting in GHG emissions.

To help reduce GHG emissions, maintain comfortable living environments, and minimize the gap between availability and demand, the concept of the use of the Earth, or in Greek *geo-*, to dissipate or store excess heat is introduced. Two specific methodologies can use the Earth to dissipate or store heat. The first is geo-exchange, which consists of deep wells that use the thermal energy that exists far beneath the Earth's surface. During the cold seasons, geo-exchange systems utilize a ground source heat pump (GSHP) to take energy from the ground (source) and bring it to the surface. Thermal energy is then used for space heating, water heating, or to meet thermal demands. During the summer months, the system works in reverse, extracting heat from

a home or building and sending it down the wells utilizing a working fluid, where the heat dissipates in the ground. A geo-exchange system's set-up consists of deep borehole heat exchangers (BHE). Borehole well spacing is far enough apart so that there is minimal thermal interaction between the boreholes. This far-spacing allows for the heat injected to dissipate into the surrounding soil, effectively keeping the temperature surrounding the BHE near-constant on an annual basis. This near-constant temperature is favorable in a geo-exchange system as it means that there is a balance in the amount of heat injected in the summer with the heat extracted in the winter [2].

The second technology, which is the primary focus of this dissertation, uses the Earth as a long-term thermal energy storage medium, referred to herein as a geothermal storage system. Typically, excess heat from the summer months is injected and stored in the ground so that it can be recovered to satisfy a portion of the peaking thermal demands during colder months. As such, geothermal storage systems offer a potential solution to bridge the seasonal mismatch between the availability and demand for thermal energy. Thus, they reduce the need to rely on GHG emitting resources. The following section presents the different types of geothermal storage systems.

1.2 Types of Geothermal storage

Geothermal storage systems are available in the form of aquifer thermal energy storage (ATES), rock cavern thermal energy storage (CTES), tank thermal energy storage (TTES), pit thermal energy storage (PTES), or borehole thermal energy storage (BTES).

1.2.1 Aquifer thermal energy storage (ATES)

An aquifer thermal energy storage system utilizes a naturally-existing aquifer. As shown in Figure 1.1, at least two separate wells are drilled into the aquifer [3], which allow the aquifer

to act as both a heat source and sink. In the winters, the water can be pumped up from the 'warm' well and used as a heat source. The used water is then pumped down into the 'cold' well [4]. The flow is reversed in the summer months to provide cooling. There are, however, temperature constraints on the underground water [3], which are imposed to limit the disruption of the existing ecosystem and water chemistry [4]. The volumetric storage capacity of typical ATES systems ranges from 30 – 40 kWh/m^3 [3].

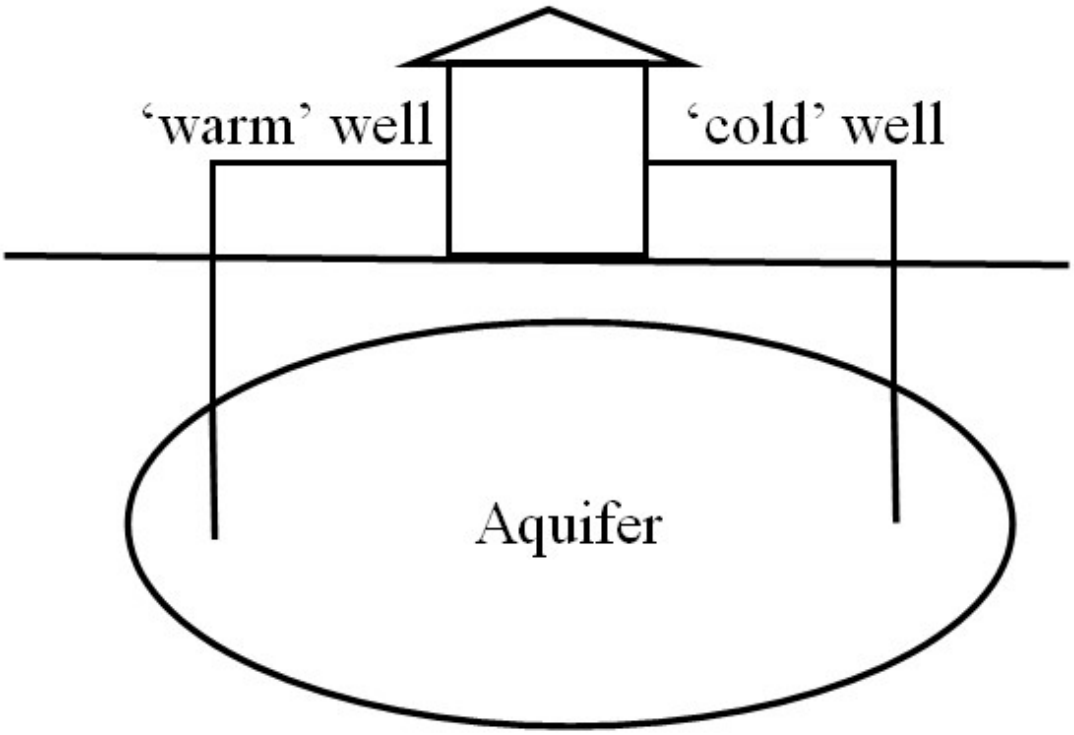

Figure 1.1 - ATES set-up

1.2.2 Rock cavern thermal energy storage (CTES)

CTES systems are essentially large stratified hot water tanks. The difference between ATES and CTES is that CTES is not a naturally occurring space. For example, there have been cases in which decommissioned mines and old oil storage facilities have been repurposed into CTESs [4]. Hot water is injected at the top of the cavern and stored seasonally. Colder water is extracted from the bottom of the cavern [4]. Figure 1.2 displays the set-up of a CTES system. The challenge of CTES systems is that they can require a volume of water up to 115 000 m^3 [4] and are very expensive to build.

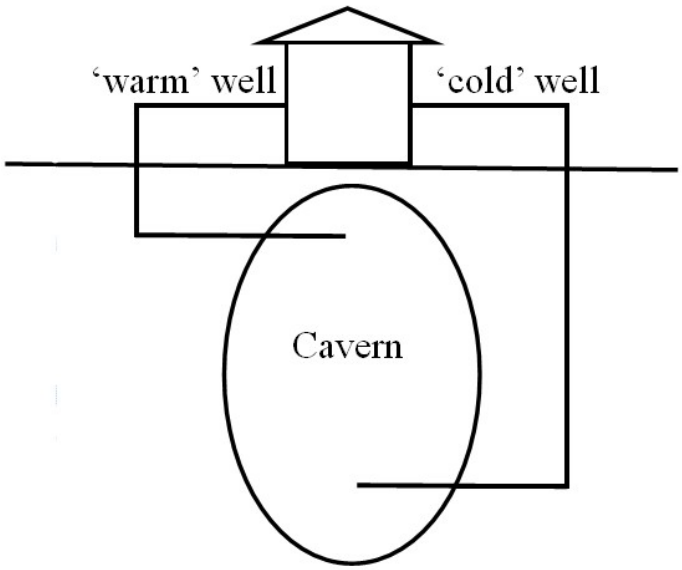

Figure 1.2 - CTES Set-up

1.2.3 Tank thermal energy storage (TTES)

TTES can be located both under and above ground. The tanks are typically steel with wood insulation per the location needs. The tanks are designed such that vertical temperature stratification occurs, similar to the CTES. The cost curve for tanks sized between 5000 and

10000 m^3 is relatively flat. However, there is an exponential relationship between the investment cost and the storage capacity for tanks less than 5000 m^3 [3]. The volumetric storage capacity of TTES systems ranges from 60 – 80 kWh/m^3 [3].

1.2.4 Pit thermal energy storage (PTES)

PTES consists of a sizeable plastic membrane placed in a large pit. The membrane covers the bottom and sides of the pit in order to prevent the storage medium (usually water) from leaking into the surrounding soil. A floating piece of insulation covers the top of the pit [3]. Similar to TTES and CTES, the pit is designed and operated to maintain thermal stratification. The volume of PTES systems is generally more significant than that of TTES systems. The specific capacity of PTES systems ranges from 60 – 80 kWh/m^3 [3].

1.2.5 Borehole thermal energy storage (BTES)

A BTES is an array of tubes feeding into and out of the Earth (referred to as boreholes), as shown in Figure 1.3. The BTES effectively uses the available surrounding soil as the storage medium. This long-term thermal energy storage is commonly referred to as a seasonal BTES. Seasonal borehole thermal energy storage combines nature with modern energy-efficient building design [5] by using the soil as a storage medium. The thermal energy that is stored in the borehole field is usually waste heat or solar thermal energy. A working fluid (typically water) is passed through a closed-circuit tube to exchange heat between the soil and the external system.

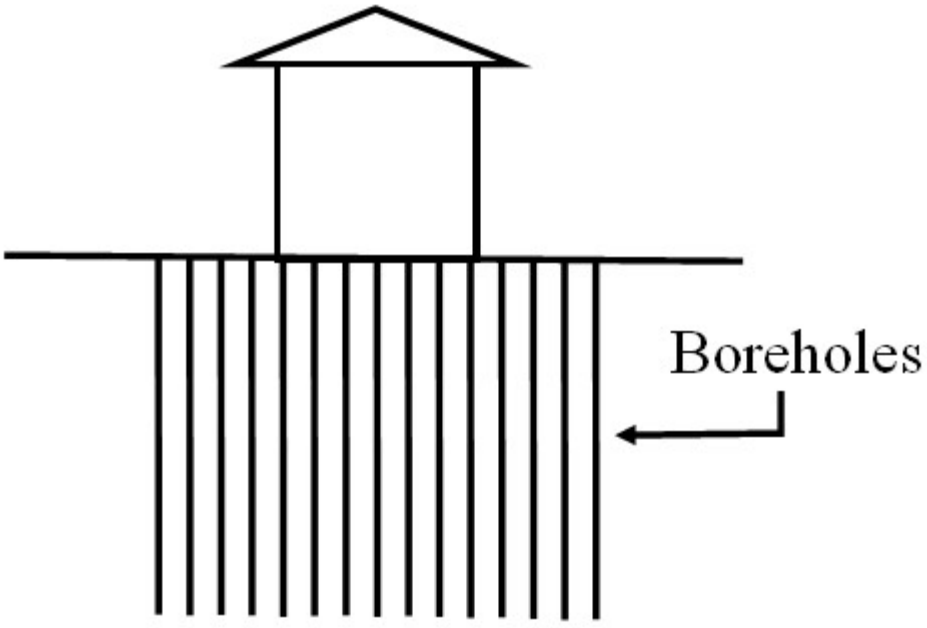

Figure 1.3 - Borehole Thermal Energy Storage

When comparing geothermal storage systems to geo-exchange systems, the main differences lie within the borehole heat exchangers' parameters. For geo-exchange systems, the spacing design between the individual boreholes is chosen in order to minimize the thermal interaction. In contrast, in geothermal storage systems, the boreholes' thermal interaction is desirable to improve system efficiency, as the heat remains concentrated within the borehole field. This allows for the heat to be extracted instead of dissipated to the far-field soil, increasing the efficiency. Geoexchange systems can reach depths greater than 1000m [6], much greater than that of geothermal storage systems, to maximize the surface area for increased heat transfer.

1.3 Application of BTES

In Okotoks, Alberta, Canada, the Drake Landing Solar Community (DLSC) uses the BTES system to store solar thermal energy in the summer to help meet peaking thermal demands during the winters. The community was built in 2007, consisting of 52 homes. Each home has

solar collectors on its roof as well as on the roof of the detached garage. DLSC has a total of 35000m^3 of soil where the borehole field is located, with 144 boreholes each 35 m deep [7]. An aerial view of the DLSC borehole field is shown in Figure 1.4.

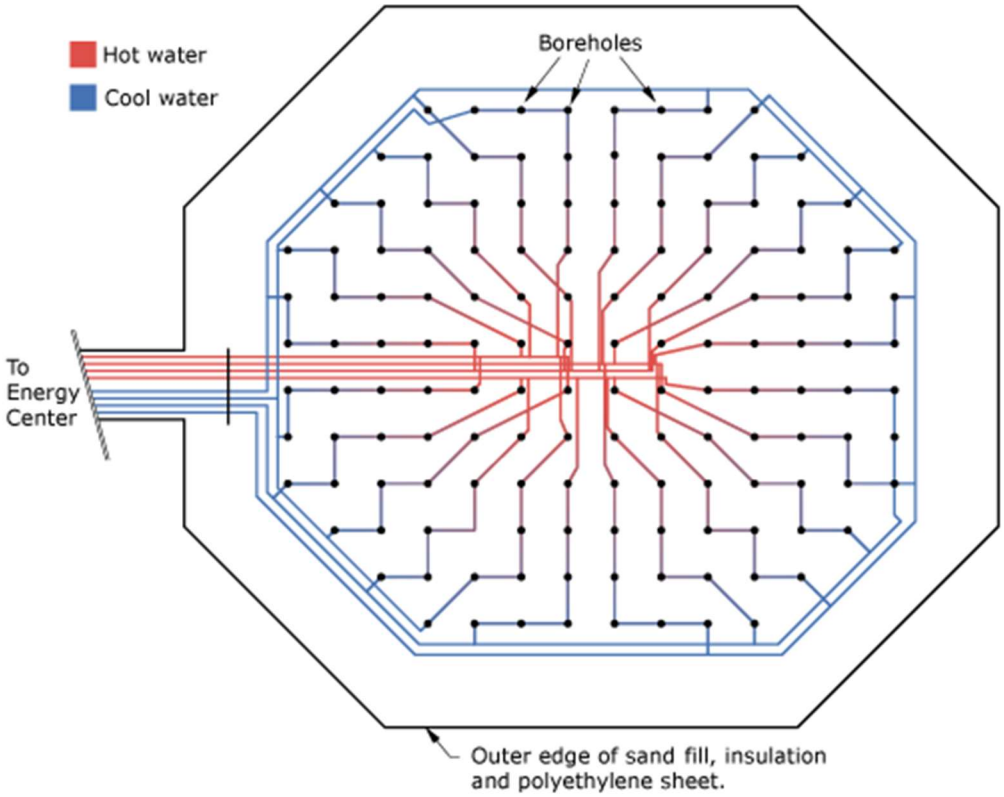

Figure 1.4 - DLSC Aerial View of Borehole Field [7]

The DLSC consists of 24 borehole strings, with one string comprising of six individual boreholes connected in series. This string configuration allows radial stratification within the field, with the motivation to limit the losses to the far-field soil surrounding the boreholes.

1.4 Design Parameters of a BTES

Boreholes can have different configurations, including coaxial, U-tube, and double U-tube (Chapter 2 will discuss these in further detail). With any configuration, the gap between the pipes and the borehole wall must be filled [8]. The filling material within the borehole can

consist of a thermally conductive grouting material or groundwater. Thermally enhanced grouting materials are recommended to reduce the boreholes' thermal resistance [9]. The selection of groundwater or a grout material is highly dependent on the geological location of the field.

Groundwater flow that exists naturally influences the operation of the BTES field [10]. It is typically not a favorable aspect of a site; however, the groundwater movement can be hard to avoid depending on the location. Further discussion on the effects of groundwater flow is presented in the next chapter.

The soil's thermal properties surrounding the boreholes have a significant influence on the heat exchanger's performance. Therefore, accurate knowledge of the thermal properties of the surrounding soil is crucial [11]. Properties include the thermal conductivity of the soil and the borehole thermal resistance. Soil properties become an essential factor when designing the borehole field. Properties such as density and specific heat capacity are of less importance compared to the thermal conductivity of the soil surrounding the borehole. The thermal conductivity will determine how well the soil can transfer the heat from the borehole into the surrounding soil and determine the charging and discharging rates of the storage system. In practice, the most common way to determine the soil's effective thermal conductivity is by employing a thermal response test (TRT) [11]. Examination of the results from a TRT can be analytical or, by using parametric estimation, numerical. Parameters such as groundwater flow and the ground thermal properties are not typically controlled, unlike the arrangement and the spacing of the boreholes within a field. Once the field's thermal properties are known, the controllable parameters can be chosen such that the field operation can be optimized,

highlighting the importance of correctly determining the soil's thermal properties at the borehole field location.

This thesis will compare the results of the typical analysis of a thermal response test completed on boreholes of a pre-existing borehole field to other means of determining the thermal properties. The typical thermal response test consists of subjecting a single borehole to steady heat injection for a pre-decided time period. The equipment used includes a heater, flow meter, and thermocouples to measure the fluid temperature at the borehole heat exchanger's inlet and outlet. The difference in the TRT completed for this thesis pertains to the borehole arrangement themselves. The boreholes tested in this thesis are three BHE connected in series with a horizontal portion buried underground leading to the inlet and outlet of the boreholes. The results from a typical TRT analysis are discussed, keeping in mind the sources of deviation of a TRT. These sources of error include groundwater flow, non-homogeneity of the soil, systematic error in equipment, assumed parameters of the soil (density and specific heat capacity), shank spacing, and horizontal portion that is connected to the boreholes in series. The effect of each of these will be discussed throughout the thesis.

This thesis will provide experimental data and will evaluate the typical analysis of a thermal response test of a pre-existing BTES system. At McMaster University in Hamilton, Ontario, the to-scale research facility consists of 66 boreholes grouped into 11 strings, each of three boreholes in series. The boreholes reach 80ft (24.4 m) in-depth and are 3 inches in diameter with 1-inch diameter U-tubes. Chapter 3 highlights the BTES characteristics and summarizes the test cases implemented on the BTES system at McMaster University. Chapter 4 presents the methods of analysis, including an analytical approach, as well as a numerical approach using a parametric estimation technique. Chapter 5 illustrates the comparison between the models and

the experimental data, taking a closer look at the effect of the physical differences between the borehole of a typical TRT and the boreholes of the pre-existing BTES field. The testing time will also be considered since repeatability tests were completed on the same borehole at different months of the year. Finally, Chapter 6 provides the conclusion and recommendations for future work.

1.5 Problem

The misalignment between thermal energy availability and thermal energy demand contributes to GHG emissions. The excess thermal energy from the summer months can be stored using BTES and used to close the gaps between availability and demand [12]. For the operation and control of the BTES system to be successful, accurate characterization of the field is essential. The thermal response test is a practical test that can be conducted on a single borehole heat exchanger to determine soil thermal properties [13]. This thesis will analyze the results of multiple thermal response tests conducted on boreholes connected in series within a pre-existing borehole field.

2 Literature Review

2.1 Introduction

This literature review provides the knowledge necessary to understand the origins and some functioning applications of BTES systems. This review focuses on previous studies on the characterization of geothermal storage borehole fields and the critical design parameters that influence a borehole field's operation. These parameters include the number of boreholes, the backfill material, the borehole spacing, the borehole configuration, the soil properties, the groundwater flow, the hydraulic gradient, and the arrangement of the boreholes (i.e., serial or parallel connection). This chapter presents the state-of-the-art application of Thermal Response Tests (TRT) to evaluate geothermal borehole fields' thermal characteristics, focusing on the soil thermal conductivity.

2.2 Design Parameters of Borehole Heat Exchanger

Borehole heat exchangers are vertical wells with diameters that typically range anywhere from 60 – 340mm (refer to Table 2.1). Pipes are inserted into the well with a backfill material added to surround the pipes. The next few sections will go through different parameters that can influence an entire BTES field's operation.

2.2.1 Borehole Heat Exchanger Configuration

Borehole heat exchangers are available in various configurations, including single U-tube, double u-tube, or coaxial (Figure 2.1). Coaxial can have two operational strategies: the hot fluid entering through the center pipe or through the outer pipe. Even though single U-tube, double U-tube, and coaxial are the most common configurations, there have been borehole heat exchangers that consisted of as many as 3 to 5 U-tubes [14]. The influence of the configuration

on the large-time scale operation of a borehole system is small. Aydin et al. [14] found that the advantage of multiple U-tubes within the borehole decreases with operational time.

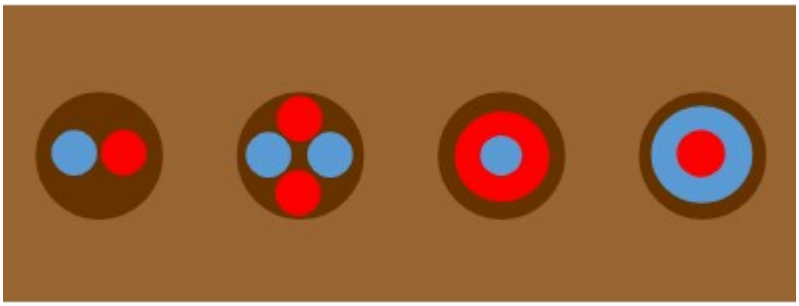

Figure 2.1 - From Left to Right: U-tube, Double U-tube, Coaxial Cold Internal, Coaxial Hot Internal

Acuna et al. [15] performed tests on both U-tube and coaxial boreholes configurations. The study found that the coaxial boreholes had a significantly lower borehole thermal resistance than the U-tube borehole. This is due to the temperature difference in the circulating fluid and soil surrounding the borehole heat exchanger.

Sivasakthivel et al. [16] compared the performance of single U-tube and double U-tube for heating and cooling operations. Findings show that the double U-tube for both operation modes obtained higher average effectiveness, defined as the "ratio of the actual rate of heat transfer to the maximum amount of heat rate that can be transferred" [16]. The findings also showed that the temperature difference between the inlet and outlet fluid was more considerable for the double U-tube heat exchanger.

Gordon et al. [17] compared experimental data with numerical models of short-term temperature variations of coaxial and U-tube boreholes. They found that the coaxial provided higher borehole thermal resistance, however with the increase in surface area of the borehole

wall it was shown to be beneficial. This was because of the increased heat-flux to the surrounding soil [17].

For single or multiple U-tube configurations, spacers can fix the location of the pipes inside the borehole. Spacers ensure that the pipes do not touch each other and remain in contact or close to the borehole wall [14] [18]. This spacing is known as "shank spacing" and is shown in Figure 2.2. Austin et al. [19] found that even significant errors in estimating the shank spacing value had minimal effect on the final thermal conductivity value found from a thermal response test. This is expected, as the thermal response test analysis excludes the first few hours of operation, where the shank spacing would have the most significant effect on heat transfer.

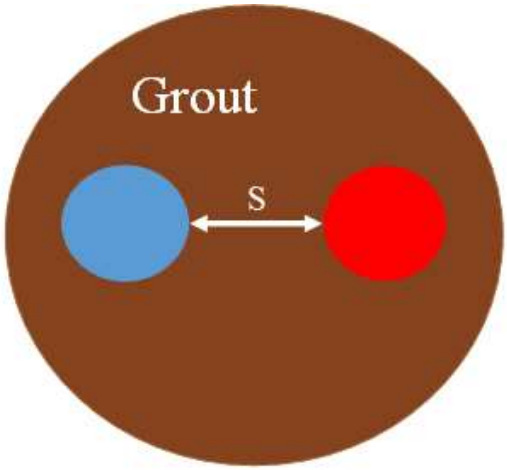

Figure 2.2 - Shank spacing, S, of a Single U-tube Borehole Heat Exchanger

Aydin et al. [14] suggested that when comparing a double U-tube configuration to a maximum of 5 U-tube configuration, the double U-tube is better suited when evaluating the total cost ratio to thermal power. Further research is required for which configuration is best suited for specific applications.

2.2.2 Tube Conductivity

Typically, the tubes within a borehole are high-density polyethylene (HDPE) that allows the boreholes to tolerate operating temperatures of 60°C under long-term operation [20]. The tubes are the fluid carriers. The tube's thermal conductivity within the borehole can vary based on the site location and budget of the project. Studies have been completed comparing the thermal conductivity of the pipe when enhanced using nano-particles (HDPE-nano) [21]. The thermal conductivity of the pipe is one of the factors that affect the total thermal resistance of the borehole [22]. The total thermal resistance of the borehole heat exchanger is dependent on the thermal resistance of the backfill material and the tubes of the heat exchanger.

Bae et al. [21] compared U-tube boreholes' performance using nano-enhanced pipes against conventional pipes. The boreholes were both 150 meters deep. Experiments showed that compared to the regular HDPE, the nano-particles could reduce the thermal resistance of the pipe slightly. By reducing the pipe's thermal resistance, the total borehole thermal resistance is also reduced, allowing the heat to more easily transfer to the borehole heat exchanger's surrounding soil.

2.2.3 Backfill Material

The backfill material of a borehole heat exchanger fills the gap between the internal pipes and the soil surrounding the borehole. Figure 2.3 shows a single U-tube heat exchanger.

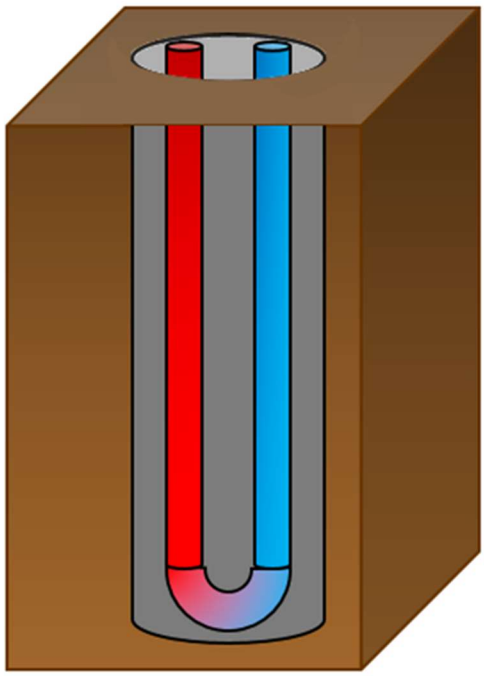

Figure 2.3 - U-Tube Heat Exchanger

Surrounding the two legs of the u-tube (red and blue) is the backfill material, also known as grout. A cross-sectional view of a U-tube heat exchanger is shown in Figure 2.4. Boreholes have grout added around the heat exchanger to minimize contamination of surrounding groundwater and provide better thermal conductance [22], [23].

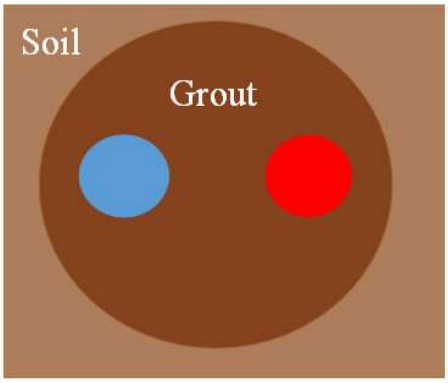

Figure 2.4 - Cross-Sectional View of Single U-Tube Borehole Showing the Backfill Material

Borehole wells can have a filling material of either a thermally conductive grout ([24], [25]), soil/silica sands ([26], [27]), or groundwater ([15], [28], [29], [30]–[32]). Backfill material commonly has a high thermal conductivity to enhance the borehole's thermal performance [8]. Boreholes will have grout added around the heat exchanger to minimize contamination of surrounding groundwater and provide better thermal conductance [22], [23]. Pahud et al. [18] showed that the borehole filling material's thermal resistance could decrease when quartz sand is used instead of bentonite. Typically, adding bentonite to grout is an environmentally friendly way to enhance thermal conductivity.

Shang et al. [33] evaluated the recovery period of single U-tube borehole heat exchangers while subjected to cycles of 12 hours of heat injection, followed by 6 hours without heat injection. The recovery time of the boreholes with three different backfill materials: cement mortar, clay, and sandy clay, were evaluated. Findings showed that the borehole containing cement mortar exhibited the shortest recovery time because of the different porosity and thermal diffusivity of the material.

Bozzoli et al. [34] found that the grout thermal properties significantly affect the short-timescale response of the borehole heat exchangers and a minor effect on the long-timescale

response. The short-timescale effect is primarily due to the close proximity of the filling material to the heat carrier fluid.

Muraya [35] stated that the backfill material should be a material that will resist drying out over time and have a high thermal conductivity. He states that the purpose of the backfill material is to create a thermal bridge between the heat exchanger and the surrounding soil.

Guan [8] evaluated different lengths of carbon fiber within a bentonite-based grout and found that the longer fibers and higher volumetric percentages were able to enhance the thermal conductivity of the grout.

The downfall of using a thermally enhanced grout as the backfill material is the adverse effect on the short-circuiting between the pipes within the heat exchanger [15]. The grout can enhance heat transfer to the surrounding soil, but it can also enhance the interaction between the upward and downward pipes.

The filling material used is also dependent on geological conditions. For example, in Sweden, it is typical that a borehole has groundwater as a filling material [31]. The groundwater-filled boreholes also have natural convection currents that will occur when the water surrounding the heat exchanger tubes begins to rise in temperature. Gustafsson et al. [31] showed that the influence of natural convection currents in the borehole is heavily dependent on heat injection rate. The natural convection occurs because of the changing density of the groundwater with the increased temperature. Groundwater filled boreholes are mostly observed in Northern European countries [15].

Acuna et al. [15] evaluated the performance of groundwater-filled boreholes subjected to forced convection currents within the borehole. Forced convection was accomplished by the

injection of nitrogen bubbles into the groundwater. Findings showed that the forced convection currents reduced the borehole thermal resistance by 30% compared to the case with natural convection currents for the U-tube borehole heat exchanger. For these boreholes, freezing is avoided by using an anti-freeze solution.

2.2.4 Borehole Thermal Resistance

The borehole configuration, pipe thermal conductivity, and backfill material contribute to the total borehole thermal resistance [36]. The total borehole thermal resistance can be estimated theoretically (either analytically ([36],[37], [38], [39]), numerically [40], or found experimentally ([41], [42])). Experimental results can be analyzed analytically using the infinite line source model or numerically with the parameter estimation technique [43]. Claesson et al. [36] stated that the simplified methods could work poorly or very well, depending on the situation.

The borehole thermal resistance is an essential parameter in the design and operation of a borehole heat exchanger [36]. The infinite line source model numerically determines the thermal resistance of the boreholes that have been subject to an experimental thermal response test.

2.3 Parameters that Influence the Borehole Field

A borehole thermal energy storage field (as seen earlier in Figure 1.3) consists of an array of borehole heat exchangers. A BTES field aims to store thermal energy over periods of months while minimizing the thermal losses to the surrounding environment. Heat lost to the soil outside of the borehole field contributes to lower efficiency of the system as the heat cannot be retrieved during extraction. The key parameters that influence how the BTES field will operate include the number of boreholes, the distance between the boreholes, the depth of the boreholes, the connection between boreholes, and finally, the properties of the soil within the borehole field. These parameters will be discussed in the next sections.

2.3.1 Number of Boreholes

The number of existing thermal storage borehole fields is limited; however, models exist that have evaluated the impact of the number of boreholes in a BTES. To evaluate the impact of the number of boreholes, Mohamad et al. [44] used TRNSYS to simulate different configurations to evaluate a geo-exchange borehole field for a case study of a 24-unit apartment building. The borehole field cases ranged from 15-40 total boreholes, with depths ranging from 54 – 145 m and spacing ranging from 3.5-8 m. This case study showed that the case with a smaller number of boreholes and deeper wells was the best solution for their cooling load and heating loads of 279 MWh and 1.83MWh, respectively. Even though this case study was for a geo-exchange system, evaluating the different spacings and depths is still valid for a geo-storage field because of the similarities in the physical set-up. Baser et al. [45] evaluated the subsurface temperature of the soil-borehole thermal energy storage (SBTES) field. The field consisted of an array of 5 boreholes, each with a depth of 9m and radial spacing of 2.5m. This study concluded that to effectively store thermal energy in the soil of the borehole field, the field should consist of more boreholes, allowing the injected heat to be concentrated in that location while minimizing the losses to the surrounding soil. These two studies show that the number of boreholes for a field is dependent on the load capacity.

McCartney et al. [46] performed a 4-month experiment on a solar-thermal SBTES that consisted of 13 boreholes, each 15 m deep, and with a spacing between boreholes ranging from approximately 1.5-3m. This field's configuration consisted of three different borehole strings to ensure uniformly distributed heat injection and maintain radial stratification. This study concluded that 70% of the solar thermal energy collected could be injected into the SBTES [46]. The 4-month heat injection period was followed by a 5-month period of ambient cooling. After

this period, the temperature showed some retained heat amongst the 13 boreholes, indicating that this number of boreholes and spacing of boreholes was successful in storing thermal energy.

Simon Chapuis [47] provides a review of the duct ground heat storage model (DTS) available in the TRNSYS environment. Chapuis used TRNSYS to validate a newly developed model that can consider non-uniformly spaced boreholes around the center axis of the soil volume. Findings showed that calculating the heat transfer could be considered more accurate for the proposed model because of the consideration for the uneven spacing. This particular model was not validated for thermally interacting borehole wells because of the large spacing (6 m) and short duration of experiments [47].

Simulations have been performed (examples include [48], [49],[33] ,[50],[51],[45],[52]) to characterise the performance of a BTES/GSHP/or SBTES system. Validation using experimental data for many of the available simulations has been complete; however, it is difficult to collect experimental data of a pre-existing BTES field. Shang et al. [33] found that soil properties had a great effect on soil recovery within their simulations after a period of heating. Austin et al. [53] state that the number of boreholes is highly dependent on the thermal properties of the soil. In the simulations mentioned it is very important that the soil properties be accurate to the field tested, and so field properties will be discussed in further detail in a later section.

2.3.2 Boreholes in Series

A borehole field can consist of each borehole connected to other boreholes in series or individually in parallel, as seen in Figure 2.5. This configuration of multiple boreholes in series will be referred to herein as a borehole string. The number of boreholes in the string depends on the application of the BTES. An advantage of boreholes in series is the radial stratification that

can be achieved when various strings' inlets are at the center of the field. The heat carrier fluid moves radially outwards to other boreholes connected in series. An example of this was shown in Figure 1.4 with DLSC. When the field is thermally charging, the hottest fluid enters the center boreholes and progresses through the borehole strings towards the outer-most boreholes of the field [54], creating radial stratification. The benefit of radial stratification is in the reduction of heat losses at the perimeter of the field.

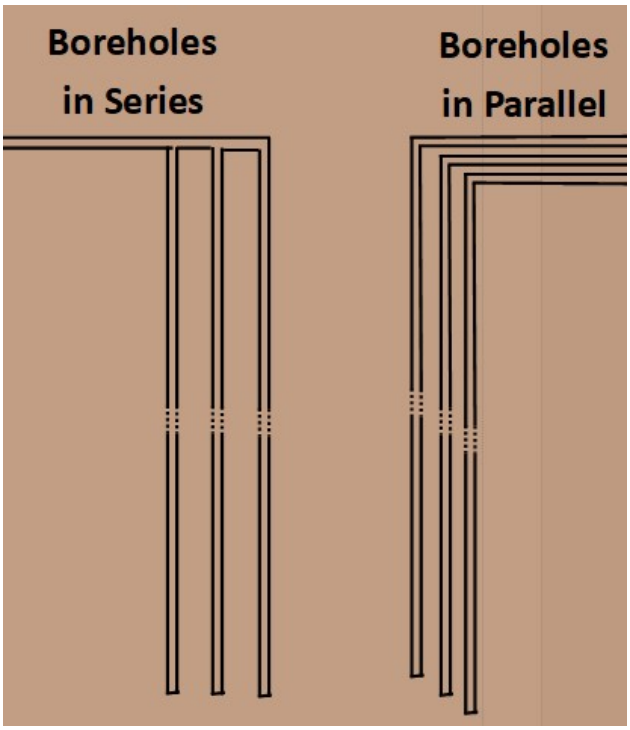

Figure 2.5 - Boreholes in Series vs. Boreholes in Parallel

2.3.3 Spacing of Boreholes

For geothermal exchange, Lee et al. [55] stated that boreholes should be spaced such that each borehole is not thermally affecting another borehole. Thermal interaction is not desired in this case study because the boreholes are used in a geo-exchange system. The desire is that the borehole heat exchanger dissipates the injected heat. This study's boreholes reached a depth of

5km, considerably deeper wells than a typical BTES system. In the case of geothermal storage, thermal interaction between the boreholes is critical to operating a successful geo-storage system, as the concentrated heat in the center of the storage can be extracted at a later season.

Gultekin et al. [56] performed multiple simulations using COMSOL Multiphysics software to determine the effect of boreholes, spacing in the range of 0.5 – 15m. They found that the thermal interaction had little impact on the temperature change between the interacting boreholes for the first week of heat injection. The impact of interaction was seen, however, after six months of continuous heat injection. This study showed that the distance between the interacting boreholes, the heat flux from the borehole, and the operation duration all influence the amount of thermal interaction experienced. When the borehole spacing is 0.5m apart, the thermal interaction is significant and becomes less significant when spacing is greater than 9m [56].

Lazzari et al. [57], Monzo et al. [58], and Koohi-Fayegh et al.[59] developed models to explore the effects of borehole spacing on the borehole temperature. Experimental data exists that can be used to validate some of these models. However, it is challenging to isolate the effects of the different boreholes spacing because of the infeasibility of drilling boreholes with different spacing for the sole purpose of experimental validation.

2.3.4 Soil Properties

Soil properties become an essential factor when designing the borehole field. Catolico et al. [54] used simulations to better understand the challenges associated with BTES fields. The objective was to improve the BTES efficiency by analyzing the heat transfer within the soil. Their findings showed that with a lower thermal conductivity, the BTES efficiency of heat extraction increased. The lower thermal conductivity created a higher temperature near the

boreholes once the injection phase was finished. This created a greater temperature gradient during the heat extraction phase. The thermal conductivity, as well as the heat capacity, governs the thermal behavior of the soil [60]. In turn, this will determine the capacity of the storage system. The thermal power of the operation of a BHE is also highly dependent on thermal conductivity [61].

The most common way to determine the soil's effective thermal conductivity surrounding the borehole heat exchanger is by utilizing the thermal response test (TRT). Parameters obtained from a TRT include the undisturbed soil temperature, the thermal conductivity of the soil, and the total resistance of the borehole. These parameters are then used to design the anticipated BTES field because cost and performance are dependent on these parameters [62].

Table 2.1 presents previous work done on TRTs performed on a single borehole. Also, Austin [53] conducted 22 different TRTs at various locations with varying parameters. Xia et al. [63] performed 31 TRTs in the Greater Toronto Area. It is common to complete a thermal response test before drilling the entire field to determine the soil's thermal properties so that the design of the field is suited for the specified location.

2.4 Parameters that Influence the Thermal Response Test

The TRT includes subjecting the borehole to a constant heat injection rate for an extended period. The test includes collecting temperature response data from the borehole heat exchanger and plotting the average temperature with time.

Table 2.1 shows a few of the different models used to determine the effective soil thermal conductivity. Spitler et al. [64] provided an excellent review of the thermal response test's history and progression since its introduction in the 1980s. It should be emphasized that the results from

a thermal response test do not account for the inhomogeneity or stratification of the existing soil. The thermal conductivity found from a thermal response test is typically known as the effective thermal conductivity [64]. Databases of known soil types and the corresponding thermal property values are available but typically consist of a wide range of values for a particular soil type and therefore are insufficient [64] to use in the design of BTES fields. The following sections of this chapter highlight the parameters that influence thermal response test results and the related research.

Table 2.1 - Experimental TRTs

Author(s)	Year	Borehole Type	Borehole Diameter (mm)	Depth (m)	Filling Material	Heat Rate (kW)	Duration of Heating (hour)	Model Used to solve thermal conductivity
Acuna, Jose [15]	2013	U-tube	140	220.4	GW	8.7	18-42	line source
Acuna, Jose [15]	2013	U-tube	140	260	GW	9	~48	line source
Acuna, Jose [65]	2013	Coaxial	115	168, 182	GW	6	76, 54, 88	line source
Acuna, Jose [29]	2011	Coaxial	140	100	GW	1.7 – 4.0	21 - 77	line source
Aydin,M et al. [24]	2017	U-tube	57.3	50	grout	T_{in} = 1.9 - 50ºC	236	cylindrical
Beier, Richard [25]	2008	U-tube	114.6	76.2	grout	2.1	~42	line source
Eklof, Catarina., Gehlin, Signhild [30]	1996	U-tube	76	31	GW	4.5	23	line source
		U-tube	130.6	160		9	96	
		U-tube	110.5	139		9	96	
Fujii, Hiraki et al. [26]	2009	U-tube	250	100	soil	~3.6	50	G function
		U-tube	340	63	silica sand	~4	72	G function
Fujii, Hiraki et al. [66]	2006	2 U-tube	160	50	silica sand	T_{in} = 35ºC	48	G function
		U-tube				T_{in} = 35ºC	48	
		coaxial	160	50	silica sand	4.2	48	G function
						T_{in} = 35ºC	48	
Gustafsson, A.M. et al. [31]	2010	U-tube		75	GW	3.2 - 6.0	57	axisymmetric heat conduction
				150		3.2 - 11.3	57	
				66		3.3 - 11.2	57	
Javed, S. et al.	2011	U-tube	110	80	GW	4.5	48 - 260	line source
Raymond, Jasmin [67]	2018			45		< 1.2	50-55	line source
			114	154	Clay/shale	9.7	81	

Luo, Jin. Et al. [68]	2013	2 U-tube	121, 165, 180	80	cement	4.0	> 5r^2 / α	line source
Witte, H. et al. [27]	2002	U-tube	250	30	Soil	-1.1	265	line source
IEA ECES Annex 21	2013	2 U-tube	133	150		7.2	84	line source
		2 U-tube	200	193.5		9.6	84	line source
Beier, R. et al. [69]	2017	U-tube	114	76.2	grout	3.93	> 200	

2.4.1 Heat Injection Rate of Thermal Response Test

A thermal response test's recommended heat injection rate is within15-25 W/ft (49-81 W/m) [70]. Kavanaugh [71] provided guidelines for TRTs and stated that the electrical power peaks should be less than ±10% of the average electrical power. The guidelines also state that the standard deviation of supplied electrical power should be less than ±1.5% of the average. It is important to monitor the power variation and peaks during a TRT as the heat injection rate needs to be constant for the data to be used for analytical solutions.

Gustafsson et al. [31] evaluated the effects of a multi-injection rate thermal response test (MIR TRT). Testing completed on fractured bedrock showed that the higher the heat injection rate resulted in a higher effective thermal conductivity. The effective thermal conductivity was not affected by the changing heat injection rates for the solid bedrock boreholes. Instead, the thermal resistance of the borehole decreased with an increasing heat injection rate.

2.4.2 Mass Flow Rate of Thermal Response Test

The heat carrier fluid's mass flow rate during a thermal response test is typically held constant. To evaluate the effect of changing the mass flow rate, Beier et al. [69] performed two multi-flow rate thermal response tests (MFR TRT). During their tests, the thermal heat injection rates were held constant using a heater with an Arduino microcontroller. The tests showed that the thermal interaction between the two pipes of the U-tube was minimized at high flow rates.

2.4.3 Soil Stratification

The simplicity of the TRT allows for the thermal conductivity of a borehole to be easily estimated. This test, however, does not account for the soil stratification that may exist. Researchers investigated other techniques to account for the soil stratification, such as distributed

thermal response testing (DTRT). Several publications by Acuña ([15], [28], [29], [65]) performed DTRTs in order to analyze the effective thermal conductivity with depth on both u-tube and coaxial boreholes. A DTRT consists of measuring the temperature response at different borehole depths while conducting a TRT [28]. The temperature sensors at different depths each provide a unique temperature response and are treated the same as the data collected from a TRT but are specific to a segment of soil along the depth of the BHE.

McDaniel et al. [72] performed a DTRT using a fiber optic cable on a borehole and compared the results to laboratory results obtained from samples taken during the drilling process. They evaluated the variability in heat transfer at different soil strata. The results showed slight differences in the thermal conductivity values found, yet the general trend of the thermal conductivity in the two sets of data was similar.

Marquez et al. [73] performed a DTRT using a heated cable instead of the conventional water-heating method. The heating cable was in one leg of the water-filled U-tube, and a fiber optic cable was in the other leg. Two tests were completed at different locations in Canada and France. One of the main advantages of this test was excluding water circulation effects within the borehole. The natural convection effects of the water within the pipe could not be avoided, however. For the different tests, one borehole was subjected to a continuous heat source cable, and the other was subjected to a cable with alternating sections of heating and non-heating. The results showed that the thermal conductivity predicted using the heated cable method was slightly higher than that determined using the typical thermal response test.

2.4.4 Influence of Groundwater Flow

Groundwater within a borehole field can exist as either a flowing current or a homogeneous spread. It is common practice for a borehole heat exchanger model made to

assume that groundwater flow is negligible because of the uncertainty in whether groundwater exists. When there are groundwater currents, the flow will cause the heat injected into the ground to be carried away from the borehole field. In this case, the borehole field would underperform, and the efficiency of the field would decrease [54]. This would produce a geo-storage field that underperforms [30]. The thermal response test results would also give a higher value than the actual case because of the added convection. The thermal conductivity value will also be artificially high in the case where groundwater is spread homogeneously throughout the field. However, in this case the groundwater current does not carry the heat away from the field.

Catolica et al. [54] examined how soil hydrological conditions and thermal parameters affect the efficiency of a BTES. They developed a three-dimensional model with transient heat transfer coupled with fluid flow to investigate the effect of groundwater flow on the BTES efficiency. The model inputs consisted of experimental temperature data obtained from the Drake Landing Solar Community [7]. The model was found to have temperatures similar to the measured temperatures and served as a base case for sensitivity analysis on the thermal and hydrological properties [54]. Under the conditions of a large hydraulic gradient (groundwater velocity of 3.6×10^{-8} m/s) the heat injected into the field was carried away from the field, resulting in the field efficiency decreasing by 0.6% compared to the case with no hydraulic gradient.

When TRT experiments are done in-situ on a BTES, and groundwater flow is present, the calculated thermal conductivity will be artificially high [74]. Angelotti et al. [75] validated the Moving Line Source (MLS) approach against experimental data from a TRT. In the convection-dominated case, the MLS provided a better estimate of the thermal conductivity. However, when

conduction and convection are comparable, MLS fails to accurately capture the groundwater movement's effect.

Darcy's law is used in saturated zones to model the flow of groundwater [76]. Darcy's velocity depends on the hydraulic conductivity and the hydraulic head. Angelotti et al. [74] performed laboratory experiments. They found that the maximum velocity at the corresponding field scale is 7×10^{-6} m/s for the groundwater flow to not have a significant effect on the results of a TRT. Darcy's law can only be applied when the Reynolds number is very low. Li et al. [77] discussed the recovery process of a ground source heat pump (GSHP). They stated that one of the difficulties encountered when using the infinite line source or cylindrical heat source to a BHE could be the existence of groundwater, especially when Darcy's velocity is greater than 10×10^{-8} m/s. The velocity can be determined in a laboratory setting or in the field.

In the historical review written by Spitler and Gehlin [64], many TRTs were shown to emphasize the effect of the groundwater in groundwater filled borehole heat exchangers. In groundwater filled borehole, as expected, natural convection affects the calculated borehole resistance [64]. Witte and Gelder [78] provided insight into the procedure to include groundwater flow effects in a typical TRT. They used a numerical model and parametric estimation technique to obtain parameters accurately and account for water movement.

Although there are quite a few models that include the influence of groundwater flow [79], [80], there is still more research required to fully understand the impact groundwater flow has on a borehole thermal storage field and the results of a thermal response test.

2.4.5 Successive TRT

It is suggested that multiple TRTs with different heat injection rates should be conducted on a borehole when the operational heat injection and extraction rates are unknown [78], [81]. Gustafsson and Gehlin [81] performed thermal response tests on a groundwater filled borehole. They conducted TRTs with different power rates on the same borehole to determine the influence of buoyancy-driven flow. In this case, there was no waiting period between different heat injection rates. Witte and Gelder [78] performed similar tests on a groundwater-filled borehole to capture the effects of the temperature difference between the circulating fluid and the surrounding groundwater. The consequence of successive TRTs is that it nullifies the assumption of a uniform temperature gradient along the length of the borehole [82].

The best practice is to allow the ground to return to its undisturbed state when conducting multiple TRTs on a single borehole. In the case of power failure or interruption, retesting should be delayed by about five days [83]. Martin and Kavanaugh (2002) [84] recommended a waiting period of 10 days between tests. Zhou et al. [82] conducted successive thermal response tests without letting the ground temperature recover to evaluate the effect on thermal conductivity. When there is not enough time between successive tests, the results may be affected by residual thermal gradients surrounding the borehole in the radial and axial directions [82].

The ground temperature before a thermal response test has begun is not directly used to find the thermal conductivity when using the line source theory. However, the initial ground temperature does affect the thermal conductivity when evaluated using numerical models, which will be discussed in this thesis. The influence of the time between successive thermal response tests will be evaluated with the data obtained. Additionally, the time of year that the thermal

response tests were completed will be evaluated, as the precipitation and near-surface temperatures could influence the thermal conductivity values found.

2.4.6 Duration of Thermal Response Test

In their historical review, Spitler et al. stated that the duration of the TRTs is an "unexpectedly controversial subject" [64]. Many studies [19], [32], [85], [86] offered insight into the minimum time duration of a thermal response test. Their findings recommended a minimum test duration of 50 hours and a maximum of 270 hours. It was also stated that the thermal conductivity value tends to converge after approximately 100 hours [85]. From field experience, Austin et al. [19] found that the thermal conductivity converges at durations within 80 – 100 hours.

Gehlin [85] provided a guideline for the minimum duration of a TRT. He stated that it is dependent on the radius of the borehole and the thermal diffusivity of the soil and showed that the stability of the effective thermal conductivity increased with increasing time intervals. This value is generally much less than 50 hours. Austin et al. [19] suggested a test time of around 50 hours, and Martin and Kavanaugh [84] suggest at least 48 hours. Javed et al. [87] found a maximum uncertainty of 4% when comparing the thermal conductivity values found at test durations of 100 hours and 50 hours for a single u-tube borehole. The international guidelines of the TRT suggest that the test should last between 48-72 hours [74].

Jain [88] used different optimization methods to determine the effective thermal conductivity using information collected during the TRTs. This method allows for effective thermal conductivity to reach stability and does not require additional time for computation. He found that of the 7 test TRTs, the average duration of a TRT is 27 hours, with a maximum error of 7.5%.

Aydin et al. [24] conducted constant temperature thermal response tests and found that the tests could be shortened compared to the typical constant flux tests.

Monzo et al. [89] did not use the first 15 hours of the test when considering the thermal conductivity calculations. It is a topic of debate about how much of the initial data to ignore, as different studies ignore anywhere from just a few hours to the first 16 hours [85], [90]. The purpose of ignoring the first few hours of heat injection is to minimize the influence of the borehole heat exchanger's resistance, focusing the results on the surrounding soil.

2.5 Summary & Objectives

This chapter presented an extensive literature review of different factors that influence the operation of a borehole heat exchanger. Borehole filling material depends on the geological location of the field, but in Canada, mainly grout filled boreholes are found. The borehole configuration is typically u-tube or coaxial, both configurations showing sufficient operation. The number of boreholes within a BTES field depends on the capacity requirements. The spacing is also dependent on the capacity requirements and the operation schedule of the field.

There is a shortage of experimental work that characterizes the performance of series versus parallel borehole configurations. The current work presents a comparison between a borehole string and a single borehole model of an equivalent length for a short-time period test that is typically used to characterize the soil surrounding a single borehole. The effect of borehole spacing will also be considered when dealing with boreholes in series. The experimental work will be further discussed and the implications the data has on future borehole heat exchanger networks.

The current state of the art practice is to complete the TRT on a single borehole before the BTES field was in place. This research extends the typical thermal response testing to include a string of boreholes, evaluating the effectiveness of the infinite line source and parametric estimation methods. The ability to successfully determine a pre-existing borehole string's thermal conductivity would allow the same procedure to be followed after a field has been commissioned. The following research provides insight into this previously overlooked portion of soil characterization.

3 Experimental Facility and Test Cases

This chapter describes the set of experimental test cases that were performed at the McMaster Institute for Energy Studies (MIES). The following section describes the test cases for the TRTs done on individual borehole strings within a pre-existing borehole field. Ten test cases were performed to test the effects of the horizontal portion, duration of the thermal response test, and average heat injection rate. The flow rate across all tests was held constant at 0.25 kg/s to minimize the number of parameters affecting the experiment results. The experimental temperature output was used to determine the borehole strings' thermal conductivity by implementing the line source model. The line source model is a well-known model that approximates the thermal conductivity by analyzing temperature change. The line source analysis also involved using the Monte Carlo method and the statistical Bootstrap method for data selection.

3.1 Geothermal Borehole Thermal Storage Field

The borehole field used in these experiments exists beneath the Gerald Hatch Building (GHB) on McMaster University campus. The field consists of 66 U-tube boreholes spaced 5 feet (1.52 m) apart, each reaching a depth of approximately 80ft (24.4m). Figure 3.1 displays a top-view schematic of the field.

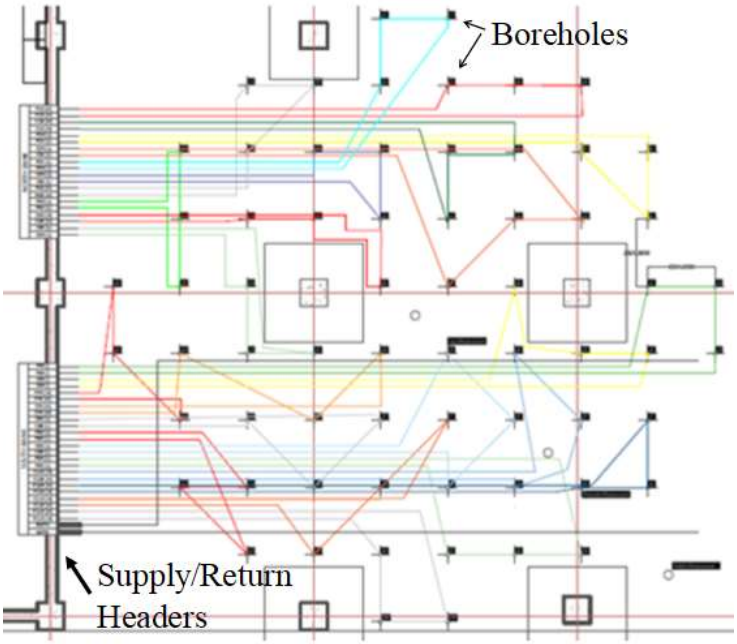

Figure 3.1- Borehole Field Layout

Each borehole is represented as a black square in Figure 3.1. This field is unique because of the structured layout of the boreholes and the connections made between boreholes. Each colored line seen in Figure 3.1 represents three serially connected boreholes (referred to herein as a borehole string), with the horizontal pipe connecting the borehole string to the supply and return headers. The field consists of a total of 22 borehole strings.

Figure 3.2 - Borehole String Connection to Header

Figure 3.2 shows the inlet and outlet of each borehole string, as well as the location of attachment to the main header pipe. The brief verical length from the inlet and outlet of the borehole string (white vertical pipe shown in Figure 11) is ignored. The pipe is insulated and is of a very short length relative to the horizontal and vertical of the borehole strings.

Specific borehole parameters are recorded in Table 3.1. There are two different types of standard dimension ratio (SDR) high-density polyethelyne (HDPE) tubes. SDR 11 used for the u-tubes within the boreholes. The two types of SDR vary in their thermal conductivity values.

Table 3.1 - Borehole Parameters

Borehole Diameter	6” (15.24 cm)
Type	U-Tube
Depth	80 ft (24.4 m)
Pipe Diameter	1” (2.54cm)
Pipe Specification	SDR 11
Pipe thermal conductivity	0.4 W/mK (LTC), 0.7 W/mK (HTC)
Grout Conductivity	1.2 W/mK

Three thermistor racks, each containing ten thermistors fixed at different depths, are placed in different locations within the field. The wells containing the thermistor racks extend to the borehole's total depth (80ft) and have thermistors placed every 8ft. The three wells are located near the core, perimeter, and outer field, as highlighted in Figure 3.3. The core and perimeter thermistor racks share wells with operational borehole heat exchangers to reduce drilling costs. These thermistor racks therefore provide the vertical temperature distribution of

these boreholes during the thermal response tests. The three thermistor racks provide data for analysing the temperature distribution radially and axially within the borehole field.

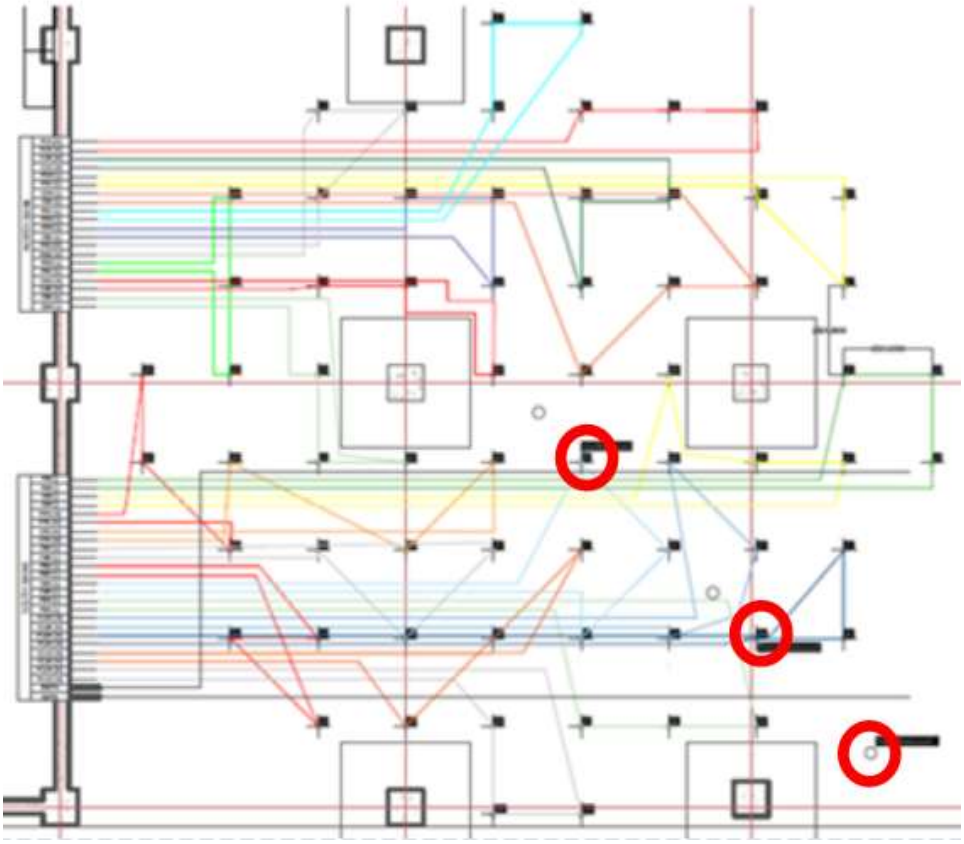

Figure 3.3 - Thermistor rack locations in three wells near the core, perimeter, and outer field of the BTES

The thermistor racks shown in Figure 12 are serviceable in the event that a thermistor needs to be replaced. These thermistor racks are also able to be removed and recalibrated if needed. Thermistors were also calibrated and installed at the inlet and outlet of each borehole string as shown in Figure 3.4.

Figure 3.4 - Inlet and Outlet Thermistors

Data from the inlet and outlet thermistors is used to calculate the heat injected and extracted for each borehole string during testing. The summation can then be compared to the total heat injected from the main header pipe temperature and flow rate.

3.2 Thermal Response Test Rig

In situ TRT testing was carried out using a GeoCube [70]. The thermal response tests do not use the temperature sensors mentioned earlier; instead, the pre-installed thermistors on the inlet and outlet of the GeoCube are used for data collection.

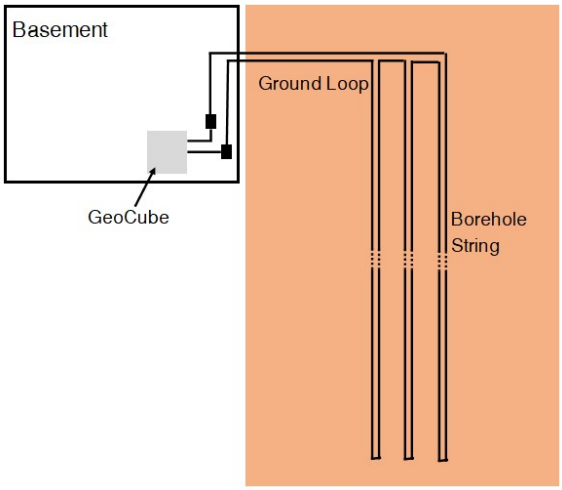

Figure 3.5 - Schematic showing the connection between the GeoCube and the borehole string

Figure 3.5 depicts the location of the GeoCube relative to the tested borehole strings. The GeoCube is a mobile piece of equipment with temperature sensors at the inlet and outlet, inline heaters, and a pump. As seen in Figure 3.6 the flow meter is not within the Geocube. However, all data was collected using the same data acquisition equipment.

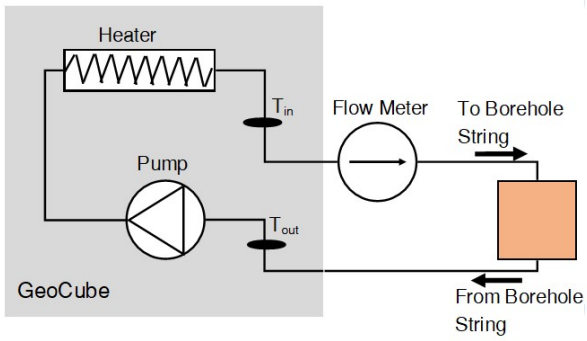

Figure 3.6 - GeoCube Schematic

The inlet and outlet of the GeoCube are connected to the borehole string valves depicted in Figure 3.7.

Figure 3.7 - Connection of the borehole string and GeoCube

The inlet and outlet temperatures, voltage, current, and mass flow rate were all recorded during the thermal response test. Recordings were either taken every 30 seconds or at 1-minute intervals, depending on the test. Figure 3.8 shows the GeoCube and mass flow meter during a TRT.

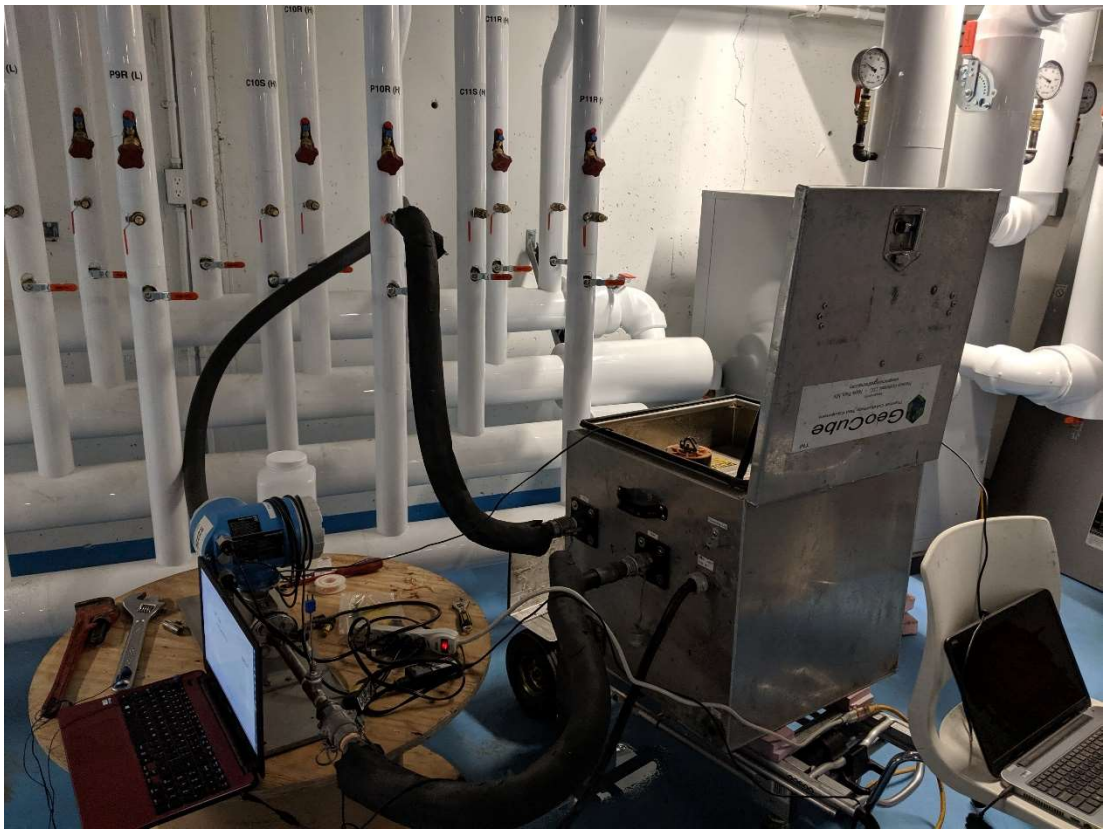

Figure 3.8 - GeoCube and Flowmeter during TRT

The GeoCube has a total of four heaters: 2× 2kW supply and 2× 3.5kW supply. The heat injection rate can then be adjusted depending on the total effective length of the borehole. This ensures that the heat injection rate is within the thermal response test guidelines of 15-25 W/ft (49-81 W/m) [70]. The ability to adjust the heaters also allows testing of the effect of different heat rates on the same borehole string. The pump has three settings. The highest setting was used for each test to keep the flow rate constant across all tests at 0.25 kg/s.

3.3 Thermal Response Tests

Thermal response tests were performed on five strings in the borehole field located at McMaster University campus. The strings, denoted as P2, P4, P5, P10, and C7, are shown in Figure 3.9. The spacing between the individual boreholes of a borehole string is dependent on

which string was tested, as shown in Table 3.2. Three of the five strings tested are in similar triangle arrangements (P2, P4, P10). Borehole string C7 was chosen because of how far the individual boreholes are from each other. The horizontal length of pipe leading to each of the borehole strings also varies. For this reason, P5 was selected for a thermal response test as the horizontal pipe length is comparatively short relative to the strings P2 and P10. Table 3.2 displays the approximate length of the horizontal portion of each tested borehole string.

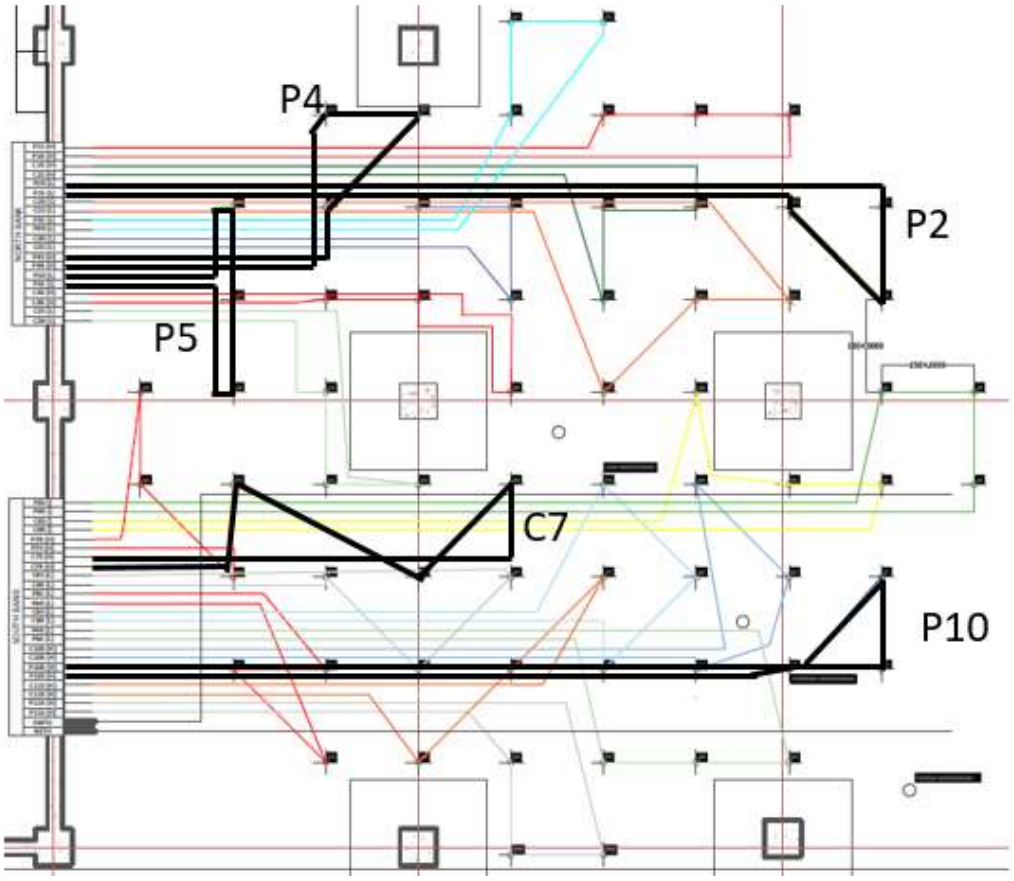

Figure 3.9 - TRT Borehole Strings

Table 3.2 - Borehole Spacing

Borehole String	Average Spacing [m]	Horizontal Length [m]	Thermal Conductivity of U-tube [W/mK]
P2	1.73	13.0	0.4
P4	1.73	4.6	0.7
P10	1.73	13.0	0.7
P5	1.52	4.6	0.4
C7	3.38	8.4	0.7

A total of ten tests were performed on the five strings. This allowed for the assessment of repeatability of experiments and the impact of altering the heat injection rate. Care was taken to ensure there was an appropriate amount of time between the tests to allow the borehole temperature to settle from the previous TRT disruption. The date of testing for each test (including the cool-down period) is shown in Table 3.3. The duration [hours], average thermal power [kW], average electrical power [kW], and average thermal heat injection rate [W/m] of each test are also displayed in Table 3.3.

When calculating the average thermal heat injection rate [W/m], the horizontal pipe length is not considered in the total length. The heat injection rate was kept as constant as possible during each test without using a generator. The variation in the heat injection rate between tests was done to evaluate the effect of different heat injection rates. Figure 3.10

displays the individual TRTs' heat injection rates and the maximum and minimum rates recommended.

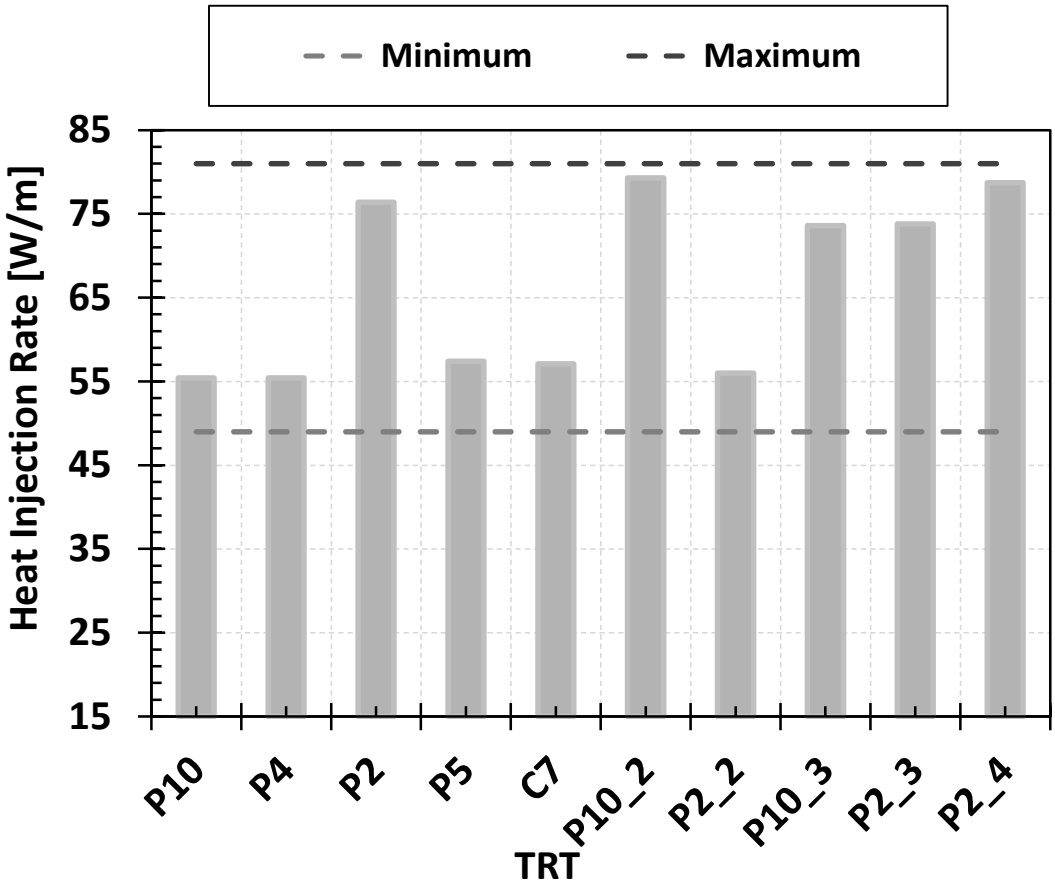

Figure 3.10 - Individual TRTs heat injection rate vs. recommended maximum and minimum rates

During the first 20-30 minutes of each test, water was circulated through the borehole string at a constant rate, with heaters turned off. This was done in order to obtain an average undisturbed fluid temperature in the boreholes. The next 70-140 hours were the heat injection stage of the thermal response test. The heat injection initiates the transient portion of heat transfer within the boreholes string.

The following chapter describes the analysis methods of the experimental data obtained for the 10 TRTs.

Table 3.3 - TRT Summary Table

Test	Infinite Line Source Thermal Conductivity [W/mK]	Duration [hours]	Average Heat Injection Rate [kW]	Electric Power [kW]	Average Thermal Heat Injection Rate [W/m]	Steady-State Circulating Fluid Temperature [°C]	Test Start Date (2019)	Test End Date (2019)	Ambient Air Temperature [°C]	Daily Precipitation [mm]	Core Thermistor Average [°C]	Perimeter Thermistor Average [°C]	Outer Field Thermistor Average [°C]
P10	1.7	71.6	4053	4310	55.4	16.4	May 13	May 16	10.2	1.9	15.9	15.6	15.7
P4	1.7	120.3	4056	4313	55.4	16.9	May 21	May 28	14.2	6.3	15.8	17.0	15.8
P2	2.3	72	5588	5680	76.4	17.0	May 31	June 6	14.9	3.3	15.8	16.2	15.8
P5	1.7	96	4198	4325	57.4	17.3	June 6	June 13	16.6	3.5	15.8	16.1	15.8
C7	1.9	113	4177	4280	57.1	16.8	June 27	July 4	22.2	1.0	15.8	17.8	16.1
P10_2	2.0	120	5801	5671	79.3	16.9	June 13	June 20	15.9	4.2	15.8	16.0	15.9
P2_2	2.1	96	4100	4291	56.0	17.8	June 20	June 26	19.5	5.4	15.8	21.5	15.9
P10_3	2.0	96	5382	5705	73.6	17.2	Oct. 10	Oct. 15	9.3	0.6	16.3	18.5	16.5
P2_3	2.1	138	5397	5659	73.8	18.8	Oct. 15	Oct. 22	8.7	3.7	16.3	32.5	16.6
P2_4	2.3	75	5727	5657	78.7	18.4	July 8	July 15	20.0	0.3	16.4	17.0	16.3

4 Analysis Methods of Test Cases

This chapter describes, in detail, the various analysis methods used in order to calculate the effective thermal conductivity of the soil surrounding the borehole strings tested. The statistical methods used to select data will be discussed, and the assumptions for each method explained.

4.1 Undisturbed Ground Temperature

The first step in determining the effective thermal conductivity of the soil surrounding the borehole is to determine the undisturbed ground temperature. The initial temperature is not used directly in the ILS method to determine the thermal conductivity; however, later in this chapter, the effects on the calculated effective thermal conductivity of the soil will be discussed. There are three methods used to determine the initial temperature. The first method uses the existing thermistors and the positions provided in the previous chapter. Due to the location of the thermistor strings, there are three different measurements of the undisturbed ground temperature profiles. The thermistor strings were installed in February of 2019 and were allowed time to settle before testing began in May 2019. The profile shown in Figure 4.1 is taken a few days before testing began. The error analysis from the calibration of the vertical thermistors can be found in Appendix A.

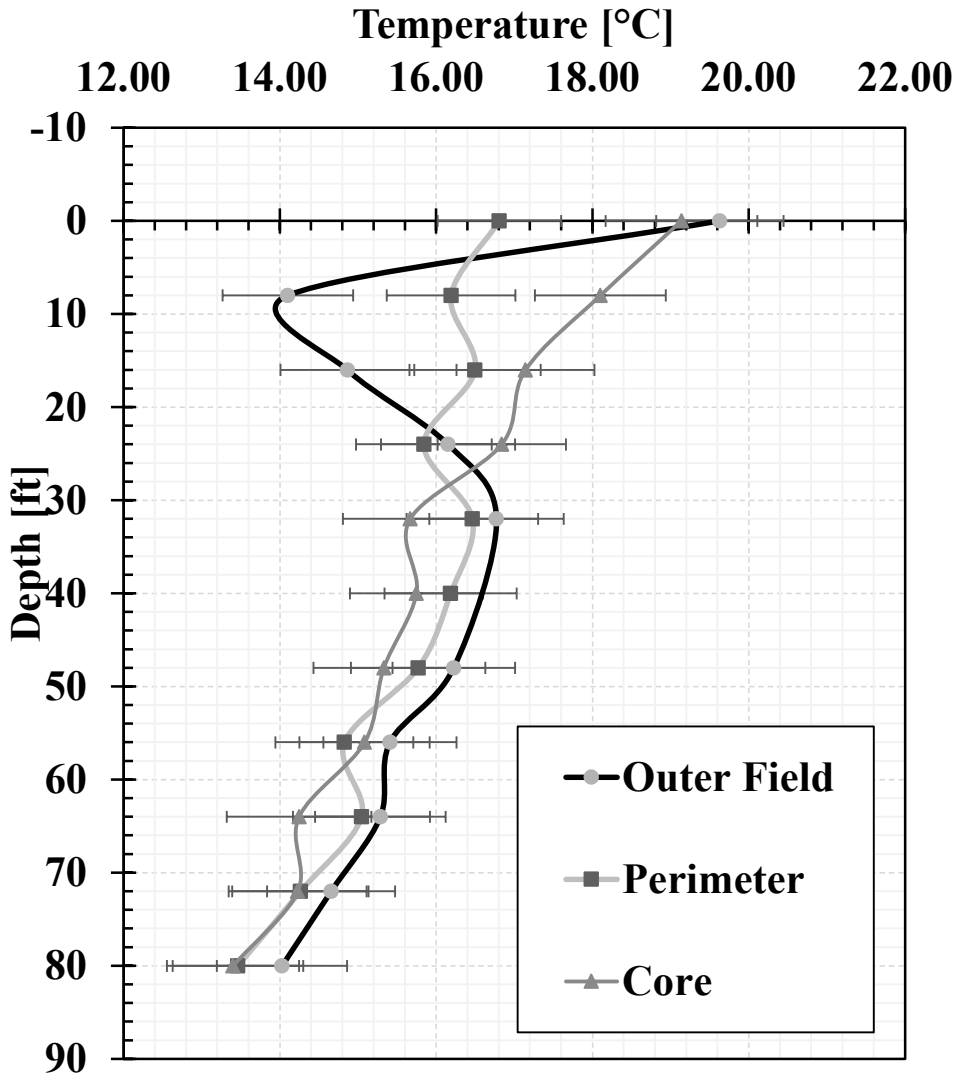

Figure 4.1 - Undisturbed Temperature Distribution

The thermistor string at the perimeter of the field is located within one of the boreholes of borehole string P10. For this reason, P10 has been selected for the full analysis to be shown. At the shallow depth of the existing boreholes, it is expected that there is a negative temperature gradient due to the influence of the surface conditions. The average temperature within each thermistor string location is displayed in Table 4.1. The variation that was seen at the near-

surface temperature sensors of the outer field string is not seen to have a prominent effect on the average temperature.

Table 4.1 - Average Undisturbed Temperature from Thermistor Strings

Location	**Average temperature [°C]**
Core	15.9
Perimeter	15.6
Outer Field	15.7

The second method to determine the undisturbed ground temperature involves circulating the water through the borehole heat exchanger without any heat. After approximately 20 minutes, the water attains thermal equilibrium with the soil surrounding the boreholes. The average water temperature can be assumed to be the average temperature along the borehole string's depth. Figure 4.2 shows the inlet temperature, the outlet temperature, and the calculated average temperature during the circulation period. Fluid circulation commences at 15 minutes and continues until the heaters are turned on at approximately 35 minutes. The profile seen shows the temperatures converging to a steady-state value.

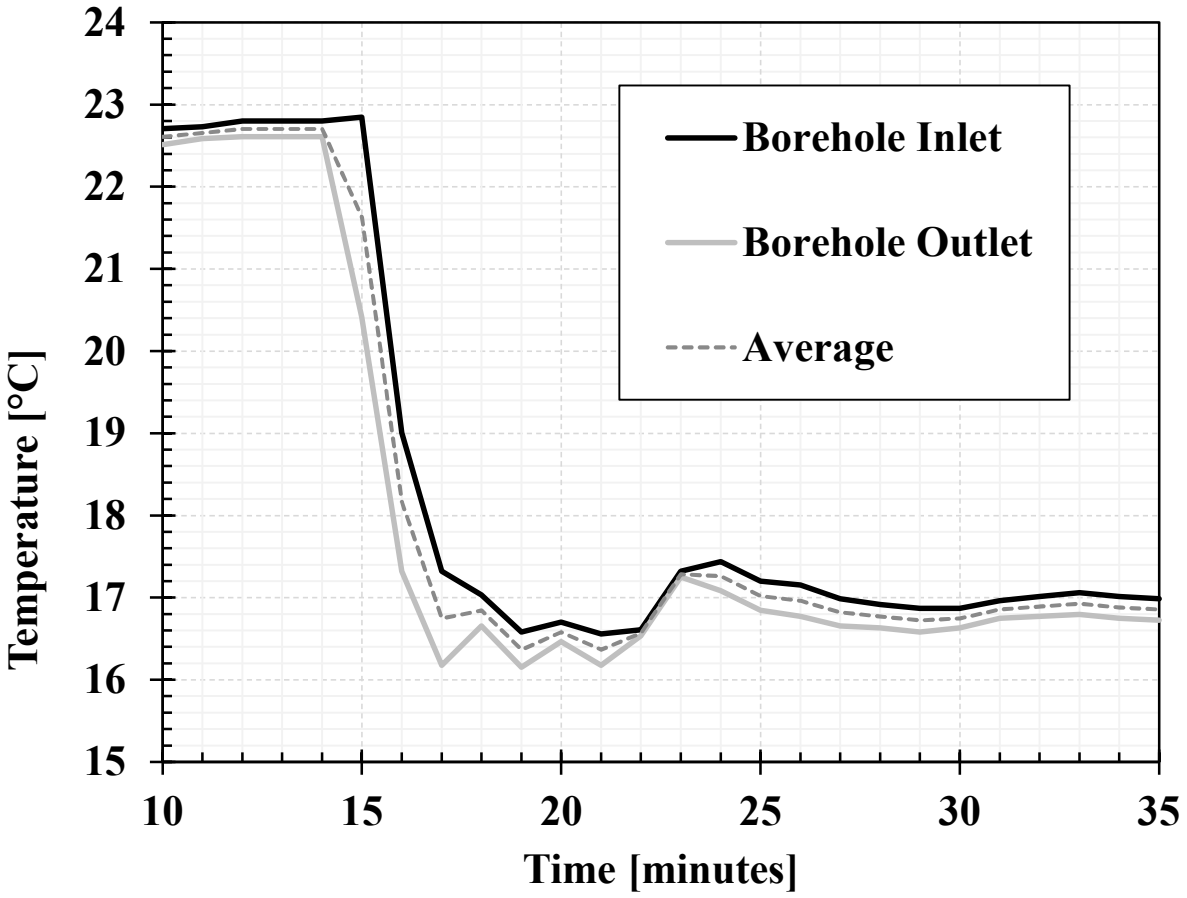

Figure 4.2 - Circulating fluid temperature with no heat injection

The steady-state temperature of the fluid after circulation can be found in Table 4.2. The circulating temperature of borehole string P10 is shown in Figure 4.2 and Table 4.2 as P10_2 as it was the second test complete on the borehole string. The steady-state circulating fluid temperature for this test was taken at the time of 35 minutes.

The third method to determine the average undisturbed temperature of the borehole heat exchanger is to analyze the initial start-up temperature of the circulating fluid. This is directly related to the time it takes for this resting fluid within the borehole heat exchangers to make the

first full pass through the string. In Figure 4.2, this can be seen by analysing minutes 15 through 25. There are three dips in the temperature that display the temperature change with depth in each of the borehole wells. These data points are then averaged to determine the average undisturbed temperature for that borehole string. The time for the fluid to make one full pass through the borehole string depends on the length of the horizontal portion leading to the borehole string inlet and outlet. The average initial start-up fluid temperature at the initial start-up is shown in Table 4.2.

Table 4.2 - Initial Circulating Fluid Temperature

Borehole String_Test Number	**Steady-State Circulating Fluid Temperature [°C]**	**Average Initial Start-up Fluid Temperature [°C]**
P5	17.3	17.8
P4	16.9	16.6
C7	16.8	16.7
P10	16.4	16.6
P10_2	16.9	16.9
P10_3	17.2	17.3
P2	17.0	16.9
P2_2	17.8	17.8
P2_3	18.8	18.9
P2_4	18.4	18.4

Finally, a temperature measurement device can be lowered down the U-tube before any heat injection occurs [91], provided that there is access to the borehole heat exchanger from the top. This method was not used, as there is not access to each individual borehole heat exchanger.

The temperature results in Table 4.1 and Table 4.2 show that the location and method of determining the temperature create discrepancy in the undisturbed temperature. The results found while circulating the fluid (Table 4.2) may be influenced by pump work, increasing the temperatures slightly. The average initial circulating temperature may vary from the steady-state circulating temperature due to the sampling rate of the temperature passing through the borehole string. The initial circulating temperature is dependent on the time it takes for the fluid to pass once through the borehole string. This time is approximately six minutes, with temperature sampling occurring every one-minute or 30-second interval, depending on the test.

4.2 Thermal Response Tests

Evaluation of the thermal conductivity was done using a direct method and a parametric estimation model with TRNSYS software. Assumptions for the evaluation of the thermal response tests include:

- Convective heat transfer within the soil is neglected and heat transfer is solely due to conduction. This is equivalent to presuming that there is no groundwater flow.
- Symmetry exists along the vertical axis
- Soil is homogeneous
- Conduction along the vertical borehole axis is neglected
- Three boreholes in series can be approximated as one borehole with an equivalent length for calculations using the infinite line source model

- The horizontal length between each of the individual boreholes is ignored
- For the TRNSYS model, the spacing between the legs of the U-tube is held constant, assuming spacers exist (spacers do not exist in reality)
- The soil's thermal diffusivity is based on Judd and Wade's (1969) value of 6.97×10^{-7} m^2/s [92]. This value was used to determine the density and specific heat capacity to be used as inputs for the simulations. Experimental data for that study is collected at a location within 500 meters of where the thermal response tests are conducted.
- The natural geothermal temperature gradient is ignored and replaced with a constant average temperature with depth
- The thermal influence from the adjacent basement to the field is assumed to be accounted for in the soil's average temperature.

4.2.1 Infinite Line Source Method

The infinite line source (ILS) model is considered a direct method to determine the effective soil thermal conductivity. The thermal response of a borehole string is the change in the temperature that occurs when the heat transfer fluid (water) is circulated through the BHE for some time [89]. The following analysis is shown for borehole string P10 and corresponds to the results of P10_2 (the second test performed on borehole string P10). Unless otherwise stated, the same analysis was completed on all other borehole strings. All further analysis on a single borehole string will be done for P10 for simplicity unless otherwise stated.

ILS makes use of the data collected from the thermal response test. Eklöf and Gehlin (1996) [30] introduced the method which was updated by Gehlin (2002) [85]. ILS is a mathematical model used to analyze many thermal response tests [62]. The method is derived from a solution to the 3-dimensional heat conduction equation:

$$\frac{\partial^2 T}{\partial x^2} + \frac{\partial^2 T}{\partial y^2} + \frac{\partial^2 T}{\partial z^2} = \frac{1}{a}\frac{\partial T}{\partial t} \quad (1)$$

After simplification, the temperature of the circulating fluid can then be approximated as:

$$\boldsymbol{T_f(t) = \frac{q}{4\pi k}\left(ln\left(\frac{4\alpha t}{\gamma r_b^2}\right)\right) + qR_b + T_{surr}} \quad (2)$$

In addition to accounting for the experimental error listed above, error estimates from implementing the ILS method need to be considered as the ILS is deemed appropriate following various assumptions [93] (refer back to section 4.2). When implementing the ILS, the relative error provided by Hellstrom [94] and revised by Eklof, C. et al. [30] stating that the minimum time duration to calculate the thermal conductivity with an error of less than 2% could be calculated using:

$$\frac{\propto t}{r^2} < 5 \quad (3)$$

This ensures that the heat capacity of the borehole filling material will not affect the results from the line source model.

In the above equation, T_f [ºC] is the circulating fluid temperature, q [W/m] is the heat injection rate, k [W/mK] is the effective ground thermal conductivity, α [m^2/s] is the thermal diffusivity, t [s] is time, γ is a constant, r_b [m] is the borehole radius, R_b [mK/W] is the borehole resistance, and T_{surr} [ºC] is the initial soil temperature.

The next few paragraphs discuss the heating process of each borehole string. Once the heater is turned on, the temperature of the fluid circulating through the borehole begins to rise. Figure 4.3 displays the temperature response during the heating portion of the TRT P10_2.

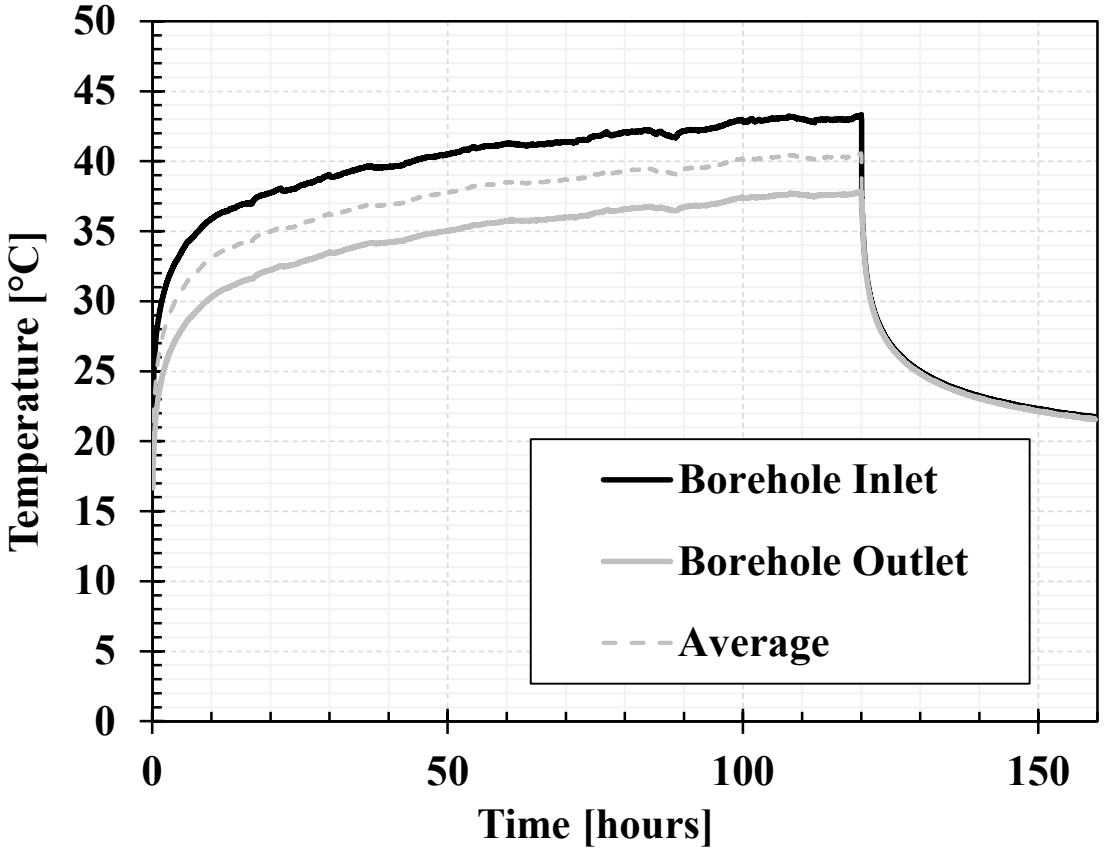

Figure 4.3 - Thermal Response of Borehole String P10

To implement the ILS, equation (2) can be simplified as:

$$T_f = mln(t) + b \quad (4)$$

As seen in Figure 4.3, the heat injection response is composed of a transient portion until the steady flux state is reached. The steady flux portion is when the curve becomes linear when plotted on a logarithmic scale. The straight line shown in Figure 4.4 is from the plot of the average temperature vs. the logarithmic time.

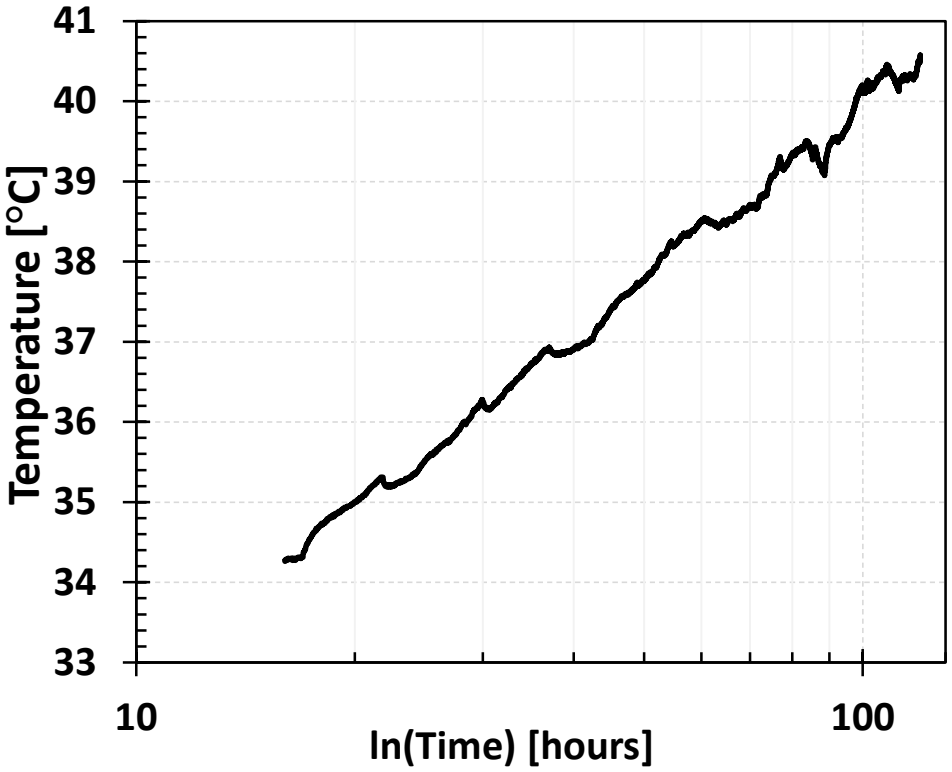

Figure 4.4 - Logarithmic Time of Average Temperature for TRT

For the infinite line source analysis, the first 16 hours of the response are discarded to eliminate the borehole thermal resistance effects when calculating the surrounding soil's thermal conductivity. Next, the slope of the line of best fit through the data is determined. This allows for the effective thermal conductivity, k_{eff}, to be approximated using the slope (m), the length of the borehole (L), and the average heat injection rate (q).

$$\boldsymbol{k_{effective} = \frac{q}{4\pi mL}} \quad (5)$$

For the line-source model to produce an accurate approximation of the effective ground thermal conductivity, the power input is recommended to be stable. This typically requires a generator to be used at the test site to ensure that any electricity grid fluctuations will not affect the test. When a generator is not used, a parametric sweep method can be implemented to ensure

that power fluctuations do not affect the thermal conductivity estimation. This will be discussed later in this chapter.

The error of the inlet and outlet temperature sensors must be accounted for when the data is selected to determine the thermal conductivity. The error of the average temperature is calculated by propagating the error from both the inlet and outlet temperature:

$$\varepsilon_{average\ temperature} = \pm\sqrt{{\varepsilon_{inlet}}^2 + {\varepsilon_{outlet}}^2} \quad (6)$$

The experimental error of the inlet and outlet sensors was equal to 0.1°C and so the average temperature error is equal to 0.14°C. The propagation of error of the average temperature to the thermal conductivity is shown in Appendix B. The error at each time step's average temperature needs to be accounted for to provide a more accurate estimation of the thermal conductivity from the linear log-trend of temperature. The Monte Carlo method is used to create several different data sets, each factor into the error.

The first step in the Monte Carlo analysis is creating a normal distribution around the average at each data point. This normal distribution comprises 1000 data points, with the distribution centered on the average temperature and a standard deviation of 0.14 (Figure 4.5).

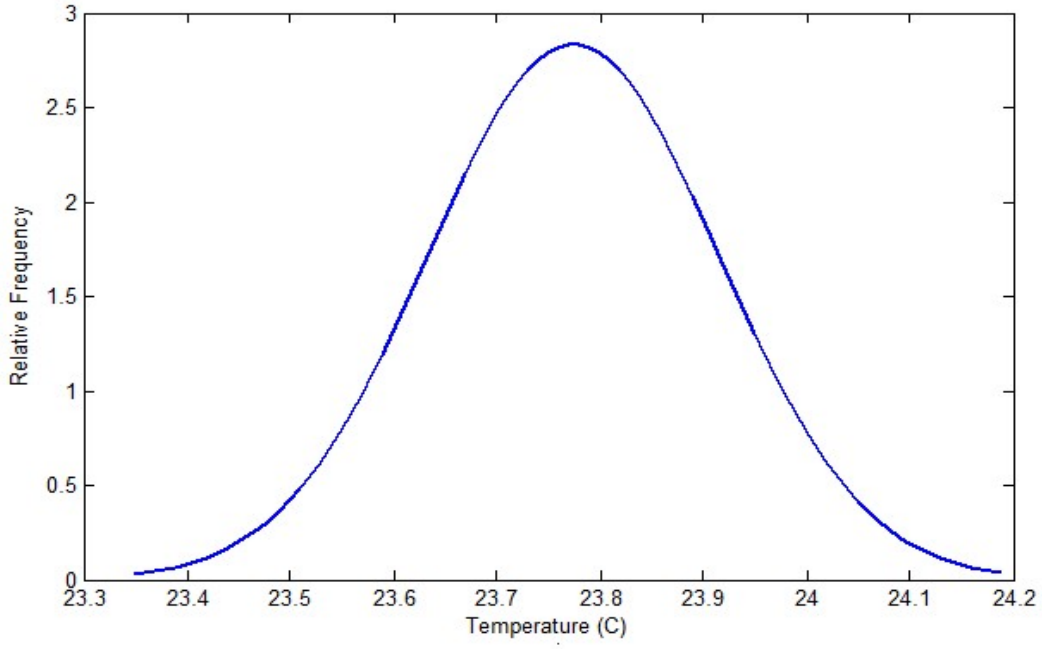

Figure 4.5 - Normal Distribution about the Average

A function is then used to select a data point from the normal distribution randomly. This new average temperature (which factors into the error) is then used to replace the experimental average temperature for that time step. This process is then repeated for each time step, creating new data sets that include the temperature variation due to the random error in the sensors.

The next step in the Monte Carlo analysis is to create multiple data sets that repeat the same process as just described. This is done to generate data sets that can be used to find the TRT's thermal conductivity.

Within each Monte Carlo data set, the statistical Bootstrap method is used to select data points to be used in the linearization trend. The Bootstrap method uses random selection with replacement to determine which data points are plotted on the log-time plot. The Bootstrap data set size should be at least 90% of the size of the population [95] (Monte Carlo sample). The key to the Bootstrap methodology is to remember that: “the population is to the sample as the sample

is to the Bootstrap samples" [95]. In this case, the 'sample' is the Monte Carlo sample previously formed. The Bootstrap sample is then plotted on a log-time plot. A linear (log) trend is found, of which the slope is used for the calculation of the thermal conductivity. A flowchart to follow each step of the Bootstrap method is displayed in Figure 4.6. This Bootstrap method is applied to each Monte Carlo sample. The final values found from each Bootstrap are averaged to give the final thermal conductivity value of the particular thermal response test.

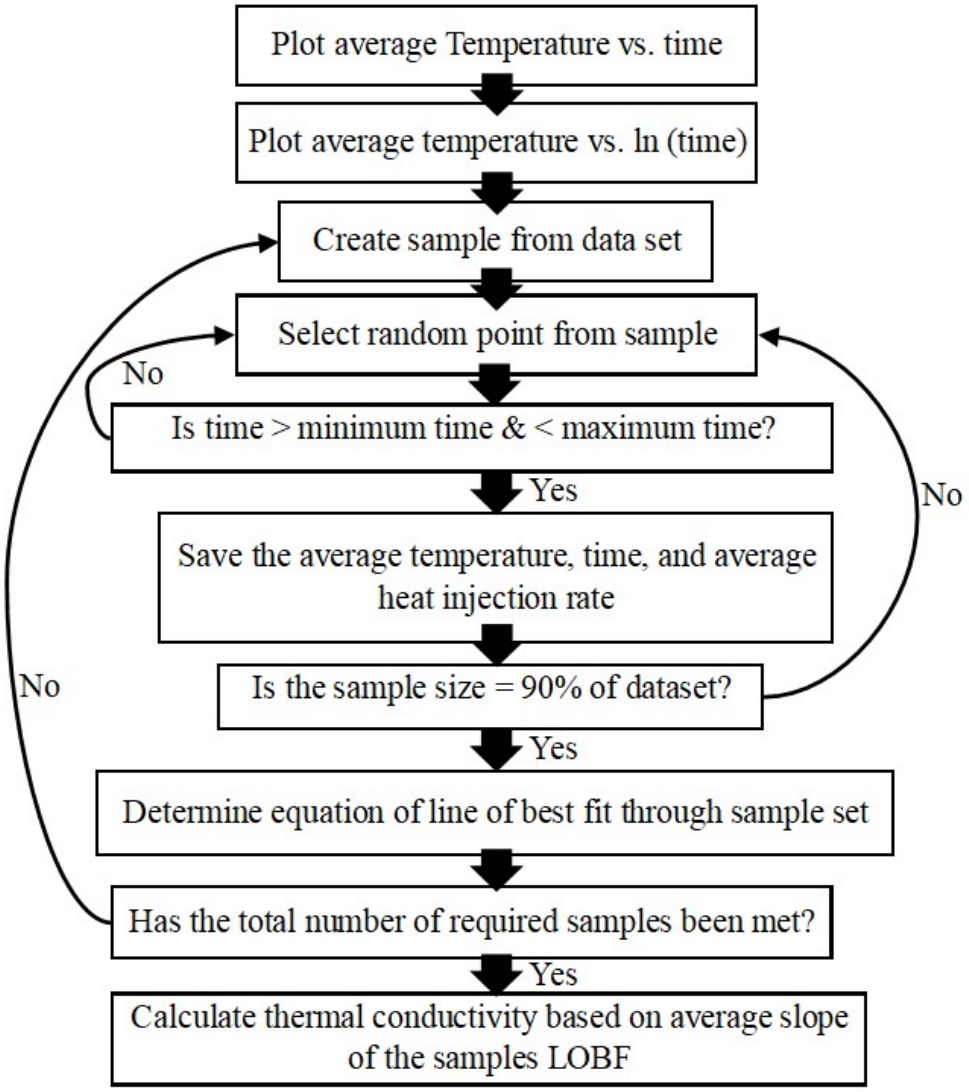

Figure 4.6 - Bootstrap Method Flowchart

A secondary resource that implements the line source theory was used to compare the above methodology to a commercial application. Ground Loop Design (GLD) was provided for use by an industry partner on the project, GeoSource. GLD uses the inlet and outlet temperature data to plot the temperature versus logarithmic time to compute the soil's effective thermal conductivity. Both the ILS and GLD do not consider the thermal interaction between the tested strings' individual boreholes. This analysis will be compared to both the above infinite line source methodology and the parametric estimation method described later in this chapter. GLD does not account for the error in the temperature measurements, power fluctuations, or the mass flow rate error.

4.2.2 Parametric Estimation Method

Transient System Simulation Tool (TRNSYS) is modeling software that can simulate transient systems. A thermal response test is a transient response of a borehole heat exchanger, and hence TRNSYS is deemed an appropriate tool to evaluate the thermal response. The parametric sweep method was used to determine the effective thermal conductivity. The model consisted of an excel worksheet input, a twin-pipe module for the horizontal portion of the pipe, and a vertical borehole heat exchanger, as seen in Figure 4.7. The input parameters of the temperature and the mass flow rate were taken from the actual data from the TRTs. The simulation time step was kept to the same sample rate as the experiment (30 seconds or 1 minute depending on the test).

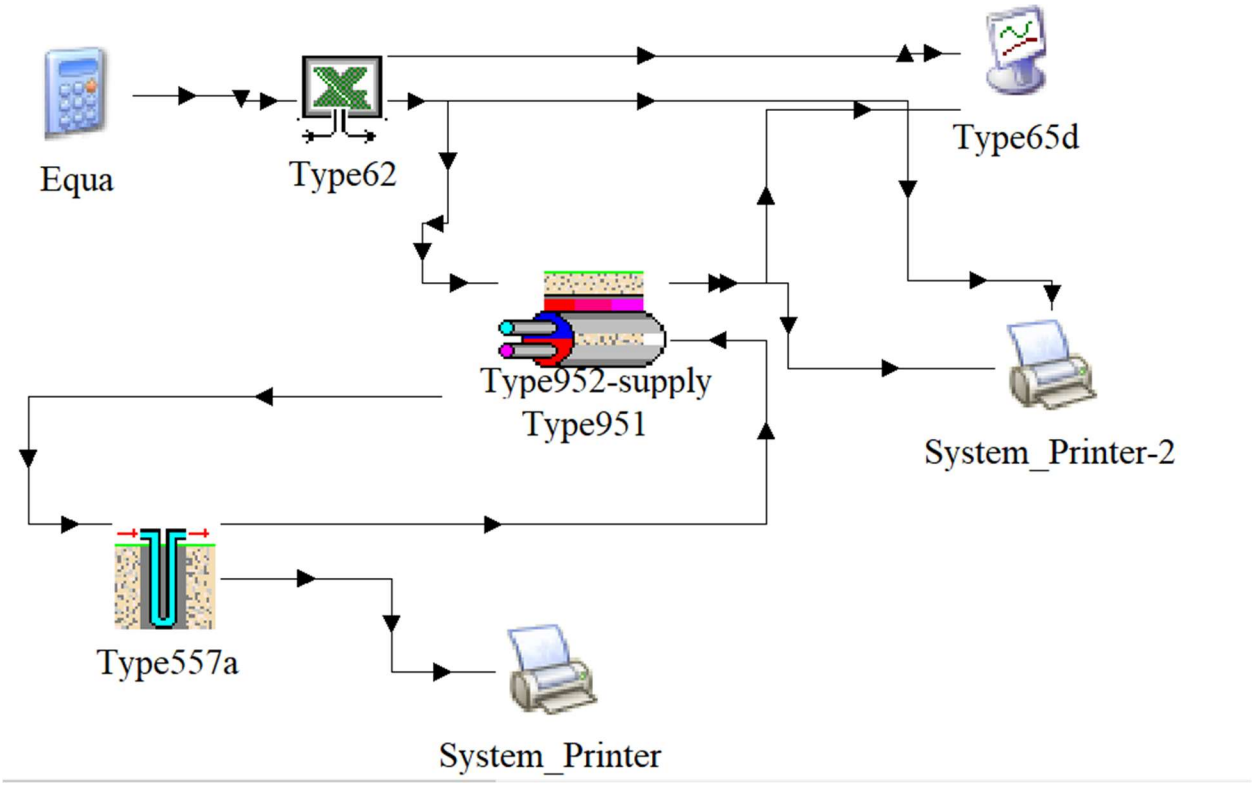

Figure 4.7 - TRNSYS Model of TRTs

To solve the heat transfer problem within and surrounding the borehole, TRNSYS can set whether the borehole exists in series or parallel. For the TRTs discussed in this thesis, all borehole strings consist of 3 boreholes in series. The model does not consider the short horizontal portion between each borehole in the series. The total volume of the storage volume (Equation 7) is dependent on the depth, spacing between boreholes, and the number of boreholes. The boreholes are assumed to be arranged in an octagonal pattern.

$$Soil\ Volume\ [m^3] = \pi \times Number\ of\ boreholes \times Depth\ [m] \times (0.525 \times Spacing[m])^2 \quad (7)$$

The spacing between the boreholes is assumed to be uniform within the cylindrical soil storage volume [96].

The pipe-to-pipe heat transfer between the pipes of the U-tube within the borehole can be enabled or disabled. For all the simulations completed, this feature has been enabled to provide a simulation environment similar to the real-world. The model uses superposition methods to determine the total temperature response within the field [96].

The soil surrounding the borehole can be segmented vertically with different thermal conductivity values for each layer. This feature is not used, as the experimental results and the line-source model used for evaluation provide an effective thermal conductivity along the entire depth of the vertical BHE.

The fluid used for the experiments is water. The density, viscosity, thermal conductivity, and specific heat are kept constant using water properties at 25°C. It is assumed that these properties' changing values do not have a significant effect on the final solution. The initial temperature of the fluid within the pipes is set as the temperature obtained from running water through the pipes for the initial 20-30 minutes of the TRTs. The average temperature of the water running through the pipes after 20-30 minutes is the standard method to determine the initial temperature of the borehole [91], as mentioned previously.

Finally, grid independence was assessed to ensure that the final values obtained for the thermal conductivity were not affected by the grid spacing in both radial and axial directions. The results from the grid dependence test are provided in Appendix E.

A design of experiments (DOE) is used to determine the best run-order of simulations. The DOE consisted of a three-factor and three-level evaluation. The factors changed included the length of the horizontal portion, the thermal conductivity of the soil, and the initial temperature of surrounding soil and water within the pipes. The length of the horizontal portion is kept to

±10% of the actual value, stated in the previous chapter. This allows for any discrepancies in the exact length of the horizontal portion to be accounted for in the analysis. A sensitivity analysis that includes the variability in the horizontal length used for the simulations is conducted.

Under normal conditions, a geothermal temperature gradient exists beneath the Earth's surface and is relatively constant throughout the year and therefore considered stationary [30]. However, in shallow borehole wells (< 50m), the annual atmospheric temperature fluctuations can affect the soil temperature. For the tested borehole strings, the temperature directly above the borehole field is held relatively constant due to insulation. This calls for the assumption that there is a small (minimal) temperature gradient due to the surface temperature variations. However, this slight temperature gradient will be averaged when the water is circulated through the boreholes before heat injection.

The thermal conductivity of the soil surrounding the horizontal portion and the vertical BHE are made equivalent in each simulation. The physical parameters, such as the borehole's depth, the diameter of the borehole, the diameter of the U-tube, and the horizontal pipe length, are all known values. The thermal properties of the borehole heat exchanger such as thermal conductivity of both the piping material and the grout material, are also known and stated as inputs in the simulation. The value of the soil's thermal conductivity is changed to produce the same outlet temperature as the experimental results. The density and heat capacity of the soil are determined based on the thermal diffusivity and the soil type [92]. A sensitivity analysis on the specific heat capacity of the soil in the simulations is carried out, and the results are provided in Appendix C. A full list of the available parameters for the TRNSYS simulations can be found in Appendix D.

The root mean square error (RMSE) was used to compare the outlet temperature of the simulations to the outlet temperature of the experiment. This method determines the average error between the two data sets, for the portion of the test where the heat transfer to the surrounding soil is dominant. This method offers a more accurate choice since the ILS, as well as GLD, both ignore a specified amount of time at the beginning of the test. The limit of the RMSE was determined using the Monte Carlo method with the experimental outlet temperature and error of the outlet temperature sensor. The limit of the RMSE is equal to 0.1.

When determining the thermal conductivity, the average power during the testing period, the error in the calculated slope, the specific heat capacity, and the mass flow rate must be known. The error propagated from calculating the heat injection rate is also accounted for when determining the average power error. The error in the mass flow rate is dependent on the flow meter used. The error is calculated as 0.2% of the highest flow rate found during the test, based on the flow meter. The specific heat capacity uncertainty is found using the tabulated water properties within the temperature range of the thermal response tests (15 - 60°C).

$$\frac{\varepsilon_{Q1}}{Q1} = \pm\sqrt{(\frac{\varepsilon_c}{c})^2 + (\frac{\varepsilon_{\dot{m}}}{\dot{m}})^2 + 2 * (\frac{\varepsilon_T}{(T_{in}-T_{out}}})^2} \quad (8)$$

To determine the average power error during the test, the standard error of the average heat injection rate of the sample is calculated.

$$\varepsilon_{Q2} = \frac{STD(sample)}{\sqrt{leng \quad (sample)}} \quad (9)$$

The maximum error of the calculated heat injection rate (MAX(ε_{Q1})), and the error due to the calculated average is used to determine the total uncertainty in the heat injection rate.

$$\varepsilon_Q = \sqrt{(\text{MAX}\,(\varepsilon_{Q1}))^2+(\varepsilon_{Q2})^2} \quad (10)$$

The uncertainty in the slope of the average temperature is found using the standard error in the line of best fit using the built-in code from MATLAB. The relative uncertainty of each component is accounted for when determining the uncertainty of the effective thermal conductivity.

$$\frac{\varepsilon_k}{k} = \pm\sqrt{(\frac{\varepsilon_Q}{Q})^2 + (\frac{\varepsilon_m}{m})^2} \quad (11)$$

5 Analysis of Results

5.1 Infinite Line Source Model

As mentioned in Chapter 4, ten thermal response tests were completed on the existing borehole thermal storage field. This section shows the results of the data obtained from the thermal response tests when the thermal conductivity is found by using both the infinite line source model and a parametric sweep method using TRNSYS. The depth, borehole filling material, and geometry are constant throughout each of the tests conducted, as mentioned in Chapter 3.

The ILS model is typically used on a single borehole in a location that is near the proposed borehole field. This section shows the results from applying the infinite line source to the data obtained from each thermal response test and will discuss the validity of the ILS model used to determine the effective thermal conductivity of the soil surrounding a borehole string within a pre-existing field. The results found from the ILS can be seen in Table 5.1. It can be seen that the values are within the range of 2.0 ± 0.3 W/mK for the tests conducted within the same field. When designing a borehole field, the thermal conductivity is used to determine the size (number of boreholes) which influences the cost of the borehole field. The broad range of thermal conductivity values found from the TRTs show the variation of results at the same location. A single test may not indicate the thermal properties of the entire field, as the soil of the borehole field could vary within the same location. As discussed in Chapter 2, some of the factors affecting the outcome from the ILS include, but are not limited to: the duration of the test, heat injection rate, length of the tested borehole.

Table 5.1 - ILS and GLD Results

Test #	Infinite Line Source Thermal Conductivity [W/mK]	GLD Thermal Conductivity [W/mK]
P5	1.7	1.71
P4	1.7	1.85*
C7	1.9	1.86*
P10	1.7	1.87
P10_2	2.0	1.98
P10_3	2.0	2.04
P2	2.3	2.21
P2_2	2.1	2.46
P2_3	2.1	2.18
P2_4	2.3	2.37*

*test failed one aspect of the GLD stability check

Thermal conductivity results from ground loop design are shown in Table 5.1. GLD also implements the infinite line source, however the results vary in some of tests. The ILS code accounts for the error in the temperature sensors, whereas GLD does not. The time frame used for the analysis could also differ between ILS and GLD, hence some varying results.

5.1.1 The Effect of Duration of Test

According to the international guidelines, the recommended duration is at least 72 hours of constant heating [74]. The tests conducted were run to different total duration to ensure that all tests conducted were in compliance with the recommendations. This allows for the comparison between duration and the thermal conductivity found at each site.

A thermal response test's duration is an essential factor because it must be long enough so that the borehole's conductivity is not considered when calculating the effective thermal conductivity. This value is generally set as a minimum, with the maximum governed by allowed time and cost at the test's specific location. Figure 5.1 shows how the thermal conductivity changes as the end time of the test was then stepped forward in time at one-hour intervals. The start time for each test was at hour 16 of heating. The results are found to agree with Gehlin's findings that the thermal conductivity value converges after approximately 100 hours [85]. The longest test run conducted on borehole string P2 was 140 hours of constant heat injection. This test, along with others displayed in Figure 5.1, shows the effective thermal conductivity to plateau after approximately 80 hours of heating.

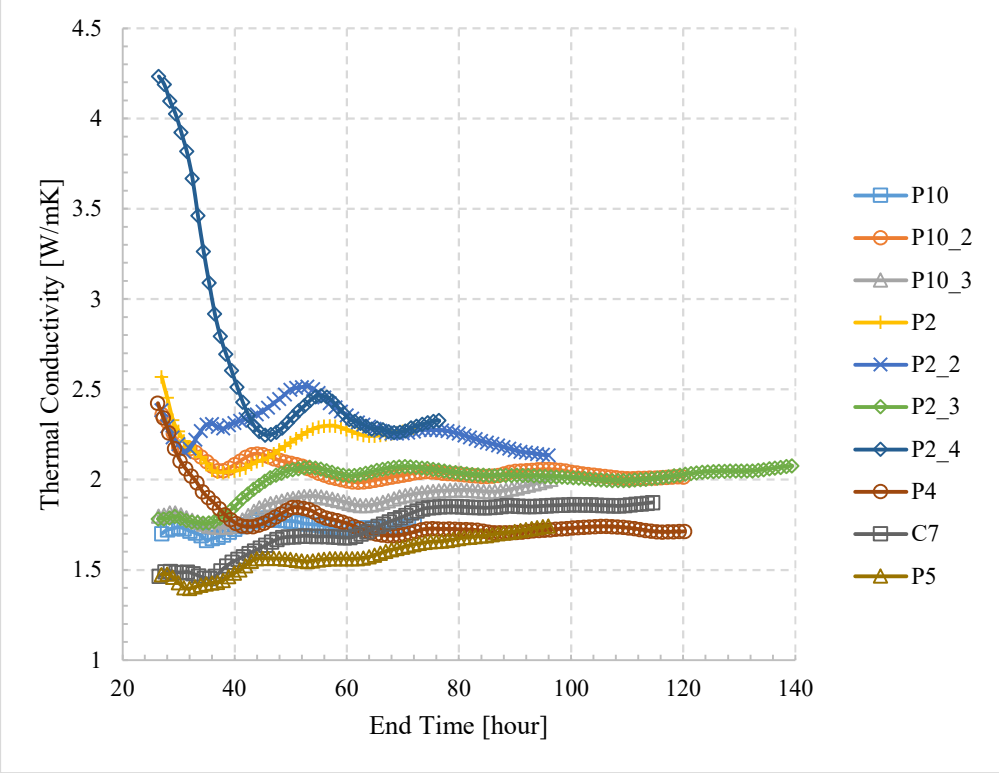

Figure 5.1 – Analysis Time Frame vs. ILS Thermal Conductivity

It is suggested that data be collected and analyzed as the TRT is running, instead of after. This allows for the data to be plotted and the effective thermal conductivity to be observed as the test continues. This could help determine an appropriate time to end the test. This graph corroborates the recommended duration of a TRT to determine an appropriate, effective thermal conductivity along the borehole length.

From Figure 5.1, it can be seen that tests P10, P2 and P2_4 do not reach a stable thermal conductivity value. Test P2_2 runs longer than 80 hours, however the thermal conductivity also does not converge. P10, P2 and P2_4 ran for less than 80 hours, showing that the minimum duration of the test should depend on the borehole string being tested.

Repeatability of the experiments was tested on borehole strings P2 and P10. When conducting multiple TRTs on the same borehole, the concern is the lasting thermal effects from the previous disturbance. The initial temperature of the borehole strings depends on the location and the number of tests that have previously been performed on that particular string. This will be discussed in the following section.

5.1.2 The Effect of the Initial Temperature of the Borehole String

It can be seen in Figure 4.1 (previous section) that the near-surface temperature varies depending on the thermistor location. This may be the result of the heated floor at the top of the borehole field. Each location shows a negative temperature gradient, as expected at these shallow depths. The procedure for determining the ground thermal conductivity from a TRT requires the undisturbed ground temperature [91]. However, it is only used when determining the resistance of the borehole heat exchanger. Therefore, when using the ILS, the difference in the undisturbed ground temperature should not significantly affect the calculated thermal conductivity.

For the tests conducted in this thesis, the undisturbed ground temperature varied between tests that were conducted on the same borehole string. Figure 5.2 displays the temperature versus the calculated thermal conductivity for a particular test.

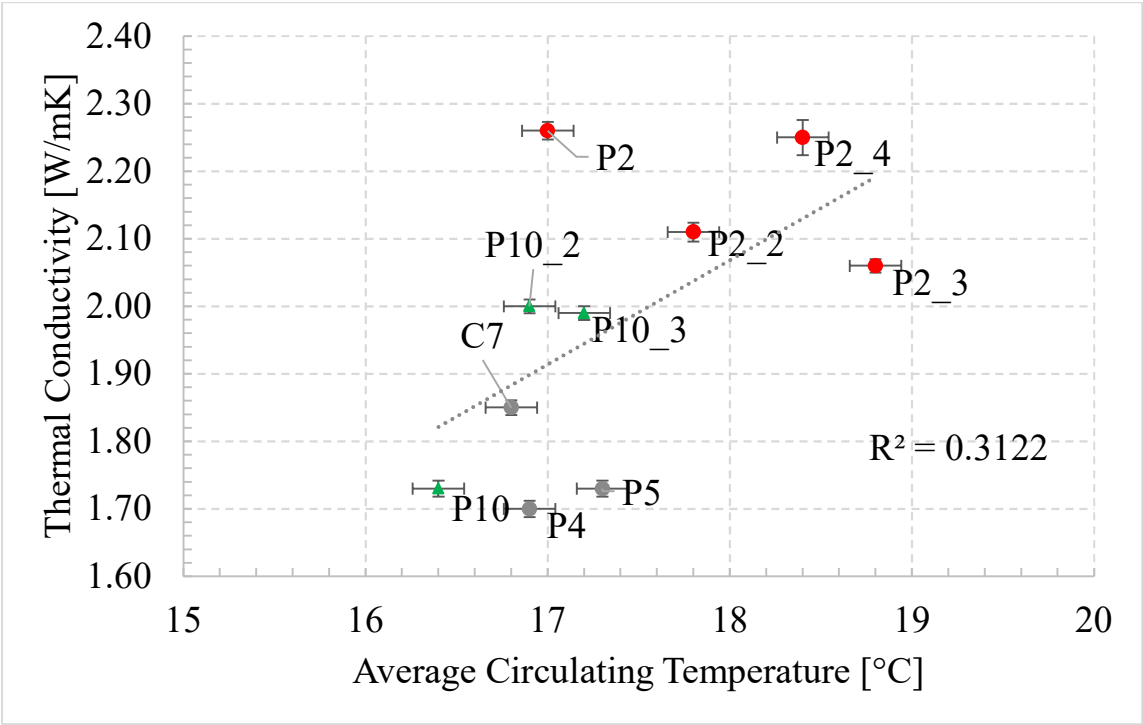

Figure 5.2 - Initial average circulating temperature of TRTs compared to the ILS thermal conductivity

There is no definitive correlation between the average circulating temperature and the thermal conductivity, as the r-squared value is 0.31 shown in Figure 5.2. Evaluating the repeated tests of string P2 (shown in red) shows that this holds true as the thermal conductivity does not increase with increased circulation temperature. Repeated tests of string P10 show an increase in thermal conductivity between the first and second test, but not between the second and third.

The borehole strings were allotted time between tests to reduce the error brought on by the previous thermal disturbance. It can be seen in Table 5.2 that the temperature from borehole

string P2 increases with each test. The same trend is seen in Table 5.3 with borehole string P10 initial temperatures increasing with each consecutive test.

Table 5.2 - Initial Steady-State Circulating Temperature [°C] of Repeated P2 Tests

Test (Date)	P2 (May 31 – June 6)	P2_2 (June 20-26)	P2_4 (July 8 – 15)	P3_3 (Oct. 1-22)
P2 [°C]	17.0	17.8	18.4	18.8

* All temperature measurements to the accuracy of ±0.14°C, all tests conducted in 2019

Table 5.3 - Initial Steady-State Circulating Temperature [°C] of Repeated P10 Test

Test (Date)	P10 (May 13 -16)	P10_2 (June 13 – 20)	P10_3 (Oct. 10-15)
P10 [°C]	16.4	16.9	17.2

* All temperature measurements to the accuracy of ±0.14°C, all tests conducted in 2019

When the heat injection rate of the regular operation of the borehole field is unknown, it is suggested that multiple thermal response tests be conducted. The tests should all be conducted with different heat injection rates to characterize the proposed field's soil accurately. The order of tests for borehole string P2 was: 1,2,4,3. P2_3, the final test, can be seen to have the highest steady-state circulating fluid temperature. The same can be seen with borehole string P10. The order is P10, P10_2, and finally, P10_3 with the highest initial temperature. The infinite line source model does not require the initial temperature to determine the thermal conductivity, so the effects are not seen here. It has been suggested that at least five days should be allowed between successive TRTs to allow the ground to return to its initial state [83]. It has also been

suggested that there should be ten days between successive tests [84]. Table 5.2 and Table 5.3 shows that ten days is not sufficient time to allow the ground to settle back to its initial temperature. One suggestion would be to follow the TRT with a heat extraction test to shorten the recovery time.

The radial variation in initial temperature from the previous disturbance is not accounted for in the TRTs. This would be caused by the soil stratification along the depth of the borehole, and the corresponding heat transfer.

This study aims to explore the effect of the different initial temperatures when looking at the results from the parametric estimation method with program TRNSYS. This will be discussed in a later section of this chapter.

5.1.3 The Effect of Heat Injection Rate

As stated before, the heat injection rate should be within 15-25 W/ft (49-81 W/m) [70]. Two borehole strings were subject to different heat injection rates between 49 and 81 W/m to test the heat injection rate effect. The purpose of these tests was to see if the heat injection rate would affect the effective thermal conductivity. The effect of the heat injection rate versus effective thermal conductivity is shown in Figure 5.3.

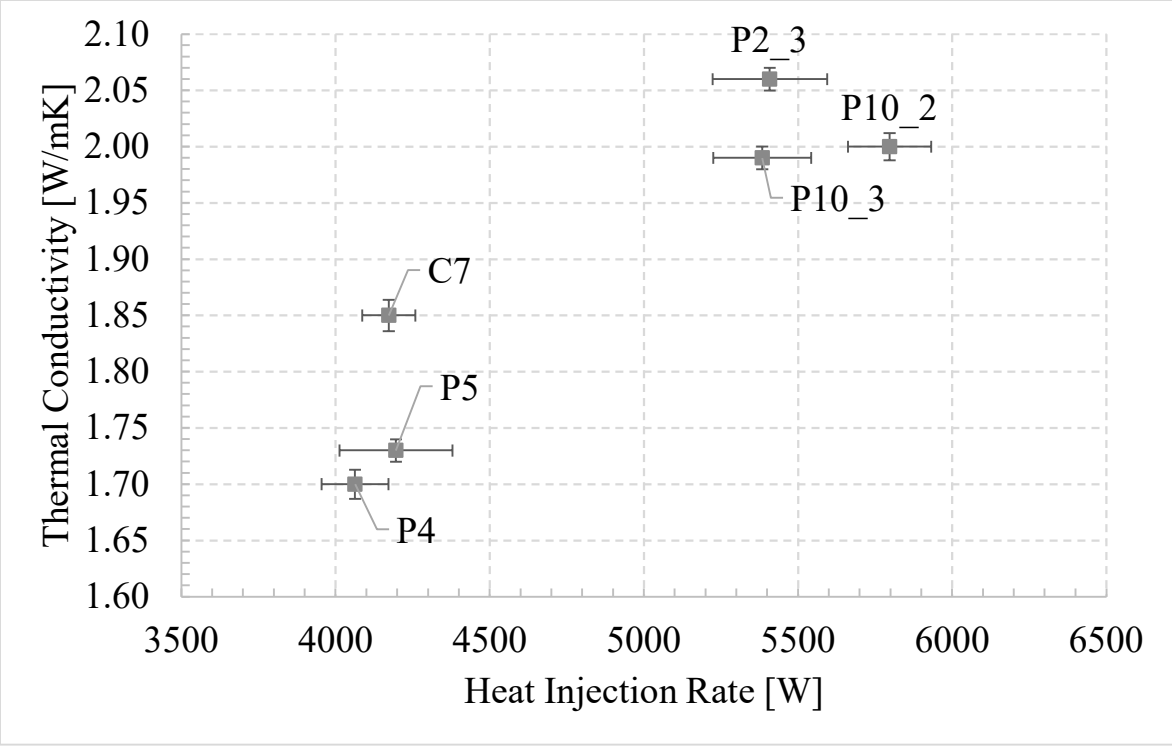

Figure 5.3 - Heat Injection Rate of TRT versus the ILS Thermal Conductivity

Test P10, P2, P2_2, and P2_4 are ignored because the thermal conductivity did not reach stability. There appears to be a positive linear relationship between thermal conductivity and the heat injection rate. P10_3, P10_2, and P2_3 have the same horizontal pipe length and P4 and P5 have the same horizontal pipe length, the influence of the horizontal pipe length will be discussed later in this chapter. Another parameter to consider is the spacing between the individual boreholes of the borehole string. Different borehole spacing with the same heat injection rate can affect the heat transfer because of the thermal interference. The spacing and heat injection rates are both fundamental parameters when it comes to the thermal interaction of boreholes of a string.

The groundwater that exists around the borehole string is also another parameter to consider. The boreholes tested all have a thermally conductive grout as the filling material. This

means that if there were any natural convection around the borehole, it would be due to existing groundwater. When the heat is injected into the borehole, the water surrounding the heat exchanger is warmed up, causing a buoyancy force that would cause the heated water to rise to create a natural convection current. This moving water would then cause an artificially high thermal conductivity because of the rate of temperature response. When evaluating groundwater filled boreholes with different heat injection rates, Gustafsson et al. [31] found that the thermal conductivity increases with increasing heat injection rates, however when evaluating solid bedrock boreholes, the thermal conductivity was not affected. This, therefore, brings forth the possibility that there is naturally occurring groundwater at some locations within the tested borehole field, which affects the effective thermal conductivity.

The answer to whether or not groundwater flow exists is inconclusive from the results in this thesis and would require more investigation. The final parameter that could cause the variation between the different borehole strings is their location within the field. As mentioned earlier, the strings are all located in the same field, but some are closer to an existing heated basement next to the borehole field. The depth of the heated basement is assumed to be a maximum of 15ft [4.57m]. The heated basement effect is assumed to be accounted for with the average temperature of the soil. The time between the borehole field construction and when the temperature sensors were installed allowed the soil temperature to settle. This methodology accounts for the heated basement in the initial temperature.

Another important factor of the heat injection rate is stability throughout the entire test. As discussed previously, Kavanaugh [71] states that the electrical power peaks should be less than ±10% of the average electrical power. The standard deviation of supplied electrical power should be less than ±1.5% of the average.

Table 5.4 - Power Stability Results of Each Test

	$\left(\frac{Electrical\ Peak}{Average\ Power} - 1\right) \times 100\%$	$\frac{Standard\ Deviation}{Average\ Power} \times 100\%$
P5	3.64	1.48
P4	3.80	1.61
C7	4.13	1.51
P10	3.66	1.14
P10_2	3.25	1.25
P10_3	2.89	1.37
P2	3.85	1.27
P2_2	3.58	1.37
P2_3	3.82	1.29
P2_4	4.36	2.08

Table 5.4 displays the final results from the stability check for each test to show the power stability of each test. It can be seen that tests P4, C7, and P2_4 all have a standard deviation of supplied electrical power that is greater than ±1.5% of the average. Test C7 sits at 1.51% over, and P4 sits at 1.61%, which are both very close to being within Kavanaugh's guidelines. All tests are within the guidelines for the electrical power peak being within ±10% of the average electrical power.

5.1.4 The Effect of Groundwater flow

Groundwater flow can give the results of a thermal response test a falsely increased thermal conductivity due to buoyancy effects. Gustaffson and Gehlin [81] mentioned using a least-squared approximation to determine whether or not groundwater flow influences the thermal conductivity values found. This method is described by Witte et al. [97], where if the estimated thermal conductivity does not change significantly with time, the effects of groundwater flow are negligible. This methodology was displayed in the section 'The Effect of Duration of Test' as the thermal conductivity was plotted as time marches forward. Comparing the results from the section 'The Effect of Heat Injection Rate,' it can be seen that some of the tests do not reach stability. The tests conducted by Witte et al. did not reach full stability, as the thermal conductivity kept rising as more data was added [97]. The stability criterion was not explicitly stated for this particular experiment. Witte attributed this to the existence of groundwater on the grout-filled boreholes. To elaborate further on this, the three most 'unsteady' tests are plotted in Figure 5.4.

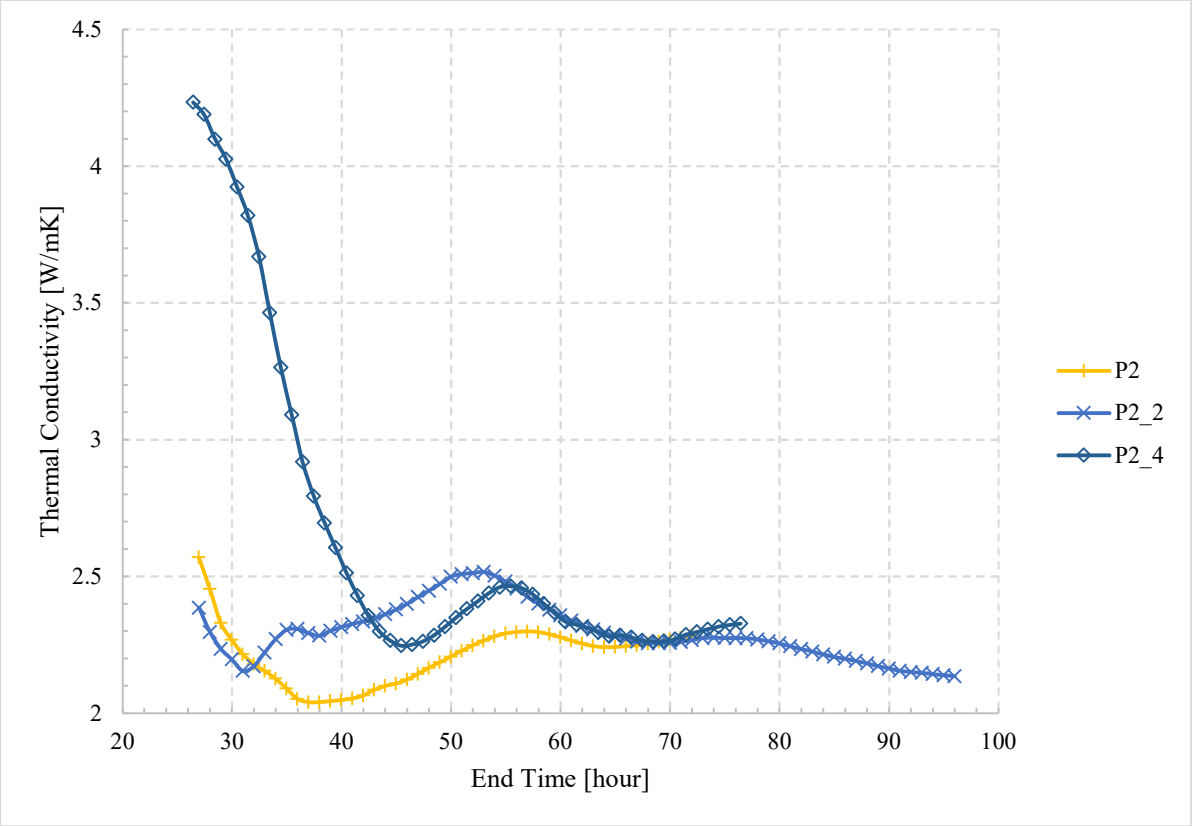

Figure 5.4 - Stability of 3 TRTs

It has already been discussed previously that of the above tests, test P2_4 failed one power stability criteria. The electrical power supply affects the thermal heat injection rate and can cause variability in effective thermal conductivity. The difference between P2 and P2_2 and the rest of the tests conducted is the time of year that the tests were done. The possibility of groundwater flow needs to be elaborated on further, with more research going into groundwater and precipitation on groundwater flow. Further research into this is not within the scope of this thesis.

5.1.5 The Effect of the Horizontal Portion of the Borehole String

The inverse relationship between the effective thermal conductivity and the total length of the borehole (Equation 5) becomes significant when considering the length of the horizontal

portion in the borehole's total length. This can be seen in Table 5.5, as each effective thermal conductivity value decreases when the appropriate horizontal length increases the length. Tests that did not reach convergence of the thermal conductivity are not shown in this table. The results forth the question of whether the horizontal portion is necessary for the analysis.

Table 5.5 - Effect of Horizontal Length on Effective Thermal Conductivity

Test	Horizontal Length [m]	Effective Length [m]	Infinite Line Source Thermal Conductivity Including Horizontal Length [W/mK]	Infinite Line Source Thermal Conductivity Excluding Horizontal Length [W/mK]
P5	4.6	77.8	1.6	1.7
P4	4.6	77.8	1.6	1.7
C7	8.4	81.6	1.7	1.9
P10_2	13.0	86.2	1.7	2.0
P10_3	13.0	86.2	1.7	2.0
P2_3	13.0	86.2	1.8	2.1

The heat transfer between the two legs of the horizontal portion is not the same as the borehole heat exchangers' two legs. Using the ILS is not the most accurate method to evaluate the horizontal runs. To adequately address this physical parameter, a more in-depth evaluation of the experimental data is considered. This is done using a parametric estimation technique with TRNSYS and will be discussed in detail in the following section.

5.2 Parametric Estimation Method

The irregularities in the power supply and the horizontal length can be accounted for in determining the thermal conductivity using parametric estimation. As mentioned, TRNSYS is used. The soil's thermal conductivity is assumed, and the step-wise inlet temperature and flow

rate are used as the inputs. The response of the borehole string is evaluated, and the thermal conductivity value changed accordingly. This was done for all borehole strings. The horizontal portion of the borehole strings was included for this part of the analysis. The properties of the soil surrounding the heat exchangers are $\rho = 1600$ kg/m^3 and $c_p = 1.579$ kJ/kg K, and the properties of the circulating water are $\rho = 1000$ kg/m^3 and $c_p = 4.18$ kJ/kg K.

5.2.1 Single Borehole TRT Validation

Data from a single borehole thermal response test was used to validate the TRNSYS library component for boreholes (Type 957a). Beier et al. [98] provide a reference data set that offers the supply temperature, return temperature, mass flow rate, heat balance, and power balance from a thermal response test performed on a single borehole with a depth of 18.3m. The paper's test parameters included the borehole dimensions, filling material, grout thermal conductivity, pipe thermal conductivity, and the thermal conductivity of the soil surrounding the borehole. The soil thermal conductivity from four different methods was given, including the line source method, parametric estimation, probe measurement, and the analytical composite model [99]. The borehole was made of a thin aluminum pipe and the U-Tube was a HDPE material. The average mass flow rate during the test was 0.197 L/s and the average heat injected by the electric heater was found to be 1056 W.

Table 5.6 - Parameters of Validation Case for TRNSYS Type 957a of Beier et al. [98]

Soil Thermal Conductivity [W/mK]	2.82 (probe measurement) 2.91 (Line source) 2.94 (Analytical composite)

	2.84 (parametric estimation)
Grout Thermal Conductivity [W/mK]	0.73
Borehole Depth [m]	18.3
Borehole Diameter [cm]	12.6
Borehole Wall Thermal Conductivity [W/mK]	0.39
U-tube Type [m]	SDR 11 (1 in.)
Volumetric Flow Rate (Average) [L/s]	0.197
Heat Input Rate (Average) [W]	1056

The parameters listed in Table 5.6, including the soil thermal conductivity from the probe measurement, were used as the input to the TRNSYS model for validation.

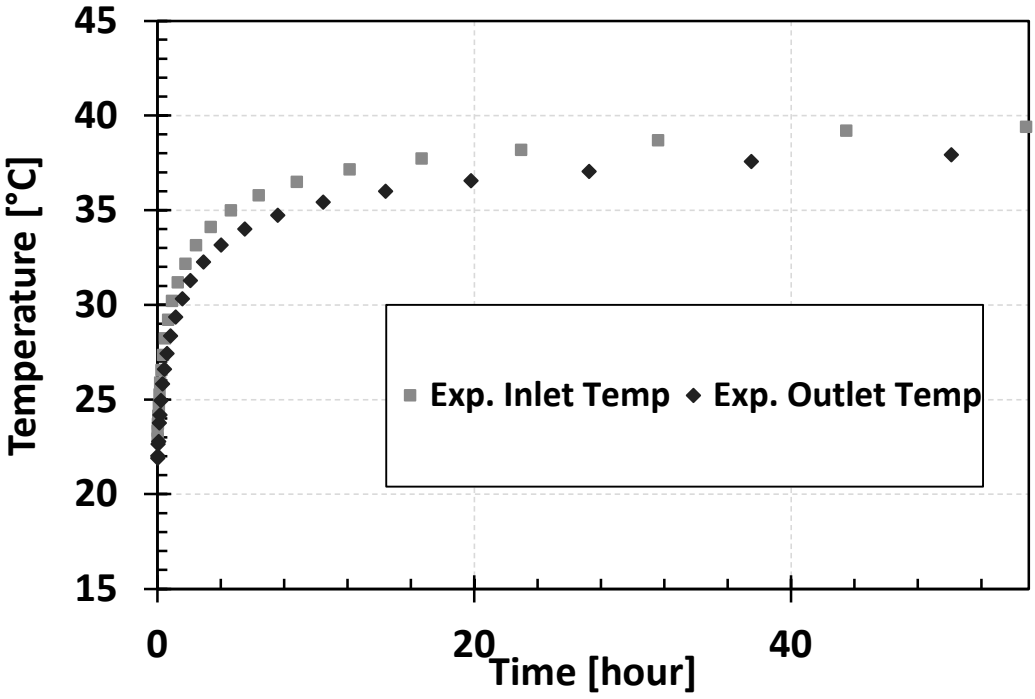

Figure 5.5 - Experimental Temperatures based on Beier et al. [98]

The data obtained from Beier's paper is shown as the 'Experimental' temperatures in Figure 5.5 [98]. The same technique was used to obtain a mass flow rate at each time step, shown in Figure 5.6.

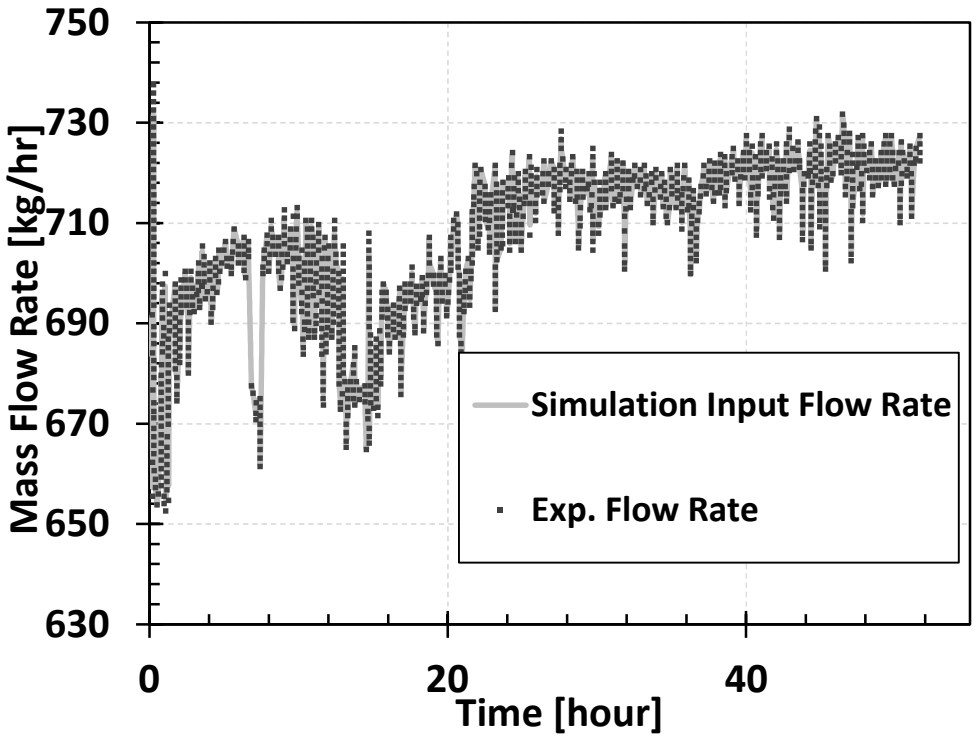

Figure 5.6 - Mass Flow Rate of Reference Data Set for Validation

The inlet temperature and the mass flow rate were used as the inputs, and the outlet temperature was obtained from the model of a single borehole heat exchanger. The thermal conductivity of the sand was set to 2.82 W/mK as per the line source findings from Beier et al. shown in Table 5.6. A range was used for the initial temperature of the borehole and surrounding sand, as this information was not given in the paper. Beier et al.'s experimental apparatus was set in a room, the initial temperature of this TRT would be significantly higher than that of an in-ground TRT.

The average temperature of the TRNSYS simulation was plotted, and the Line Source model was used to find the effective simulation thermal conductivity. The simulation inlet temperature data points are from the experimental data and have been interpolated to have data at

every one-minute interval for the TRNSYS simulation. The outlet and inlet temperature of the simulation is shown in Figure 5.7.

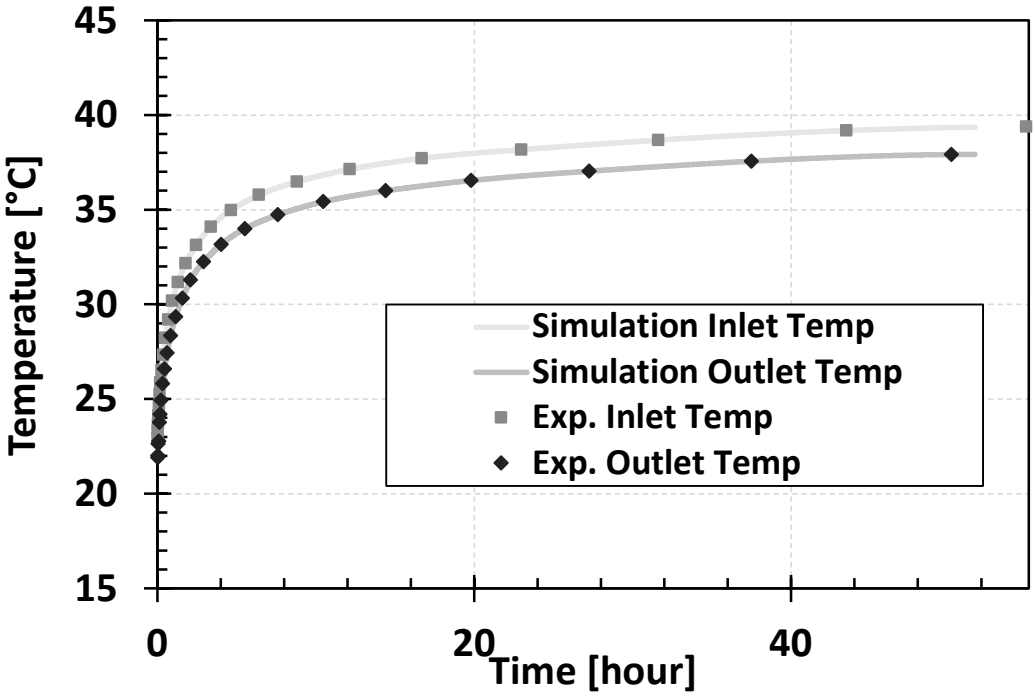

Figure 5.7- Simulation temperature

The root mean square error (RMSE) was also calculated for the simulation and experimental outlet temperatures. This method has been previously used by Gordon et al. [17] to compare different evaluation methods. The results should be that the line source model's output thermal conductivity is equal to 2.82 W/mK input. The RMSE should also be limited by the outlet temperature sensor error (0.1 °C). As mentioned above, the initial temperature of the soil was not disclosed in the paper. Therefore, this parameter was varied in the simulations to see the effect on the RMSE and LS thermal conductivity. The LS thermal conductivity was calculated by using the simulation inlet and outlet temperature and applying the ILS model.

Table 5.7 - Results from TRNSYS Type 957a Validation

Initial Temperature [°C]	RMSE of Outlet Temperature	LS Thermal Conductivity [W/mK]	Average Heat Injected [W]
16	0.16	3.31	1220
17	**0.13**	3.17	1167
18	0.14	3.04	1113
19	0.18	**2.9**	1056
20	0.23	**2.76**	1006

Results from varied initial temperature are shown in Table 5.7. Column three of Table 5.7 shows the results of applying the LS method to the simulation output temperatures. For each of the simulations the input sand thermal conductivity was held at 2082 W/mK. The minimized RMSE at a temperature of 17°C gives an LS thermal conductivity that is overestimated compared to Beier et al's results of 2.82 W/mK when applying the LS method. The average heat injected in Table 5.7 is calculated using the simulation outlet temperature, inlet temperature, and mass flow rate. It should be noted that the average heat injection is closest to the average heat injected from the experimental data of 1164.4 W when the LS thermal conductivity is 3.17 W/mK. The LS thermal conductivity closest to the simulation input thermal conductivity occurs when the initial temperature is between 19 and 20°C. The average heat injection rate at this temperature is significantly less than the experimental heat injection rate.

The conclusions drawn from the validation case are that the initial soil temperature significantly affects the output temperature response. Since the TRNSYS model Type 957a is typically used for thermally interacting boreholes of a BTES field, perhaps it does not correctly calculate the thermal resistance of a single borehole subjected to a short heat injection period. Further research into how the TRNSYS model models one borehole is suggested.

The TRTs conducted in this thesis consist of three boreholes connected in series and a horizontal portion leading to the borehole heat exchangers' inlet and outlet. Due to the individual proximity, heat injection rates, and the test duration, thermal interaction amongst the boreholes is expected to occur. This, therefore, allows the assumption that TRNSYS will be able to model the thermal response test of a borehole string correctly due to the assumed ability that TRNSYS can account for thermal interaction correctly.

5.2.2 Borehole String Modelling

The simulations assume a single layer of homogenous soil characteristics. It also assumes that groundwater flow through the soil area of the borehole heat exchangers does not exist. The groundwater flow in the experimental field is unknown. This attributes to the error that exists between the thermal conductivity values found from the infinite line source and parametric estimation.

5.2.2.1 Grid Sensitivity

Before simulating the different thermal response tests, a grid sensitivity analysis was performed to ensure the results are not dependent on the spatial discretization of the domain. A constant 5 kW heat input was used within the TRNSYS platform. No horizontal pipe connections were used in this portion.

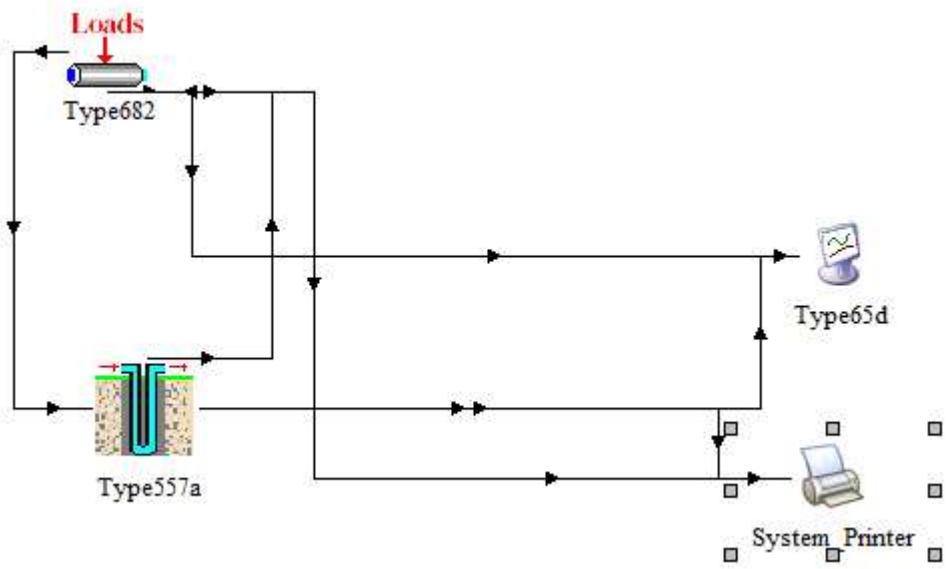

Figure 5.8 - Constant Heat Injection Model

The constant heat injection input is used to mimic a very stable thermal response test. For the grid sensitivity testing, the number of radial regions and vertical regions is tested. The volume of soil for all the simulations was held at 57,046m^3. The volume is calculated based on Equation (7) (recall section 4.2.2) with a string of three boreholes that reach a depth of 24.4 meters and spacing of 30 meters that ensure there will be no thermal interaction. The restrictions set by TRNSYS are as follows: number of radial regions: less than or equal to the number of boreholes connected in series, vertical regions: number of vertical sub-regions multiplied by the number of radial regions must be less than 121.

Table 5.8 - Grid Sensitivity Results

Volume [m^3]	57045						
Number of Radial Regions	1	1	1	3	6	60	119
Number of Vertical Regions	1	3	119	60	60	3	1
LS Thermal Conductivity [10-72hrs]	2.22	2.23	2.24	2.24	2.24	2.24	2.23

Table 5.8 shows the various number of radial and vertical regions tested. In some cases, the product value exceeds the maximum value of 121 to observe the effect. In those cases, the simulations end up with the same output, suggesting that the program does not allow for the maximum value of 121 to be exceeded. Three radial regions and 60 vertical regions are sufficient for the thermal conductivity to remain stable with a changing number of regions. Three radial regions and 60 vertical regions are used for all the following simulations unless stated otherwise.

5.2.2.2 The Impact of the Borehole String Spacing

When considering geostorage or geo-exchange systems, it is crucial to consider the spacing between the individual boreholes of a borehole string. The thermal interaction that may occur during a thermal response test depends on the test duration and the spacing. To discuss the effect of the spacing on the TRT, 5 sample volumes were used in TRNSYS to see the effect on the outlet temperature. The average temperature was then calculated so that the slope moving forward with time could be evaluated, and the line source effective thermal conductivity. The

spacing and corresponding volumes are displayed in Table 5.9. Volumes B, C, and D are the same volumes of the borehole strings discussed throughout this thesis. Volume A corresponds to a closely packed borehole string, with a spacing of 1 meter, and volume E represents an arbitrary spacing within the range of what could occur in a geo-exchange field of 4.6m (13ft). The volume of soil is calculated using the following equation:

$$Volume = \pi * Number\ of\ Boreholes * Borehole\ Depth * (Spacing * 0.525)^2 \quad (7)$$

Table 5.9 - Spacing and Volumes of TRNSYS Simulations with Number of Boreholes, Borehole Depth, and Borehole Properties held Constant

Simulation	Borehole Spacing [m]	String Soil Volume [m^3]
A	1	63
B	1.52	146
C	1.73	190
D	3.38	724
E	4.57	1325
Base Case	17.76	20 000

Using TRNSYS, the experimental inlet conditions are extended to provide data that would resemble a TRT with a duration of approximately one month. All cases ignore the natural temperature gradient that would exist axially in the soils surrounding the borehole. A logarithmic fit was placed over the data obtained from test P10 to reduce the simulation time. The simulation time step was then set to one hour using the equation of the logarithmic fit. The properties of soil for all the tests were: k = 1.5 W/m.K, C_p= 2526 kJ/m^3.K. The length of the horizontal portion was held constant at 1 meter to minimize the horizontal heat loss effect on the outlet temperature. This is not consistent with the large borehole spacings; however it could be achieved with a highly insulated horizontal pipe.

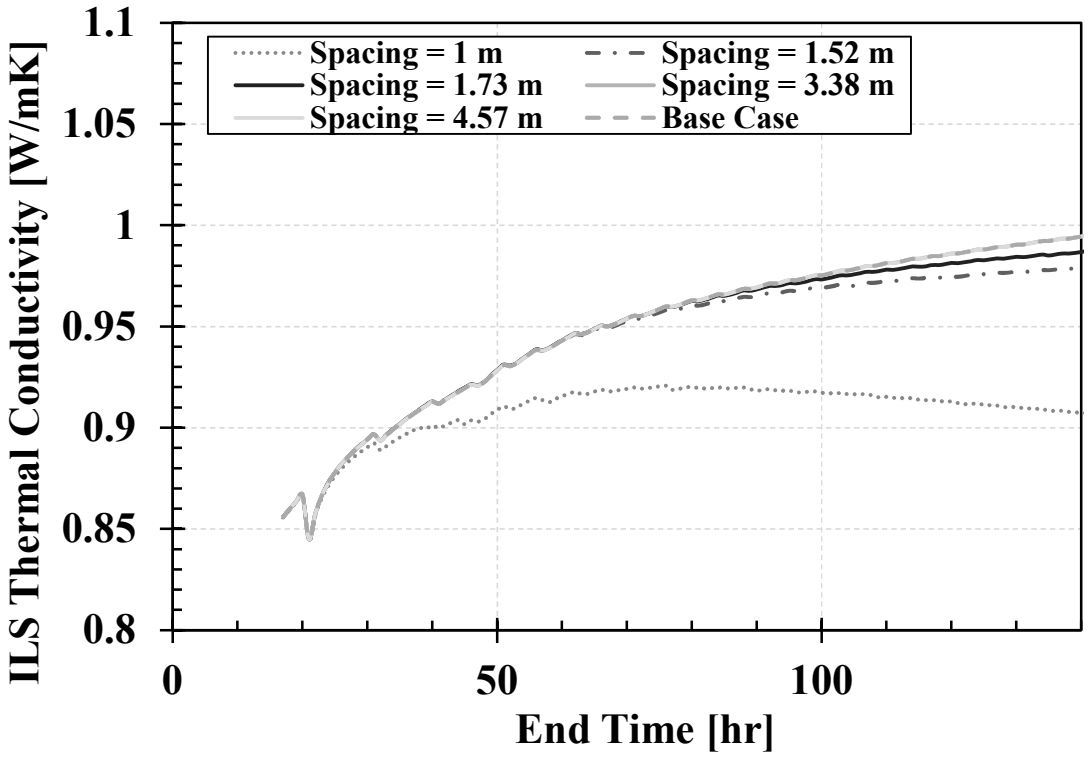

Figure 5.9 – Effective Thermal Conductivity Based on ILS versus Duration of Test and Spacing of Boreholes

Once the outlet temperature was obtained, the average fluid temperature is calculated. The slope of the average temperature vs. logarithmic time is then determined, holding the analysis start time as 16 hours after the heating period started and stepping forward with time. This is done to see the effect on the slope as the duration of the test is extended. The results of this analysis can be seen in Figure 5.9. Here it can be seen that the proximity of the other boreholes has a substantial effect on the slope of the average temperature and hence the thermal conductivity. The base case scenario shows where the thermal interaction would be obsolete, as the spacing is substantial. In all cases, the thermal conductivity is much lower than the TRNSYS input soil thermal conductivity of 1.5 W/mK.

The effective thermal conductivity based on the ILS is shown at different end times, up to the total one-month test (650 hours). The results are plotted in Figure 5.10 below. It can be seen that even after the one-month duration, the effective thermal conductivity is still greatly underestimated by TRNSYS.

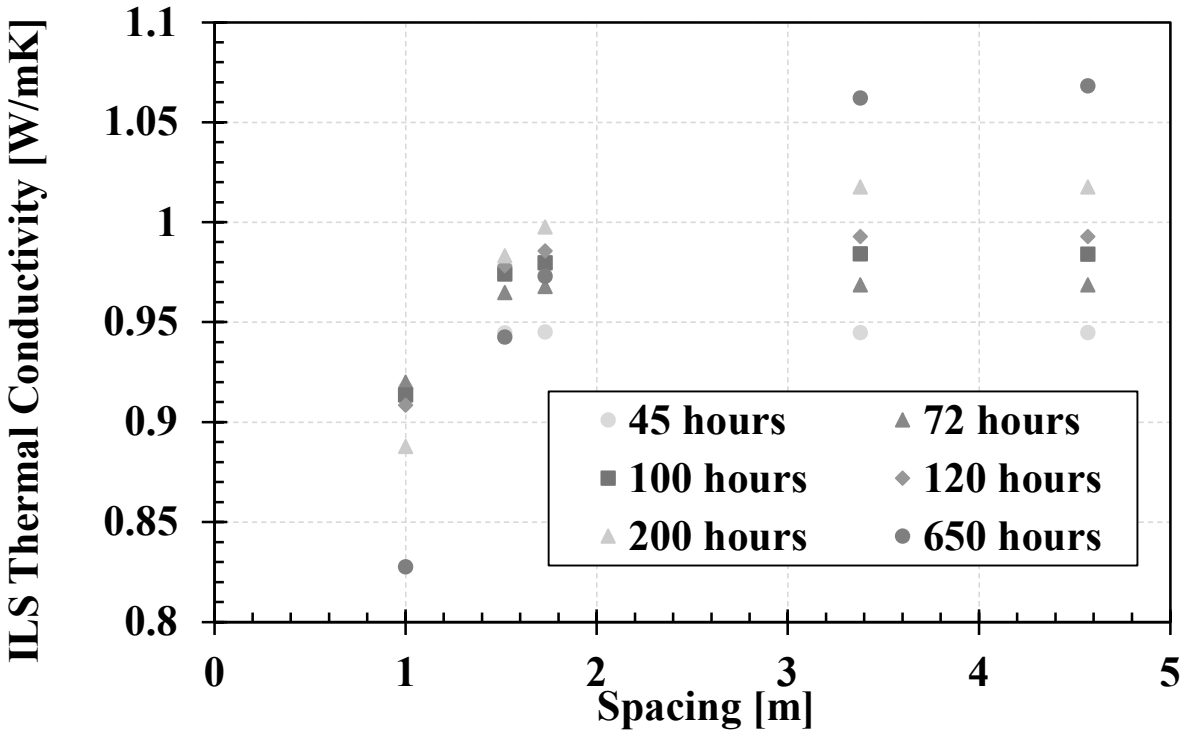

Figure 5.10 – ILS Effective Thermal Conductivity Versus Spacing at Different Total Durations

The general trend of the data shows that TRNSYS may be able to account for thermal interaction, however the approximation is not correct. This is seen as the closer spaced borehole strings (1 m) show a lower effective thermal conductivity. This is expected, as if the boreholes of the string are interacting, it is expected that the temperature response would increase faster, causing the ILS effective thermal conductivity to be decreased. Further investigation needs to be done to determine a relationship between the spacing of the boreholes in the string and the

maximum duration of the test before interaction, and how TRNSYS accounts for the thermal interaction. The time before interaction occurs is also dependent on the soil's initial temperature and the thermal properties of the soil.

Typically, a minimum duration of the thermal response test is recommended [19], [32], [85], [86] to limit the length of the test to minimize cost. As mentioned earlier, guidelines suggest that the thermal response tests should last between 48-72 hours [74]; however, extending the test is sometimes required to allow the thermal conductivity to converge [85]. Results from further investigation regarding the spacing and interaction time would be beneficial to determine the upper limit to the duration of the TRT before interaction and allow time for the thermal conductivity to converge.

5.2.2.3 Series Vs. String

TRNSYS is designed to give an approximation of how a BTES field will operate. This allows for the thermal interaction between adjacent boreholes to presumably be correctly accounted for when simulating the TRT data. The following section explains the methodology of choosing the simulation parameters. The typical thermal response test is applied to a single borehole heat exchanger, giving the effective thermal conductivity of the surrounding soil. Having three boreholes connected in series is believed to increase the TRT's temperature response rate, decreasing the effective thermal conductivity based on the inverse relationship between the slope of the log-temperature response curve and the thermal conductivity.

5.2.2.4 Design of Experiments

The first step to setting up simulation was determining the design of experiments (DOE) for the TRTs. A three-factor, three-level full-factor analysis was constructed for each TRT. The three factors included: the length of the horizontal portion, the initial temperature of the soil

surrounding the borehole string, and the thermal conductivity of the soil. The specific levels of each TRT are shown in Table 5.10.

The initial temperatures displayed in Table 5.10 that have been bolded show the initial experimental temperature for each TRT. For each parameter, the three levels consist of a LOW, MEDIUM, and HIGH value. This referencing will be used later. The length of the horizontal portion is not known with full accuracy. The approximated horizontal length is designated as the MEDIUM value, and a ±10% error bracket is used for the HIGH and LOW values to compensate for this. The analysis includes comparing the experimental outlet temperature to the simulation outlet temperature by means of the lowest RMSE.

The following sections investigate the individual factors that help determine the thermal response tests' outcome from the parameter estimation.

Table 5.10 - DOE parameters for TRTs

	Test	P5	P4	C7	P10	P10_2	P10_3	P2	P2_2	P2_3	P2_4
Levels of Parameters	Length of Horizontal (L) [m]	4.14	4.14	7.56	11.7	11.7	11.7	11.7	11.7	11.7	11.7
		4.6	4.6	8.4	13	13	13	13	13	13	13
		5.06	5.06	9.24	14.3	14.3	14.3	14.3	14.3	14.3	14.3
	Initial Soil Temperature [°C]	15.8	15.9	15.8	15.9	15.9	15.9	15	15.8	15	15
		16.8	**16.9**	**16.8**	**16.4**	**16.9**	**17.2**	**17**	**17.8**	17	17
		17.3	17.9	17.8	17.8	17.9	17.9	17.8	18.8	**18.8**	**18.4**
	Thermal Conductivity of Soil (k) [W/mK]	1.1	1.1	1.1	1.1	1.1	1.1	1.1	1.1	1.1	1.1
		1.3	1.3	1.3	1.3	1.3	1.3	1.3	1.3	1.3	1.3
		1.5	1.5	1.5	1.5	1.5	1.5	1.5	1.5	1.5	1.5

5.2.2.5 The Effect of the Initial Temperature of the Borehole String

The experimental inlet and outlet temperature and the three simulated results for P5 are shown in Figure 5.11. The three simulation runs chosen hold all parameters constant (k = 1.1 W/mK, L = 4.6 m), except for the initial temperature. Figure 5.11 shows that the simulations provided an outlet temperature with a similar logarithmic relationship for each of the three cases. The difference in the three simulation results plotted is the initial temperature of the soil and the initial temperature of the water within the legs of the U-tubes. The initial increased temperature shifts the response curve upwards. The root mean square error (RMSE) was used to evaluate the outlet temperatures.

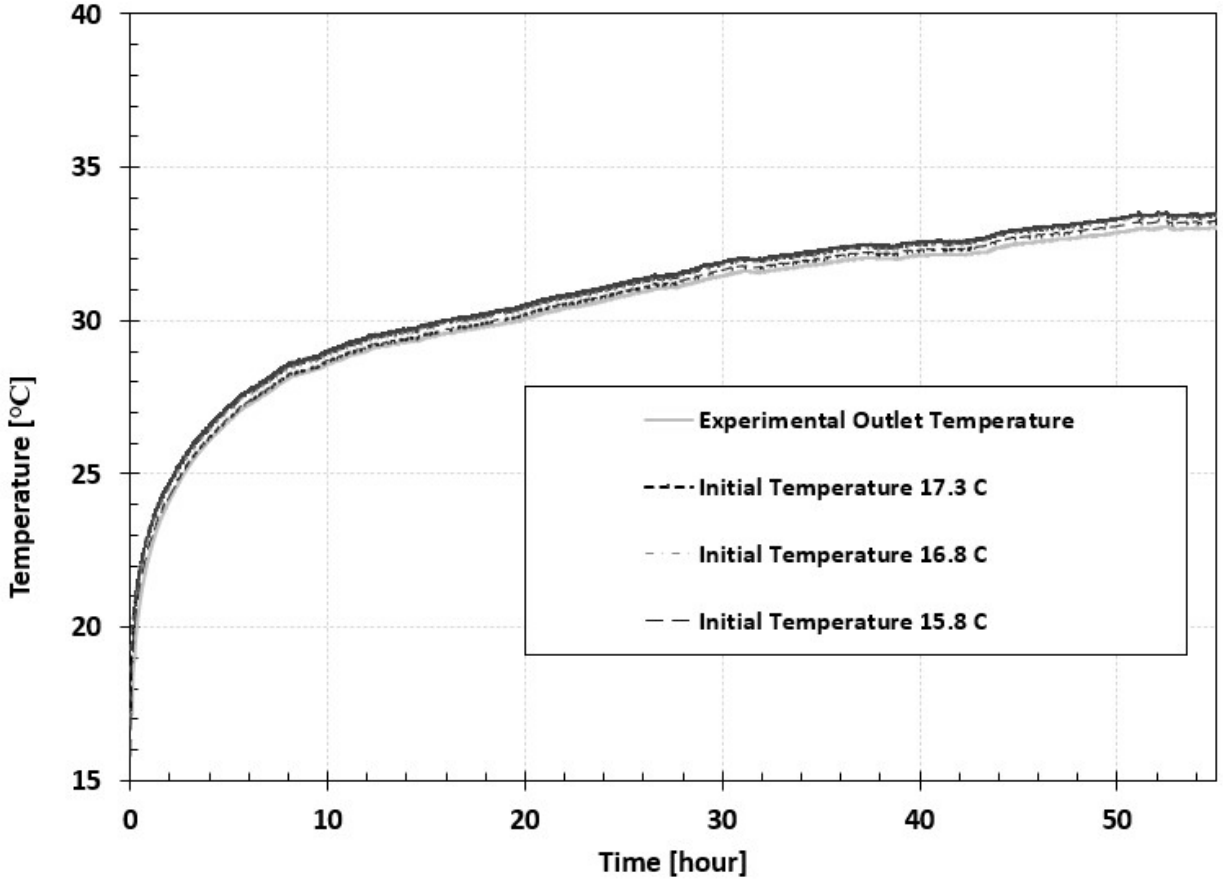

Figure 5.11 – P5 Simulations with Different Initial Temperatures

This method allows for the error from the entire duration of the test to be considered. The residual error between the experimental and simulated outlet temperature is also shown in Figure 5.12. The error is most significant at the beginning when the effect of the starting temperature in the pipes is most influential.

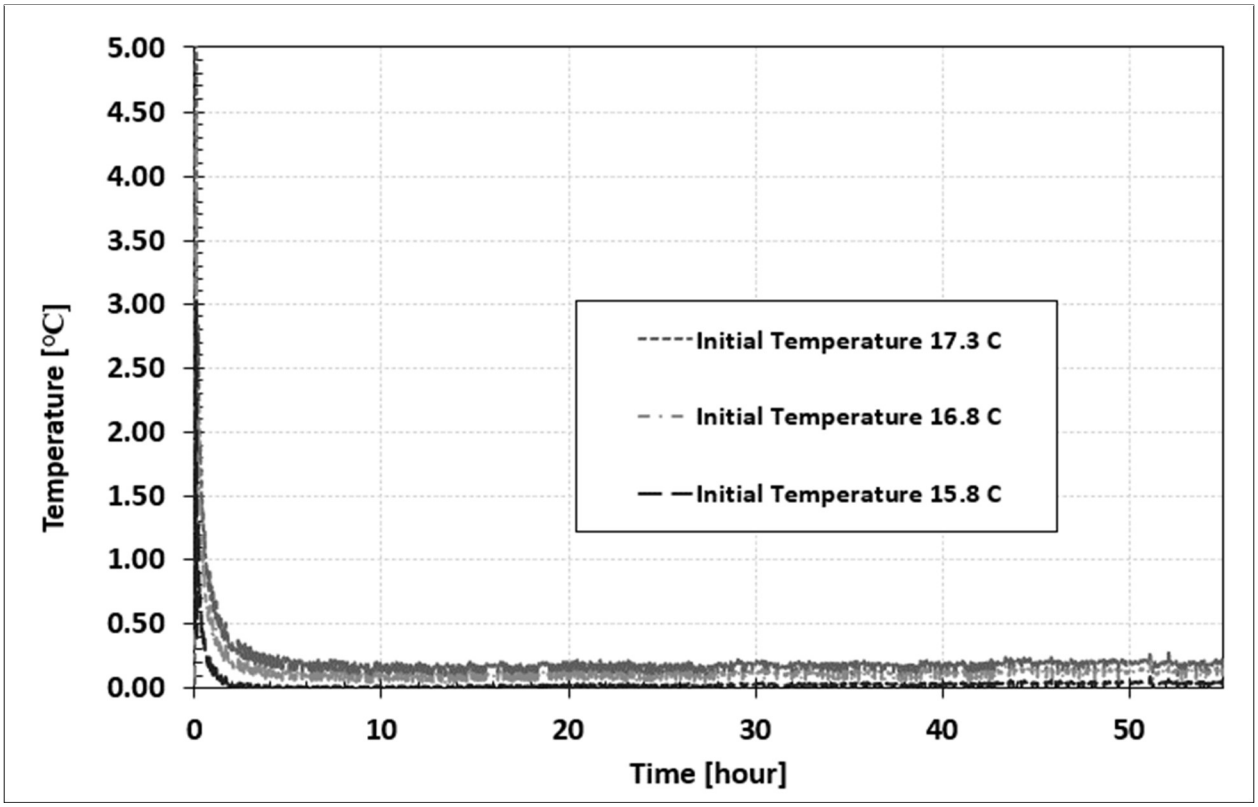

Figure 5.12 - Residual Error Plot of 3 sample Simulations for P5

When plotting the results from the DOE for each TRT, the minimum RMSE of 0.1 is used as the threshold value. This value is related to the experimental error from the temperature readings. For demonstration purposes, additional simulations were conducted for TRT P5 with higher thermal conductivity values closer to the value found using the ILS. This was to show the minimization of the RMSE as a function of the thermal conductivity.

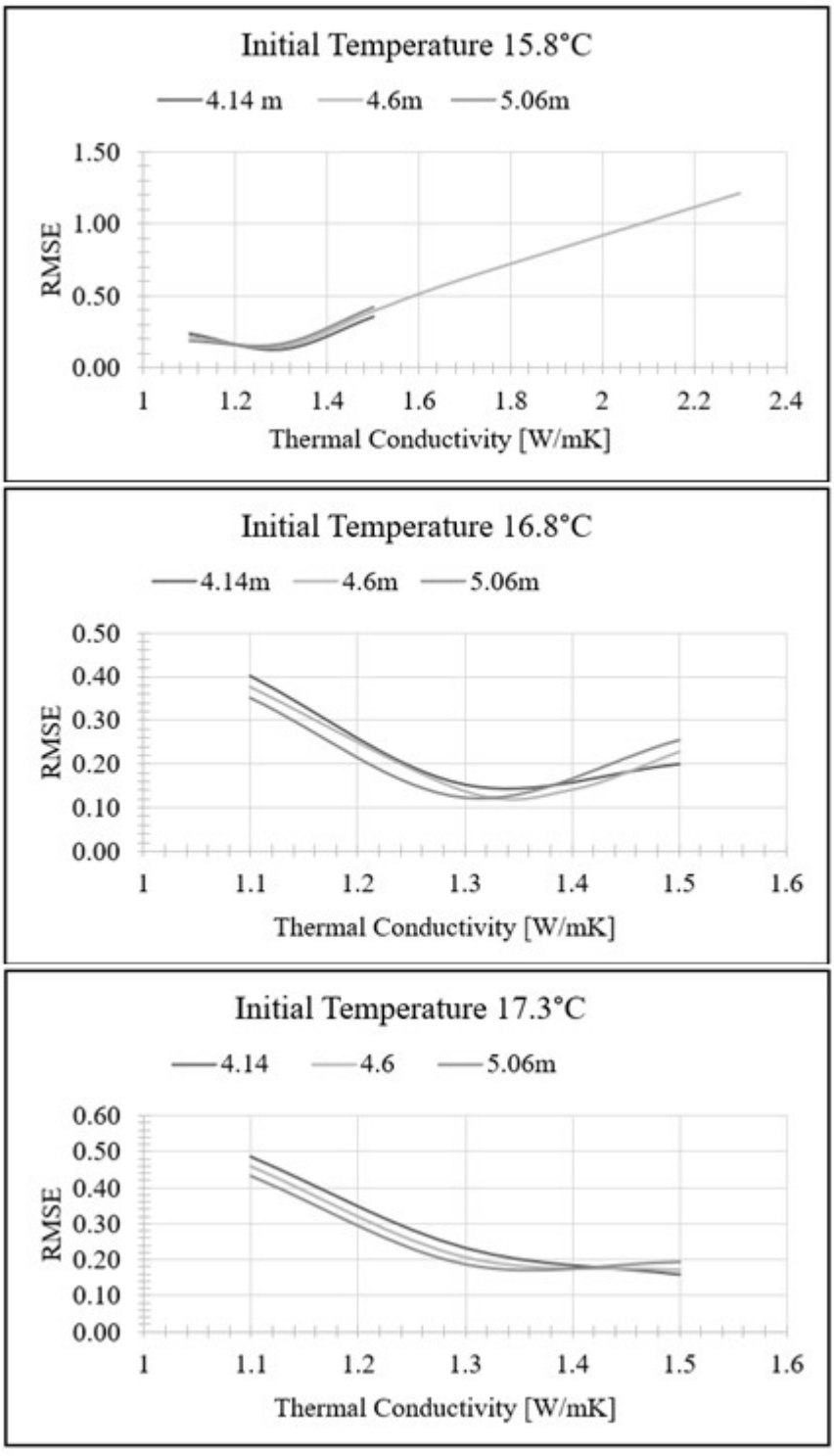

Figure 5.13 – P5 Simulation RMSE Results

The above three graphs of Figure 5.13 individually display the results when the initial temperature is held constant, and the horizontal length (L) and thermal conductivity are varied.

From these graphs, when the initial experimental temperature is used (Figure 5.13 bottom), the smallest RMSE occurs when k = 1.5 W/mK and horizontal length is 4.14 meters. The RMSE for these particular parameters is equal to 0.16. When the horizontal length is 4.6 meters, the RMSE becomes 0.17 with a 1.5 W/mK thermal conductivity. Table 5.11 shows the average thermal conductivity value when the minimum RMSEs are calculated from each different horizontal length, highlighting the initial temperature effects. For example, in Figure 5.13 (middle), the minimum RMSE for the horizontal lengths of 4.14, 4.6, and 5.06 m are 0.15, 0.14, and 0.12, respectively. The corresponding thermal conductivity values are 1.3, 1.3, and 1.3 W/mK. This results in an average value of 1.3 W/mK.

Table 5.11 - Average Thermal Conductivity Based on Initial Temperature

	Average Thermal Conductivity [W/mK] at Specified Initial Temperature [°C] (Refer to Table 5.10)		
Initial Temperature Setpoint	Low	Medium	High
P5	1.3	1.3	1.4
P4	1.3	1.4	1.5
C7	1.1	1.2	1.3
P10	1.1	1.1	1.3

P10_2	1.2	1.3	1.4
P10_3	1.1	1.1	1.2
P2	1.2	1.4	1.5
P2_2	1.1	1.3	1.4
P2_3	1.1	1.1	1.3
P2_4	1.1	1.3	1.4

Table 5.11 above shows the variability in the estimated thermal conductivity when the initial temperature is varied. These findings suggest that the predicted conductivity is dependent on the grout temperature, where spatially uniform temperatures are assumed. A simple, average temperature of the borehole depth is insufficient to find an accurate solution so perhaps a spatially non-uniform temperature gradient should be explored in future work. This suggestion will be discussed in more detail in the next chapter.

5.2.2.6 The Effect of the Horizontal Portion of the Borehole String

The horizontal length for each borehole string was displayed in an earlier chapter; however, a ±10% error margin is considered when simulating, seen in Table 5.10. The results from TRT P5 are shown in Figure 5.14.

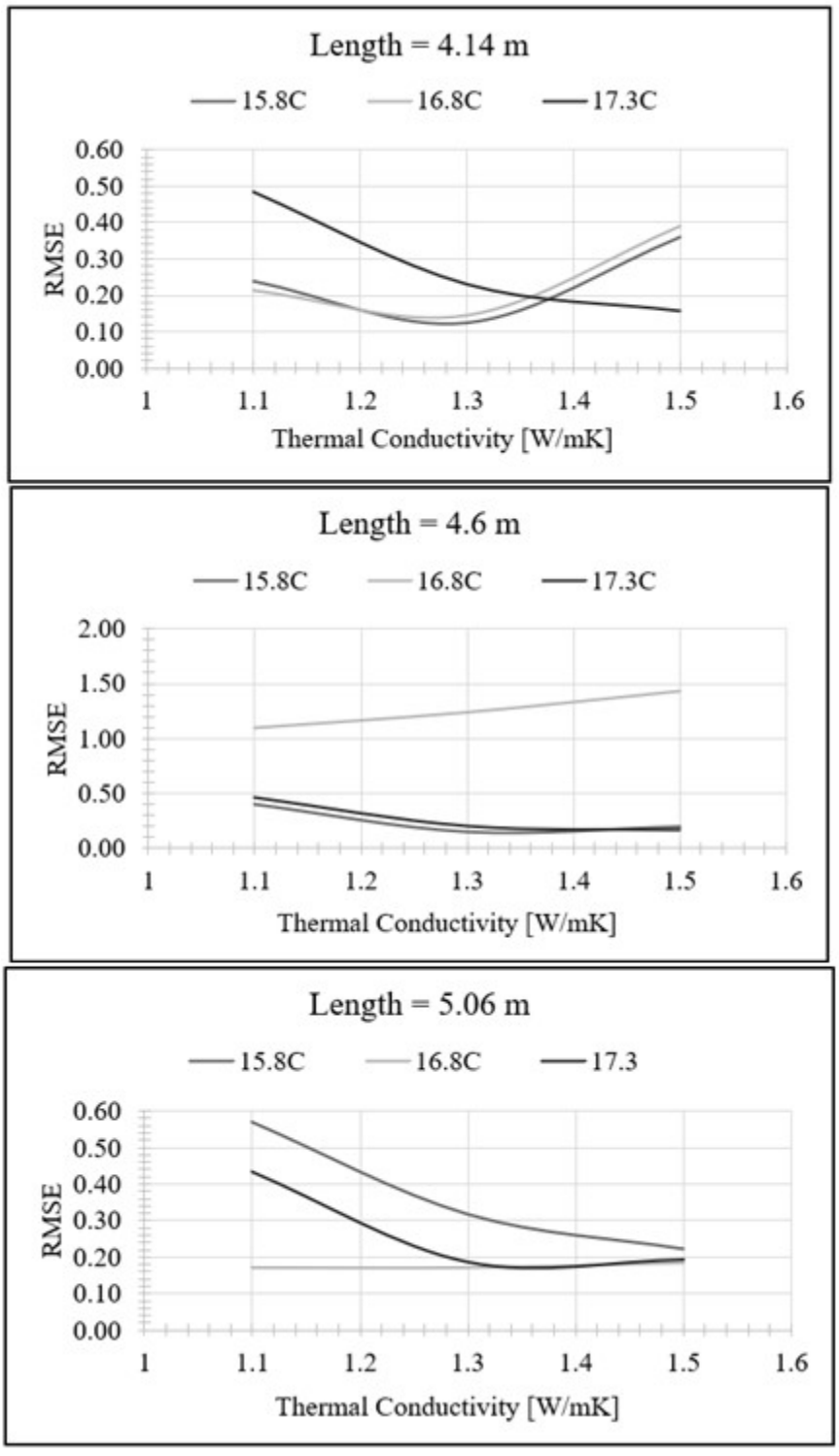

Figure 5.14 - Effect of Horizontal Length on P5

These are the same data points from Figure 5.13 but separated by horizontal lengths to evaluate the effects.

Table 5.12 - Thermal Conductivity at Specific Horizontal Lengths

	Average Thermal Conductivity [W/mK] at Specified Horizontal Length (Refer to Table 5.10)		
Horizontal Length Setpoint	Low	Medium	High
P5	1.4	1.4	1.4
P4	1.4	1.4	1.4
C7	1.2	1.2	1.2
P10	1.2	1.2	1.2
P10_2	1.4	1.3	1.2
P10_3	1.2	1.1	1.1
P2	1.4	1.4	1.3
P2_2	1.3	1.3	1.2
P2_3	1.2	1.2	1.1
P2_4	1.3	1.3	1.2

From Table 5.12, the TRT with the longest horizontal lengths (tests conducted on P2 and P10) have the most significant variability in thermal conductivity values across all three horizontal lengths tested. This shows that the input length of the horizontal portion affects the total heat transfer and must be analyzed in further detail. Another horizontal length to consider is the portion between the individual boreholes of the string. The heat transfer of this portion is not accounted for in the TRNSYS model. The average distance between the boreholes is used when considering the radial thermal interaction but is not considered in the heat carrier fluid flow path. This portion of the model setup is discussed further in the next chapter.

To identify the effects of the horizontal portion on the simulation results, the thermal response tests were simulated in TRNSYS while excluding the horizontal portion that leads to the borehole string inlet and outlet.

Table 5.13 - Thermal Conductivity of TRNSYS Simulations excluding the horizontal portion

Thermal Response Test	TRNSYS [no horizontal] Thermal Conductivity by Minimized RMSE [W/mK]
P5	1.7
P4	1.7
C7	1.7
P10	1.7
P10_2	2
P10_3	1.7
P2	2.3
P2_2	2.2
P2_3	2
P2_4	2.5

The results from simulations excluding the horizontal portion leading to the inlet and outlet of the borehole strings are shown in Table 5.13. The horizontal twin-pipe model was never validated because of the lack of experimental data available. The twin-pipe model, TYPE 951, is recommended to be validated or verified to determine the error associated with using the component in the borehole string model. The next section will compare the line source model

results and all of the TRNSYS simulation configurations. The expected results will be discussed and compared to the actual results, with suggestions and conclusions drawn from the findings.

5.2.2.7 Comparison between the ILS and TRNSYS Effective Thermal Conductivity Values

The final effective thermal conductivity of both the parametric estimation and the infinite line source method is shown in Table 5.14. In this table, the effective thermal conductivity values are chosen based on the lowest average RMSE. The horizontal length and the initial temperature at this lowest RMSE are also displayed.

Table 5.14 - Final Thermal Conductivity value found using ILS and TRNSYS

	Effective Horizontal Length [m]	Average Borehole Spacing [m]	Effective Initial Temperature [°C]	TRNSYS Thermal Conductivity with Horizontal Length Included [W/mK]	Minimum RMS Error [K]	ILS Thermal Conductivity (no Horizontal) [W/mK]	ILS Thermal Conductivity (with Horizontal) [W/mK]
P5	5.06	1.52	16.8	1.3	0.12	1.7	1.6
P4	4.14	1.73	15.9	1.3	0.10	1.7	1.6
C7	9.24	3.38	15.8	1.1	0.11	1.9	1.7
P10	13	1.73	15.9	1.1	0.14	1.7	1.5
P10_2	13	1.73	16.9	1.3	0.18	2.0	1.7
P10_3	13	1.73	17.2	1.1	0.19	2.0	1.7
P2	11.7	1.73	15	1.3	0.16	2.3	1.9
P2_2	11.7	1.73	15.8	1.1	0.11	2.1	1.8
P2_3	11.7	1.73	17	1.1	0.18	2.1	1.8
P2_4	11.7	1.73	17	1.3	0.16	2.3	1.9

The variability in the thermal conductivity found using the ILS with no horizontal is 2.0±0.3 W/mK, ILS accounting for the horizontal is 1.7±0.2 W/mK and when modeling is 1.2±0.1 W/mK. The results in Table 5.14 show that applying the infinite line source overestimates the effective thermal conductivity when compared to the parametric estimation, opposite to the expected trend. The thermal conductivity, while using the parametric estimation, was approximated to only a single decimal point. This was done because the accuracy limits of the thermal conductivity are determined using the experimental data.

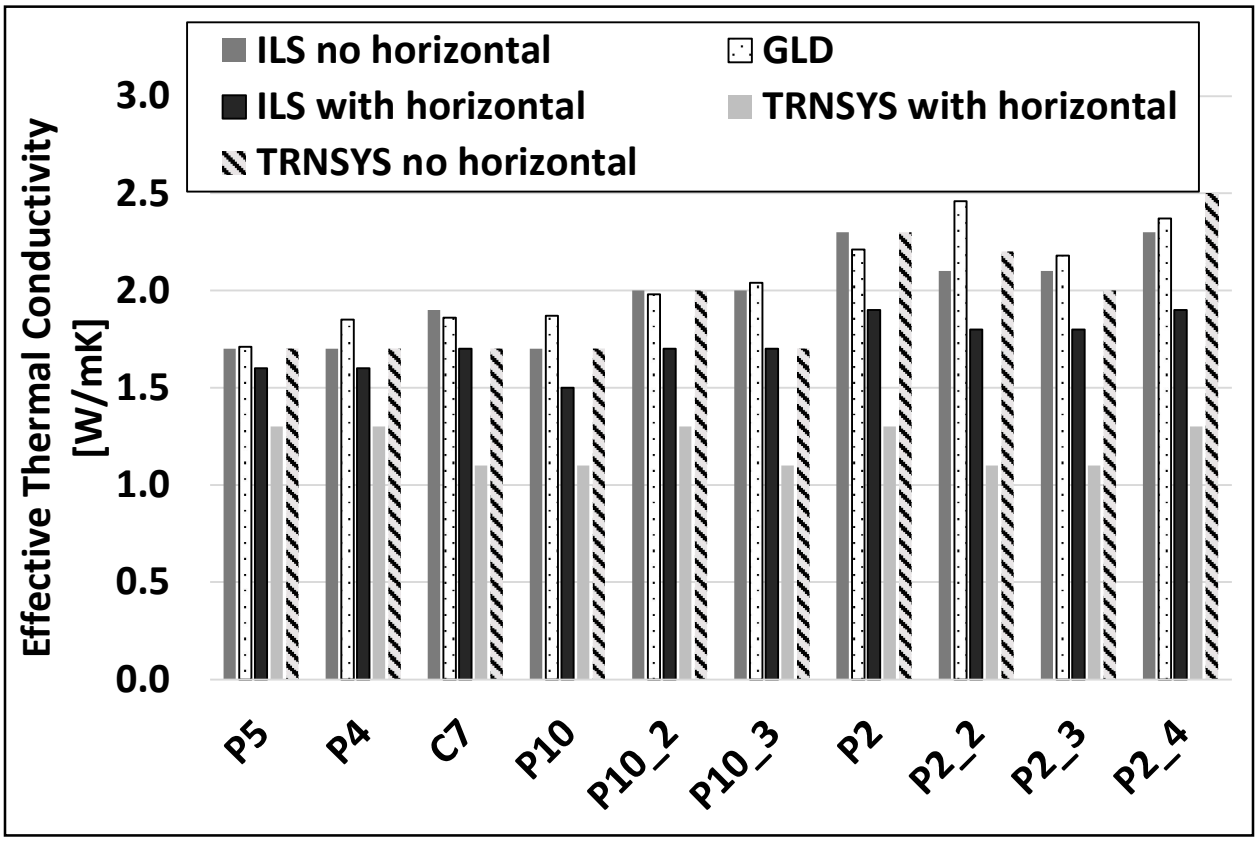

Figure 5.15 - Soil Thermal Conductivity Values of Different Analysis Methods

When comparing the results from the ILS, GLD, and TRNSYS simulations, it can be seen that the ILS without horizontal runs and GLD both provide similar values. The GLD analysis does not include the horizontal length. This verifies that the program code created to find the thermal conductivity correctly implements the ILS since GLD is also based on the ILS

model. The results for test P2_2 show that the GLD and ILS vary by 0.3 W/mK. The reason for this is not explicitly known.

Once the horizontal lengths are included in the ILS thermal conductivity calculation, the thermal conductivity becomes smaller. This is because of the inverse relationship between the total length and the effective thermal conductivity. Figure 5.15 displays the data presented in Table 5.13 and Table 5.14. The analysis methods used that excluded the horizontal portion, the tests C7, P10_3, and P2_3, give a lower effective thermal conductivity using TRNSYS than the ILS. P2_2 and P2_4 give a higher effective thermal conductivity from TRNSYS compared to ILS.

The thermal conductivity found using TRNSYS, including the horizontal length, is so greatly underestimated that the TRNSYS model's reliability is questioned for short-time and few-borehole simulations. It was shown earlier with the validation case that thermal conductivity found using the line source model on the output of a single borehole TRT output does not provide the correct thermal conductivity as the input.

Overall it can be seen that the thermal conductivity value found when applying the infinite line source to a pre-existing borehole string with a horizontal portion is overestimated. This highlights the importance of correctly accounting for the borehole heat exchangers' physical setup subjected to a TRT in the analysis. It is recommended that the horizontal twin-pipe model be validated in order to determine reliability. TRNSYS borehole model Type 957a does not correctly account for the interaction between the boreholes of the strings. The interaction is not correctly accounted for as the spacing between the boreholes is approximated thermal resistance instead of physical spacing. The listed spacing, and the spacing used as the TRNSYS input, is the

average spacing between each of the three boreholes of the string, as TRNSYS does not allow for the individual spacing to be used as an input.

The heat transfer that occurs within the horizontal portion leading to the first borehole of the string is not correctly accounted for in the ILS and, therefore, affects the final thermal conductivity value. This characteristic requires more in-depth heat transfer analysis in order to determine the soil properties properly. This analysis did not account for the horizontal portions between the individual boreholes and would need to be considered.

The comparison between which method is most appropriate to determine the soil's thermal conductivity surrounding a borehole string is inconclusive. It is recommended that the effective thermal conductivity be determined either by standard TRT methods (single borehole), thermal probe method, or independent thermal properties testing. This would allow for a benchmark value that would provide a flawless comparison between the different analysis methods and allow proper conclusions to be drawn.

5.3 Additional Methods

In addition to the work presented above, a TRT test was run by a third-party [100] which was conducted on a single borehole heat exchanger reaching a depth of 182 meters near the location of the borehole strings tested for this thesis. The thermal conductivity value was found to be 2.3 W/mK which is within the range of the values determined when applying the ILS to the borehole strings. When comparing to the thermal conductivity determined by this third-party thermal response tests, the depth of the tested boreholes should be taken into consideration. The maximum depth of the boreholes reached for the borehole strings tested in this thesis was approximately 24 metres. At this depth, the soil consisted of a silty clay loam. The additional third-party [100] TRT provided drilling information which showed that the formation up to a

depth of 47.2m consisted of clay, sand, and gravel followed by shale formation until the final depth of 182 metres. This corresponds to 74% of the borehole length to be surrounded by shale formation. Typical values of the thermal conductivity for shale rock are dependent on the quartz percentage and the water content. The United States Department of the Interior Geological Survey provide data which shows that shale with water in the shale pores can have a thermal conductivity range of 1.48 – 19.35 W/mK [101] depending on solidity (related to water content). The final effective thermal conductivity of 2.3 W/mK is most likely higher then the previously stated 1.7±0.2W/mK due to this shale rock formation.

Laser Flash Technique (LFA) was also used to determine the thermal conductivity of three dry soil samples. The density of the samples was determined by weighing the soil sample 'disks' and measuring the dimensions of the disks. One of the soil sample disks is shown in Figure 5.16 below.

Figure 5.16 - Compressed Soil Sample (1 Inch Diameter) Used for LFA Testing

The results of the three samples, referred to as A, B, and C are shown in Table 5.15 below. Each sample was subjected to a total of three laser flashes to determine an average effect thermal conductivity of the samples. LFA fires a laser 'burst', typically around 15 Joules [102] at the soil sample, and a thermocouple located on the other side of the sample measures the thermal response of the sample. Using the temperature-time profile, a built-in program determines the thermal diffusivity, specific heat capacity, and inputted density of the sample to determine the thermal conductivity.

Table 5.15 - LFA Results of Dry Soil Samples of Soil Surrounding the Borehole Strings

Soil Sample	Flash #	C_p [J/kgK]	Thermal Diffusivity [cm^2/sec]	Density [kg/m^3]	Thermal Conductivity [W/mK]	Average k per sample [W/mK]
A	1	1136.958	0.0052	2081	1.23	1.17
	2	1206.556	0.0046	2081	1.16	
	3	1154.589	0.0047	2081	1.13	
B	1	852.1639	0.0054	2065	0.95	0.89
	2	762.7917	0.0053	2065	0.83	
	3	815.4287	0.0052	2065	0.88	
C	1	775.3246	0.0051	1947	0.77	0.72
	2	688.3181	0.005	1947	0.67	
	3	740.3416	0.0049	1947	0.71	

The thermal conductivity values are low relative to the TRT results, however it is typically seen that the thermal conductivity of the soil increases with increasing the moisture content [103]. The samples shown in Table 5.15 were made of dry soil and the compression of the sample to create the disk with minimum water or air 'pockets' in the sample. The relationship between the thermal conductivity and the moisture content is logarithmic, however more parameters such as porosity, grain size, and saturation ratio are needed to determine the effective thermal conductivity of an in-situ sample. Alrtimi et al.'s prediction of the thermal conductivity of wet Tripoli sands was proven with experimental work [104]. Roshankhah et al. provide a summary of empirical models (Chen [105], Johansen [106]) and an analytical model (Haigh

[107]) [108]. Haigh also provided a list of alternative prediction models to determine the thermal conductivity of various soil types, ranging from crushed rock particles (Cote & Konrad [109]) to sandy soils (Gangadhara Rao & Singh [110]). The relationship between the thermal conductivity (k) of a saturated soil of the models mentioned above are determined using some or all the following parameters: the thermal conductivity of water (k_{water}), sand grain thermal conductivity $k_{sand\ grain}$), saturation ratio (S_r), moisture content, unit weight, and the porosity (n) of the sand. To estimate the effect of moisture on the thermal conductivity of the soil, the empirical model proposed by Chen [105] which was determined by 80 needle-probe tests on sandy soils, was used. Chen [105] proposed the following equation:

$$k = k_{water}^{n} k_{sand\ grain}^{1-n} [(1-b)S_r + b]^{cn} \quad (12)$$

Empirical parameters, b and c, were obtained from fitting the experimentally measured data and are equal to 0.0022 and 0.78, respectively [105].

The empirical model proposed by Lu et al. [111] was also used to compare the thermal conductivity with water content. Their model is a modification of a model proposed by Johansen [106], and estimates the thermal conductivity of sandy soils using the following equation:

$$k = [k_{water}^{n} k_{sand\ grain}^{1-n} - (b-an)] exp[\propto (1 - S_r^{\propto - 1.33}] + (b-an) \quad (13)$$

Where a, b, and α are empirical parameters with values of 0.56, 0.51, and 0.96 recommended for sandy soils.

The thermal conductivity value of the sand grains is assumed as being 4 W/mK and 7.5 W/mK to give a range of possible effective thermal conductivities. The results of applying Chen

and Lu et al.'s model are shown in Figure 5.17. Two different porosity values, $n = 0.4$ and $n = 0.5$, at a range of saturation ratio are shown.

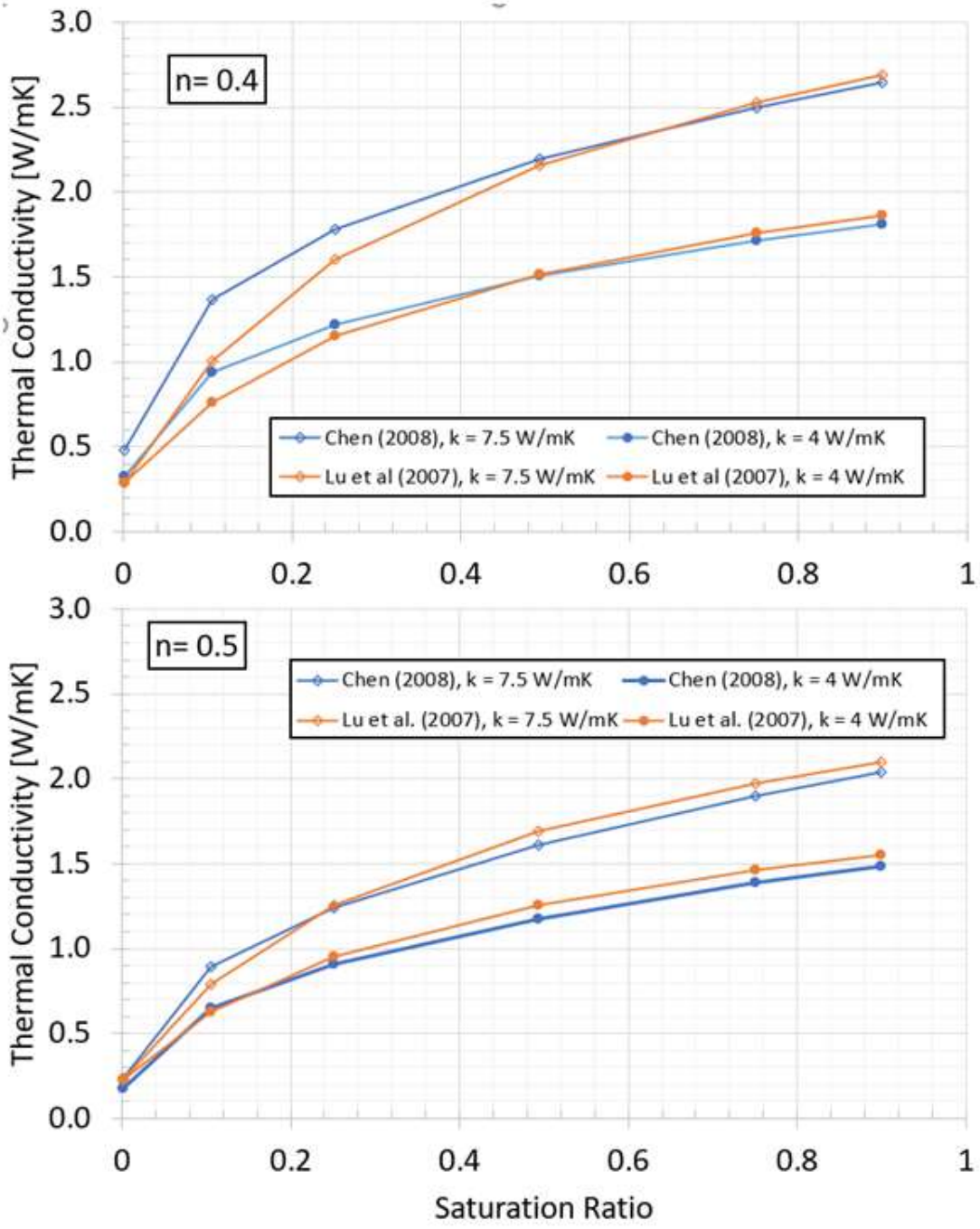

Figure 5.17 – Comparison of the thermal conductivity based on Chen [105] and Lu et al. [111] at porosity, n = 0.4 and n = 0.5, and thermal sand grain thermal conductivity, k = 4 W/mK and k = 7.5 W/mK.

As seen above, the effective thermal conductivity has a logarithmic relationship with the saturation ratio. The results from the dry sample LFA results (k = 0.72, 0.89, and 1.17 W/mK) correspond to a lower saturation ratio within the sample, which was expected. This shows that LFA wet samples of the soil surrounding the borehole strings will provide a higher thermal conductivity than those obtained from the dry samples. These results also show that the LFA thermal conductivity value shown below in Figure 5.18 is low relative to the expected thermal conductivity.

Finally, the results of experiments performed by Judd and Wade (1969) are analysed to determine the thermal conductivity given the thermal diffusivity of 6.967E-7 m^2/s (0.027 ft^2/s) [92]. For consistency, the storage heat capacity used for the TRNSYS simulations was used to determine the thermal conductivity of 1.76 W/mK. The results are also presented below in Figure 44.

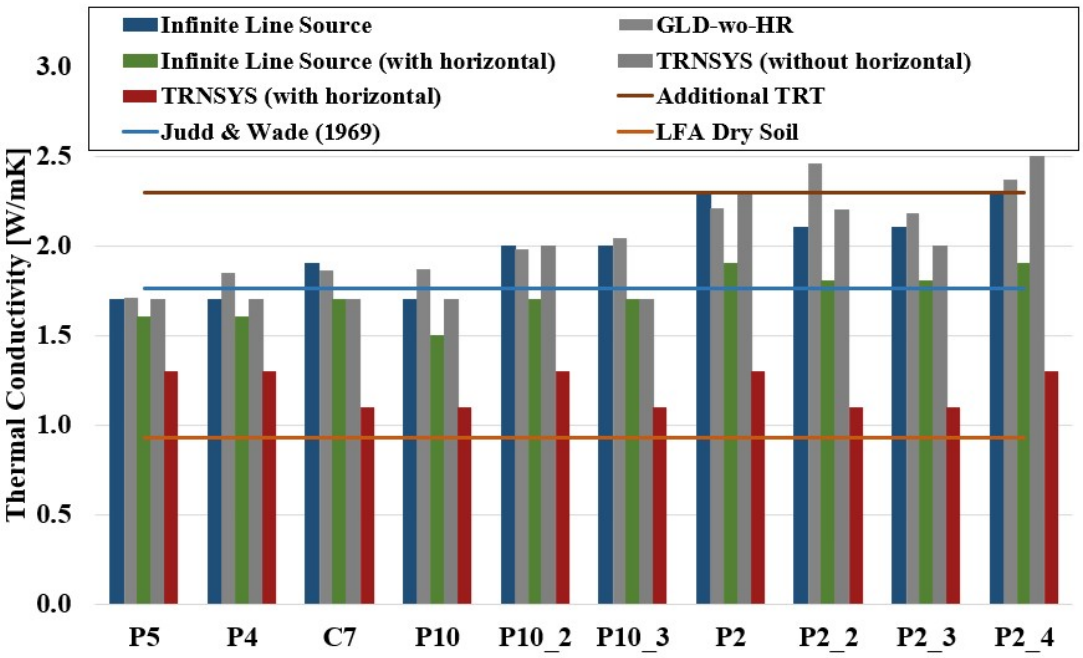

Figure 5.18 - Effective thermal conductivity comparison of all analysis methods of the soil surrounding borehole strings

6 Conclusions and Recommended Work

This thesis's goal was to assess the validity of the conventional thermal response test evaluation methods when performing the test on a string of boreholes. This evaluation allows for a borehole field to be drilled in its location in the same configuration as its planned operation, allowing for the characterization to represent the actual field as best as possible. The evaluation of multiple borehole strings within the same borehole field location allowed for the characterisation of the soil in different areas, giving a range of the effective thermal conductivity. This array of thermal conductivity based on location allows for better planning and operational control especially when dealing with seasonal BTES.

The infinite line source and TRNSYS were used to determine the soil's effective thermal conductivity surrounding pre-existing borehole strings. The thermal conductivity of the soil within a BTES is a determining factor of the operation, control, and capacity of the field. It is, therefore, an essential parameter to determine correctly. This thesis presented a design of experiments for the simulations to minimize the root mean square error between experimental data and the simulation output. The parametric estimation method results were compared to the typical thermal response test analysis results, using the infinite line source.

When the spacing was below 1.73 m the interaction between adjacent boreholes of the borehole string would invalidate the Infinite Line Source method's central assumption. TRNSYS was then used based on the assumption that it had the capability to account for the thermal interaction between the boreholes. The findings were that the thermal conductivity found using TRNSYS was significantly lower than that of the ILS, with values of 1.2±0.1W/mK when accounting for the horizontal portions. Contrary to the findings, the interaction of the boreholes

should increase the temperature response more rapidly which in turn would decrease the effective thermal conductivity (by lowering the slope of the temperature vs. time curve). This provides evidence that TRNSYS is unable to properly represent a borehole string and the horizontal portion of the string. TRNSYS is a very well-known program with capabilities extending much further than modeling just borehole heat exchangers with input temperatures and mass flow rate, however this thesis found that in the case of few boreholes and shorter time scales, the model does not correctly account for the geometry. TRNSYS is a proven design tool when applied to a large borehole field with long-term simulations, but the model cannot account for short-term interaction well. It is recommended that the TRNSYS horizontal pipe model be investigated further as the work done in this thesis shows that the results are scattered and not consistent when evaluating the borehole strings with the horizontal portion. It should be mentioned, however, that when evaluating a single borehole heat exchanger TRT, the TRNSYS results were a good prediction of the experimental results of Beier et al. [98].

The spacing between boreholes used to determine soil volume within TRNSYS is an insufficient way to model the borehole string. Therefore, the reliability of the results is questioned. Within TRNSYS, the spacing of boreholes is used to determine a thermal resistance of the borehole heat exchanger, allowing for the heat transfer problem to be solved. This is sufficient in the case of obtaining an estimate of a long-term full-field response for a BTES, but in the case of a TRT conducted on a borehole string, it is insufficient. The twin-pipe model in TRNSYS has also been shown to affect the outcome of the simulation significantly. It is recommended that the twin-pipe model be evaluated in greater detail, including verification or validation. The length of the horizontal portion can be up to 18% of the borehole strings' total length and is significant enough to contribute to the thermal response.

The horizontal portion leading to the inlet of the first borehole of each string was accounted for with the ILS by adding the total horizontal length of tubing to the effective length of the borehole heat exchanger. This method provides reasonable thermal conductivity values, however the geometry of the horizontal piping is not an exact match to that of the BHE, as there is no borehole pipe material, no grout, and the return and supply pipe spacing is not constant. It was found that the ILS method provides a thermal conductivity of 1.7±0.2 W/mK when accounting for the horizontal length of the borehole strings. This error value also accounts for the error associated with using the ILS (see section 4.2.1) provided by Eklof and Gehlin [30]. The ILS therefore has been proven to give reasonable results when applied to the borehole string, however it is recommended that future work includes an approximation of the effect of the length of horizontal on the effective thermal conductivity.

When repeating a test on a single BHE (i.e. P2,_2, P2_3, P2_4 and P10_2, P10_3), it is recommended that the waiting period between the successive tests be extended to the amount of time that is required for the borehole to return to its undisturbed temperature, rather than a set number of days (see section 2.4.5 of 2 Literature Review). The ground temperature before a thermal response test has begun (undisturbed temperature) is not directly used to find the thermal conductivity when using the line source theory. However, the initial ground temperature does affect the thermal conductivity when evaluated using numerical models which should be done when evaluating a string to correctly account for thermal interaction.

Modelling software such as ANSYS CFX or COMSOL Multiphysics are recommended for future comparison of the borehole strings. Implementing such models would allow for the horizontal portions leading to the string and the horizontal portion between each borehole of the string (i.e. the spacing) to be correctly accounted for in the geometry. TRNSYS could also be

revisited again in the future, taking a closer look at the horizontal pipe model and re-evaluating the borehole resistance model that TRNSYS uses when determining the response of a borehole string.

It is also recommended that wet soil samples be obtained and tested using the LFA. This would further aid the thermal conductivity estimation of the field, as it would better represent soil that exists within the BTES field.

This in-situ testing provided valuable thermal properties of the field as these thermal properties will dictate the operation and control of a borehole thermal energy storage field. The balance of heat injected and heat extracted into the BTES during operation becomes the most important control characteristic as it will dictate the lifetime of the field and the efficiency. Detailed analysis of a thermal response test is therefor recommended by use of the aforementioned modelling software in order to enhance the estimation of the thermal conductivity by creating a more accurate reduced model in the future.

7 References

[1] N. R. Canada, “Renewable Energy Facts,” 2020. https://www.nrcan.gc.ca/science-data/data-analysis/energy-data-analysis/energy-facts/renewable-energy-facts/20069#L1 (accessed Aug. 31, 2020).

[2] P. Kandiah, “CFD Study of a Large Buried Tank Within a Borehole Field,” 2014.

[3] L. L. Jensen, D. Trier, F. Bava, I. Ben Hassine, and X. Jobard, “D2.3 Large Storage Systems for DHC Networks.” [Online]. Available: https://w4u0es9f4.wimuu.com/Download?id=file:68931000&s=5624676745098706070.

[4] B. Nordell, “Large-scale Thermal Energy Storage,” no. February, pp. 1–10, 2000.

[5] H. Paksoy, *Thermal Energy Storage for Sustainable Energy Consumpton*. Springer, 2005.

[6] B. Harris, “A CFD Study on the Extraction of Geothermal Energy from Abandoned Oil and Gas Wells,” 2017.

[7] N. R. Canada, “Drake Landing Solar Community,” 2012. http://www.dlsc.ca/index.htm (accessed Aug. 31, 2020).

[8] Z. Guan, “Thermal enhancement of bentonite-based grouting material by using carbon fibers in ground heat pump system,” *Masters Thesis*, p. McMaster University, 2017.

[9] B. Sanner, “Current status of ground source heat pumps in Europe,” 2003, [Online]. Available: https://www.buildingphysics.com/download/Futurestock 1.pdf.

[10] M. Sauer, E. Mands, E. Grundmann, and B. Sanner, “Experiences from use of TRT (Thermal Response Test) in the design praxis for BHE (Borehole Heat Exchanger): lessons learned, enhanced information, new developments,” *Eur. Geotherm. Congr. 2016*, pp. 19–24, 2016, [Online]. Available: http://ubeg.de/Lit/2016 Sauer et al egc 2016.pdf.

[11] X. Zhang, T. Zhang, B. Li, and Y. Jiang, “Comparison of Four Methods for Borehole Heat Exchanger Sizing Subject to Thermal Response Test,” 2019.

[12] A. Hesaraki, S. Holmberg, and F. Haghighat, “Seasonal thermal energy storage with heat pumps and low temperatures in building projects — A comparative review,” *Renew. Sustain. Energy Rev.*, vol. 43, pp. 1199–1213, 2015, doi: 10.1016/j.rser.2014.12.002.

[13] B. Sanner, G. Hellström, J. D. Spitler, and S. Gehlin, “Thermal Response Test – Current Status and World-Wide Application,” *Proc. World Geotherm. Congr.*, no. April, pp. 24–29, 2005.

[14] M. Aydın and A. Sisman, “Experimental and computational investigation of multi U-tube boreholes,” vol. 145, pp. 163–171, 2015, doi: 10.1016/j.apenergy.2015.02.036.

[15] J. Acuña, “Distributed thermal response tests – New insights on U-pipe and Coaxial heat exchangers in groundwater-filled boreholes,” KTH Industrial Engineering and Management, 2013.

[16] T. Sivasakthivel, M. Philippe, K. Murugesan, V. Verma, and P. Hu, “Experimental thermal performance analysis of ground heat exchangers for space heating and cooling applications,” *Renew. Energy*, vol. 113, pp. 1168–1181, 2017, doi: 10.1016/j.renene.2017.06.098.

[17] D. Gordon, T. Bolisetti, D. S. K. Ting, and S. Reitsma, “Short-term fluid temperature variations in either a coaxial or U-tube borehole heat exchanger,” *Geothermics*, vol. 67, pp. 29–39, 2017, doi: 10.1016/j.geothermics.2016.12.001.

[18] D. Pahud and B. Matthey, “Comparison of the thermal performance of double U-pipe borehole heat exchangers measured in situ,” *Energy Build.*, vol. 33, no. 5, pp. 503–507, 2001, doi: 10.1016/S0378-7788(00)00106-7.

[19] W. A. Austin, C. Yavuzturk, and J. D. Spitler, “Development of an in-situ system and analysis procedure for measuring ground thermal properties,” *ASHRAE Trans.*, vol. 106, no. 1, pp. 365–379, 2000.

[20] D. Mendrinos, S. Katsantonis, and C. Karytsas, “Pipe materials for borehole heat exchangers,” *Eur. Geotherm. Congr. 2016*, no. September 2016, pp. 19–24, 2016.

[21] S. M. Bae, Y. Nam, J. M. Choi, K. Ho Lee, and J. S. Choi, “Analysis on thermal performance of ground heat exchanger according to design type based on thermal response test,” *Energies*, vol. 12, no. 4, 2019, doi: 10.3390/en12040651.

[22] H. Zeng, N. Diao, and Z. Fang, “Heat transfer analysis of boreholes in vertical ground heat exchangers,” *Int. J. Heat Mass Transf.*, vol. 46, no. 23, pp. 4467–4481, 2003, doi: 10.1016/S0017-9310(03)00270-9.

[23] W. Yang, M. Shi, G. Liu, and Z. Chen, “A two-region simulation model of vertical U-tube ground heat exchanger and its experimental verification,” *Appl. Energy*, vol. 86, no. 10, pp. 2005–2012, 2009, doi: 10.1016/j.apenergy.2008.11.008.

[24] M. Aydin, A. Gultekin, and A. Sisman, “The effects of test temperature and duration on the results of constant temperature thermal response test,” no. July 2018, 2017.

[25] R. A. Beier, “Soil Thermal Conductivity Tests,” Stillwater, 2008. doi: 10.1080/02757259009532137.

[26] H. Fujii, H. Okubo, K. Nishi, R. Itoi, K. Ohyama, and K. Shibata, “An improved thermal response test for U-tube ground heat exchanger based on optical fiber thermometers,” *Geothermics*, vol. 38, no. 4, pp. 399–406, 2009, doi: 10.1016/j.geothermics.2009.06.002.

[27] H. J. L. Witte, G. J. Van Gelder, and J. D. Spitler, “In situ measurement of ground thermal conductivity: A dutch perspective,” *ASHRAE Trans.*, vol. 108 PART 1, no. 1, pp. 263–272, 2002.

[28] J. Acuña, P. Mogensen, and B. Palm, “Distributed Thermal Response Test on a U-Pipe Borehole Heat Exchanger,” *Appl. Energy*, 2008, doi: 10.1017/CBO9781107415324.004.

[29] J. Acuña, P. Mogensen, and B. Palm, “Distributed thermal response tests on a multi-pipe coaxial borehole heat exchanger,” *HVAC &R Res.*, vol. 17, no. 6, pp. 1012–1029, 2011, doi: 10.1080/10789669.2011.625304.

[30] C. Eklöf and S. Gehlin, “TED - a mobile equipment for thermal response test : testing and evaluation,” 1996, [Online]. Available: http://www.diva-portal.org/smash/record.jsf?pid=diva2%3A1032479&dswid=3663.

[31] A. M. Gustafsson and L. Westerlund, “Multi-injection rate thermal response test in groundwater filled borehole heat exchanger,” *Renew. Energy*, vol. 35, no. 5, pp. 1061–1070, 2010, doi: 10.1016/j.renene.2009.09.012.

[32] S. Javed, J. D. Spitler, and P. Fahlén, “An Experimental Investigation of the Accuracy of Thermal Response Tests Used to Measure Ground Thermal Properties,” *ASHRAE Trans.*, vol. 3, no. July 2015, pp. 13–22, 2011.

[33] Y. Shang, S. Li, and H. Li, “Analysis of geo-temperature recovery under intermittent operation of ground-source heat pump,” *Energy Build.*, vol. 43, no. 4, pp. 935–943, 2011, doi: 10.1016/j.enbuild.2010.12.017.

[34] F. Bozzoli, G. Pagliarini, S. Rainieri, and L. Schiavi, “Estimation of soil and grout thermal properties through a TSPEP (two-step parameter estimation procedure) applied to TRT (thermal response test) data,” *Energy*, vol. 36, no. 2, pp. 839–846, 2011, doi: 10.1016/j.energy.2010.12.031.

[35] N. K. Muraya, “Numerical modeling of the transient thermal interference of vertical U-tube heat exchangers,” Texas A&M University, 1994.

[36] J. Claesson and S. Javed, “Explicit Multipole Formulas for Calculating Thermal Resistance of Single U-Tube Ground Heat Exchangers †,” 2018, doi: 10.3390/en11010214.

[37] S. P. Kavanaugh, “Simulation and experimental verification of ground-coupled heat pump systems,” Oklahoma State University, 1985.

[38] J. A. Shonder and J. V. Beck, “Determining effective soil formation thermal properties from field data using a parameter estimation technique,” *ASHRAE Trans.*, vol. 105, 1999.

[39] Y. Gu and D. O. Neal, “Development of an equivalent diameter expression for vertical U-Tubes used in ground-coupled heat pumps,” *ASHRAE Trans.*, no. January 1998, 1998.

[40] R. Al-chalabi, “Thermal Resistance of U-tube Borehole Heat Exchanger System : Numerical Study,” The University of Manchester, 2013.

[41] P. Eskilson, “Thermal Analysis of Heat Extraction Boreholes,” 1987.

[42] M. H. Sharqawy, E. M. Mokheimer, and H. M. Badr, “Effective pipe-to-borehole thermal resistance for vertical ground heat exchangers,” *Geothermics*, vol. 38, pp. 271–277, 2009, doi: 10.1016/j.geothermics.2009.02.001.

[43] D. Bauer, W. Heidemann, H. Mu, and H. G. Diersch, “Thermal resistance and capacity models for borehole heat exchangers,” *Int. J. Energy Res.*, vol. 35, pp. 312–320, 2011, doi: 10.1002/er.

[44] Z. Mohamad and F. Fardoun, “Energy performance evaluation of Geothermal Boreholes,” *Int. J. Civ. Eng. Technol.*, vol. 9, no. 5, pp. 978–983, 2018.

[45] T. Başer, N. Lu, and J. S. McCartney, “Operational response of a soil-borehole thermal energy storage system,” *J. Geotech. Geoenvironmental Eng.*, vol. 142, no. 4, pp. 1–12, 2016, doi: 10.1061/(ASCE)GT.1943-5606.0001432.

[46] J. S. McCartney, T. Başer, N. Zhan, N. Lu, S. Ge, and K. M. Smits, “Storage of Solar Thermal Energy in Borehole Thermal Energy Storage Systems,” in *IGSHPA Technical/Research Conference and Expo*, 2017, no. 1981, doi: 10.22488/okstate.17.000512.

[47] S. Chapuis, “Stockage thermique saisonnier dans un champ de puits géothermiques verticaux en boucle fermée,” 2009.

[48] S. Chapuis and M. Bernier, “Seasonal storage of solar energy in borehole heat exchangers,” *IBPSA 2009 - Int. Build. Perform. Simul. Assoc. 2009*, pp. 599–606, 2009.

[49] P. Eskilson and J. Claesson, “Simulation Model for Thermally Interacting Heat Extraction Boreholes,” *Numer. Heat Transf.*, vol. 13, pp. 149–165, 1988.

[50] A. Moradi, K. M. Smits, N. Lu, and J. S. McCartney, “Heat transfer in unsaturated soil with application to borehole thermal energy storage,” *Vadose Zo. J.*, vol. 15, no. 10, 2016, doi: 10.2136/vzj2016.03.0027.

[51] S. Javed, *Thermal modelling and evaluation of borehole heat transfer*. 2012.

[52] S. Javed and J. Claesson, “New analytical and numerical solutions for the short-term analysis of vertical ground heat exchangers,” *ASHRAE Trans.*, vol. 117, no. PART 1, pp. 3–12, 2011.

[53] W. A. Austin, “Development of an in Situ System for Measuring Ground Thermal Properties,” Oklahoma State University, 1995.

[54] N. Catolico, S. Ge, and J. S. McCartney, “Numerical modeling of a soil-borehole thermal energy storage system,” *Vadose Zo. J.*, vol. 15, no. 1, 2016, doi: 10.2136/vzj2015.05.0078.

[55] J. Lee, G. Kim, D. Bae, H. Choi, and K. Kim, “An analysis on the borehole spacing for deep borehole disposal of HLW,” *15th Int. High-Level Radioact. Waste Manag. Conf. 2015, IHLRWM 2015*, pp. 638–641, 2015.

[56] A. Gultekin, M. Aydın, and A. Sisman, “Determination of Optimal Distance Between Boreholes,” *Thirty-Ninth Work. Geotherm. Reserv. Eng.*, pp. 1–8, 2014.

[57] S. Lazzari, A. Priarone, and E. Zanchini, “Long-term performance of BHE (borehole heat exchanger) fields with negligible groundwater movement,” *Energy*, 2010, doi: 10.1016/j.energy.2010.08.028.

[58] P. Monzó, M. Bernier, J. Acuña, and P. Mogensen, “A monthly based bore field sizing methodology with applications to optimum borehole spacing,” *ASHRAE Conf.*, vol. 122, pp. 111–126, 2016.

[59] M. A. Rosen and S. Koohi-Fayegh, “Modelling Thermally Interacting Multiple Boreholes with Variable Heating Strength,” p. 1165, 2019, doi: 10.3390/wsf2-01165.

[60] O. T. Farouki, “Thermal Properties of Soils.,” *CRREL Monogr. (US Army Cold Reg. Res. Eng. Lab.*, 1981.

[61] R. Wagner and C. Clauser, “Evaluating thermal response tests using parameter estimation for thermal conductivity and thermal capacity,” *Geophys. Eng.*, vol. 2, pp. 349–356, 2005, doi: 10.1088/1742-2132/2/4/S08.

[62] W. Choi and R. Ooka, “Interpretation of disturbed data in thermal response tests using the infinite line source model and numerical parameter estimation method,” *Appl. Energy*, 2015, doi: 10.1016/j.apenergy.2015.03.097.

[63] R. Xia, McMlymont & Rak Engineers, R. Mancini, R. Mancini and Associates Ltd., and G. Di Rezze, “In Situ Thermal Response Tests in Greater Toronto Area,” in *10th IEA Heat Pump Conference*, 2011, pp. 1–12.

[64] J. D. Spitler and S. Gehlin, “Thermal response testing for ground source heat pump systems — An historical review,” *Renew. Sustain. Energy Rev.*, vol. 50, pp. 1125–1137, 2015.

[65] J. Acuña and B. Palm, “Distributed thermal response tests on pipe-in-pipe borehole heat exchangers,” *Appl. Energy*, vol. 109, pp. 312–320, 2013, doi: 10.1016/j.apenergy.2013.01.024.

[66] H. Fujii, H. Okubo, and R. Itoi, “Thermal Response Tests Using Optical Fiber Thermometers,” *Geotherm. Resour. Counc.*, vol. 30, pp. 545–552, 2006.

[67] J. Raymond, “Colloquium 2016: Assessment of subsurface thermal conductivity for geothermal applications,” *Can. Geotech. J.*, vol. 55, no. 9, pp. 1209–1229, 2018, doi: 10.1139/cgj-2017-0447.

[68] J. Luo, J. Rohn, M. Bayer, and A. Priess, “Thermal efficiency comparison of borehole heat exchangers with different drillhole diameters,” *Energies*, vol. 6, no. 8, pp. 4187–4206, 2013, doi: 10.3390/en6084187.

[69] R. A. Beier, M. S. Mitchell, J. D. Spitler, and S. Javed, “Validation of borehole heat exchanger models against multi-flow rate thermal response tests,” *Geothermics*, vol. 71, pp. 55–68, 2018, doi: 10.1016/j.geothermics.2017.08.006.

[70] “GeoCubeTM User ’ s Guide.” Precision Geothermal, LLC, pp. 0–56, 2013, [Online]. Available: www.precisiongeotheral.com.

[71] S. P. Kavanaugh, “Specifications for Formation Thermal Conductivity Test,” 2008. http://geokiss.com/wp-content/uploads/2018/06/TCTestingSpecs.pdf.

[72] A. Mcdaniel, J. Tinjum, D. J. Hart, Y. Lin, A. Stumpf, and L. Thomas, “Distributed thermal response test to analyze thermal properties in heterogeneous lithology,” *Geothermics*, vol. 76, pp. 116–124, 2018, doi: 10.1016/j.geothermics.2018.07.003.

[73] M. I. V. Marquez *et al.*, “Distributed Thermal Response Tests Using a Heating Cable and Fiber Optic Temperature Sensing,” *Energies*, vol. 11, 2018, doi: 10.3390/en11113059.

[74] A. Angelotti and L. Molinaroli, “A laboratory apparatus to study Thermal Response Test

in the presence of groundwater flow," vol. 67, no. 201 9.

[75] A. Angelotti, F. Ly, and A. Zille, "On the applicability of the moving line source theory to thermal response test under groundwater flow : considerations from real case studies," *Geotherm. Energy*, 2018, doi: 10.1186/s40517-018-0098-z.

[76] A. Chiasson, S. J. Rees, and J. D. Spitler, "A Preliminary Assessment of the Effects of Groundwater Flow on Closed-Loop Ground-Source Systems," *ASHRAE Trans.*, vol. 106, no. 1, pp. 380–393, 2000.

[77] C. Li, J. Mao, Z. Xing, J. Zhou, and Y. Li, "Analysis of geo-temperature restoration performance under intermittent operation of borehole heat exchanger fields," *Sustain.*, vol. 8, no. 1, pp. 1–14, 2016, doi: 10.3390/su8010035.

[78] H. J. L. Witte and A. J. Van Gelder, "Geothermal Response Tests using controlled multi-power level heating and cooling pulses (MPL-HCP): Quantifying ground water effects on heat transport around a borehole heat exchanger," 2006.

[79] J. Raymond, R. Therrien, L. Gosselin, and R. Lefebvre, "Numerical analysis of thermal response tests with a groundwater flow and heat transfer model," *Renew. Energy*, vol. 36, no. 1, pp. 315–324, 2011, doi: https://doi.org/10.1016/j.renene.2010.06.044.

[80] V. Wagner, P. Blum, M. Kübert, and P. Bayer, "Analytical approach to groundwater-influenced thermal response tests of grouted borehole heat exchangers," *Geothermics*, vol. 46, pp. 22–31, 2013, doi: https://doi.org/10.1016/j.geothermics.2012.10.005.

[81] A. M. Gustafsson and S. Gehlin, "Thermal Response Test - Power Injection Dependence," 2002.

[82] S. Zhou, W. Cui, and K. Gao, "Application of linear superposition theory in successive thermal response tests without ground temperature recovery Application of linear superposition theory in successive thermal response tests without ground temperature recovery," *Sci. Technol. Built Environ.*, vol. 24, no. 3, pp. 220–227, 2018, doi: 10.1080/23744731.2017.1341803.

[83] X. Liu and R. A. Clemenzi, "Advanced Testing Method for Ground Thermal Conductivity," Oak Ridge, 2017.

[84] C. Martin and S. P. Kavanaugh, "Ground thermal conductivity testing - controlled site analysis," *ASHRAE Trans.*, vol. 108, no. 1, pp. 945–952, 2002.

[85] S. Gehlin, "Thermal Response Test: method development and evaluation," Lulea University of Technology, 2002.

[86] J. Spitler, S. J. Rees, and C. Yavuzturk, "More Comments on In-Situ Borehole Thermal Conductivity Testing," *The Source*, vol. 12, no. 2, pp. 4–6, 1999.

[87] S. Javed and P. Fahlén, "Thermal response testing of a multiple borehole ground heat exchanger," *Int. J. Low-Carbon Technol.*, vol. 6, no. 2, pp. 141–148, 2011, doi: 10.1093/ijlct/ctr004.

[88] N. K. Jain, "Parameter estimation of ground thermal properties," *(Master's*

Thesis).Oklahoma State Univ. Stillwater., 1999, [Online]. Available: http://www.hvac.okstate.edu.

[89] P. Monzó, "Comparison of different Line Source Model approaches for analysis of Thermal Response Test in a U-pipe Borehole Heat Exchanger," 2011.

[90] P. Bujok *et al.*, "Assessment of the influence of shortening the duration of TRT (thermal response test) on the precision of measured values," *Energy*, vol. 64, pp. 120–129, 2014, doi: 10.1016/j.energy.2013.11.079.

[91] S. Gehlin and B. Nordell, "Determining Undisturbed Ground Temperature for Thermal Response Test," *ASHRAE Trans.*, pp. 151–156, 2003.

[92] R. Judd and J. Wade, "Temperature Distribution in the Soil," *Eng. J.*, pp. 22–25, 1969.

[93] H. J. L. Witte, "Error analysis of thermal response tests," *Appl. Energy*, vol. 109, pp. 302–311, 2013, doi: 10.1016/j.apenergy.2012.11.060.

[94] G. Hellström, "Ground heat storage: Thermal analyses of duct storage systems," *Lund Univ.*, p. 310, 1991, [Online]. Available: http://search.proquest.com/docview/303983441?accountid=14357.

[95] J. Fox, "Bootstrapping Regression Models," *An R S-PLUS Companion to Appl. Regres.*, no. January, pp. 1–14, 2002.

[96] TESS, "TESS Component Libraries: General Descriptions." pp. 22–23, [Online]. Available: http://www.trnsys.com/tess-libraries/TESSLibs17_General_Descriptions.pdf.

[97] H. J. L. Witte and G. B. V Valschermkade, "Geothermal Response Tests with Heat Extraction and Heat Injection : Examples of Application in Research and Design of Geothermal Ground Heat Exchangers," vol. 31, no. 0, 2001.

[98] R. A. Beier, M. D. Smith, and J. D. Spitler, "Reference data sets for vertical borehole ground heat exchanger models and thermal response test analysis," *Geothermics*, vol. 40, no. 1, pp. 79–85, 2011, doi: 10.1016/j.geothermics.2010.12.007.

[99] R. A. Beier and M. D. Smith, "Minimum Duration of In-Situ Tests on Vertical Boreholes," *ASHRAE Trans.*, vol. 109, pp. 475–486, 2003.

[100] Egmond Associates LTD, "Geothermal Thermal Condutivity Report Prepared for McMaster University," Hamilton, 2021.

[101] E. C. Robertson, "Thermal properties of rocks. Report 88-441," *US Dep. Inter. Geol. Surv.*, p. 106, 1988.

[102] tec-science, "Laser-Flash method for determining thermal conductivity (LFA)," 2020. https://www.tec-science.com/thermodynamics/heat/laser-flash-method-for-determining-thermal-conductivity-lfa/ (accessed Oct. 22, 2021).

[103] G. Al Nakshabandi and H. Kohnke, "Thermal conductivity and diffusivity of soils as related to moisture tension and other physical properties," *Agric. Meteorol.*, vol. 2, no. 4, pp. 271–279, 1965, doi: 10.1016/0002-1571(65)90013-0.

[104] A. Alrtimi, M. Rouainia, and S. Haigh, “Thermal conductivity of a sandy soil,” *Appl. Therm. Eng.*, vol. 106, pp. 551–560, 2016, doi: 10.1016/j.applthermaleng.2016.06.012.

[105] S. X. Chen, “Thermal conductivity of sands,” *Heat Mass Transf.*, vol. 44, no. 10, p. 1241, 2008, doi: 10.1007/s00231-007-0357-1.

[106] O. Johansen, “Thermal Conductivity of Soils,” no. June, 1977.

[107] S. K. Haigh, “Thermal conductivity of sands,” no. July 2012, 2015, doi: 10.1680/geot.11.P.043.

[108] S. Roshankhah, A. M. Asce, A. V Garcia, and J. C. Santamarina, “Thermal Conductivity of Sand-Silt Mixtures,” no. December, 2020, doi: 10.1061/(ASCE)GT.1943-5606.0002425.

[109] J. Côté and J.-M. Konrad, “A generalized thermal conductivity model for soils and construction materials,” *Can. Geotech. J.*, vol. 42, pp. 443–458, Jan. 2011, doi: 10.1139/t04-106.

[110] B. Rao, “A generalized relationship to estimate thermal resistivity of soils,” *Can. Geotech. J.*, vol. 36, pp. 767–773, Jan. 2011, doi: 10.1139/cgj-36-4-767.

[111] S. Lu, T. Ren, Y. Gong, and R. Horton, “An Improved Model for Prediting Soil Thermal Conducivity from Water Content at Room Temperature,” *Soil Sci. Soc. Am. J.*, vol. 71, pp. 8–14, 2007, [Online]. Available: http://dx.doi.org/10.2136/sssaj2006.0041.

[112] L. Mesquita, D. Mcclenahan, J. Thornton, J. Carriere, and B. Wong, “Drake Landing Solar Community : 10 Years of Operation,” 2017, doi: 10.18086/swc.2017.06.09.

[113] N. R. Canada, “Residential Sector Ontario,” 2017. https://oee.nrcan.gc.ca/corporate/statistics/neud/dpa/showTable.cfm?type=CP&sector=res&juris=on&rn=2&page=0 (accessed Aug. 28, 2020).

8 Appendix A - Calibration of Vertical Thermistor and Uncertainty Analysis

NTC thermistors were used in three boreholes designated for temperature sensing, located in the core, perimeter, and the outer field of the borehole field underneath the HATCH building at McMaster. All of the thermistors were calibrated using a water bath and a Resistance Temperature Detector (RTD) to ensure accuracy in any further field temperature readings. An Omega DP251 Precision Thermometer (an RTD) was used during this calibration, with a manufacturer's reported accuracy of +/- 0.01C. The data acquisition system for this calibration consisted of an Arduino Nano3 (https://store.arduino.cc/usa/arduino-nano) with two 16-channel analog multiplexers (SparkFun Analog/Digital MUX Breakout – CD74HC4067, (https://www.sparkfun.com/products/9056).

8.1 Calibration of the Thermistors

The thermistors calibrated were the R_{25} at 10 KOhm using the RTD as reference temperature. All of the thermistors were placed at random locations in a temperature-controlled thermal bath. The temperature of the bath was initially set to 10°C. During calibration, the thermistors' temperatures and RTD temperature were taken every 5 minutes for a total of 5 samples at the set temperature. Each sample was an average of 100 data points taken and averaged by the Arduino. The Arduino is a 10bit Analog-to-Digital Converter (ADC) with a reported uncertainty of +/- 5 mV by the manufacturer. The thermal bath temperature was then increased to a maximum of 80°C at 10°C intervals, with temperature measured at each setpoint temperature [112][113].

A known mathematical equation was used to convert the output resistance values to temperature. This equation is known as the Steinhart Equation:

$$T_{steinhart} = \frac{1}{\left(\frac{1}{\beta}\right) * LN\left(\frac{R_{thermistor}}{R_{series}}\right) + \frac{1}{T_{O+273.15}}} - 273.15$$

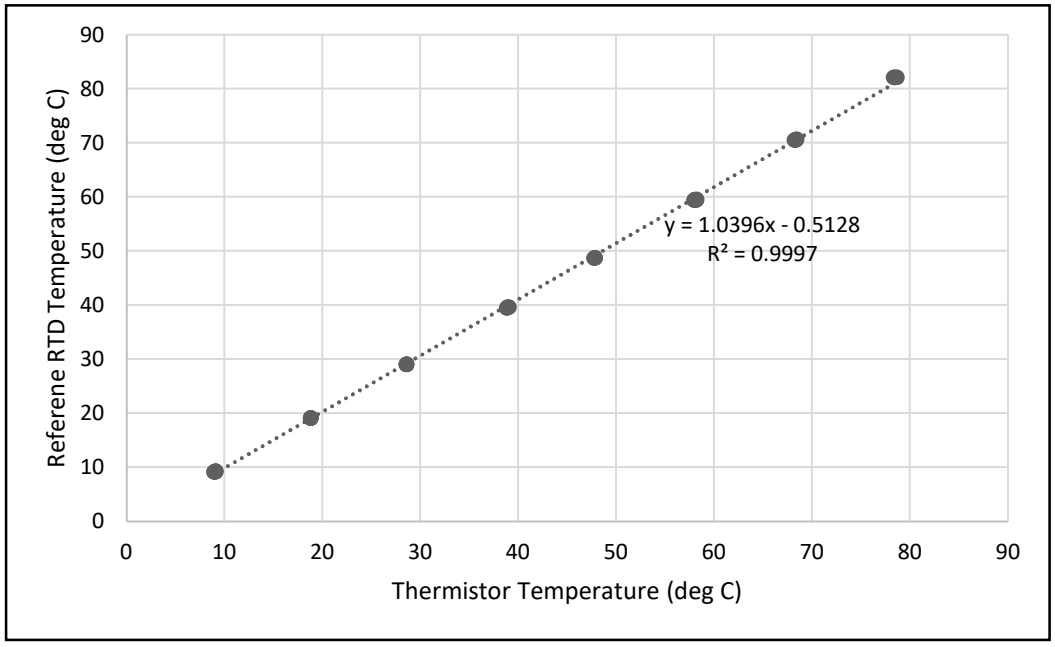

Figure 8.1- Temperature measurement from the RTD versus the temperature measured by the thermistors

Figure 8.1 shows the temperature measured by the RTD plotted against the Steinhart temperature of one thermistor.

Linear Regression was then applied to the Steinhart temperature vs. RTD temperature in order to calibrate the results of the thermistors further. The linear fit equations for each of the thermistors were then used to correct the temperature. The corrected thermistor temperature plotted against the RTD temperature is plotted in Figure 8.2 for one thermistor (same thermistor as Figure 8.1). Table 8.1 shows the corrected linear fit of the thermistors and the corresponding R^2 values.

Table 8.1 - Linear Fit Equations After Thermistor Calibration

Location	Thermistor	Linear Fit	R^2 Value
Core	1	Y = X + 5E-06	0.9997
	2	Y = X - 1E-05	0.9998
	3	Y = X - 3E-05	0.9997
	4	Y = X + 6E-06	0.9998
	5	Y = X - 3E-05	0.9997
	6	Y = X - 4E-05	0.9998
	7	Y = X - 9E-06	0.9997
	8	Y = X + 5E-05	0.9998
	9	Y = X - 4E-05	0.9997
	10	Y = X + 3E-05	0.9998
	11	Y = X - 2E-05	0.9998
Perimeter	12	Y = X - 2E-05	0.9998
	13	Y = X - 2E-05	0.9997
	14	Y = X - 4E-05	0.9997
	15	Y = X - 5E-05	0.9997
	16	Y = X - 3E-05	0.9997
	17	Y = X + 6E-05	0.9997
	18	Y = X + 6E-05	0.9997
	19	Y = X - 5E-05	0.9997
	20	Y = X + 3E-05	0.9998
	21	Y = X + 2E-05	0.9998
	22	Y = X + 4E-05	0.9998
Outer Field	23	Y = X + 3E-05	0.9998
	24	Y = X - 2E-05	0.9998
	25	Y = X - 7E-05	0.9998
	26	Y = X - 2E-05	0.9997
	27	Y = X + 3E-06	0.9998
	28	Y = X + 5E-06	0.9998
	29	Y = X - 2E-05	0.9997
	30	Y = X + 2E-06	0.9997
	31	Y = X + 4E-05	0.9998
	32	Y = X - 8E-06	0.9998
	33	Y = X - 2E-05	0.9997

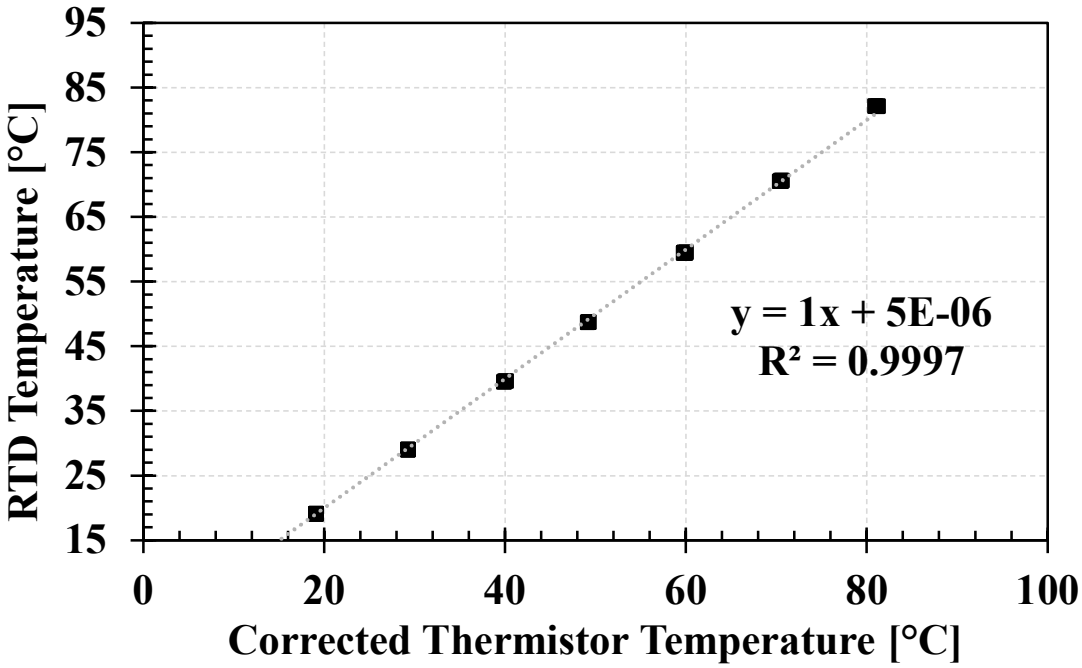

Figure 8.2 - Corrected Thermistor Temperatures After Calibration Versus RTD Temperature

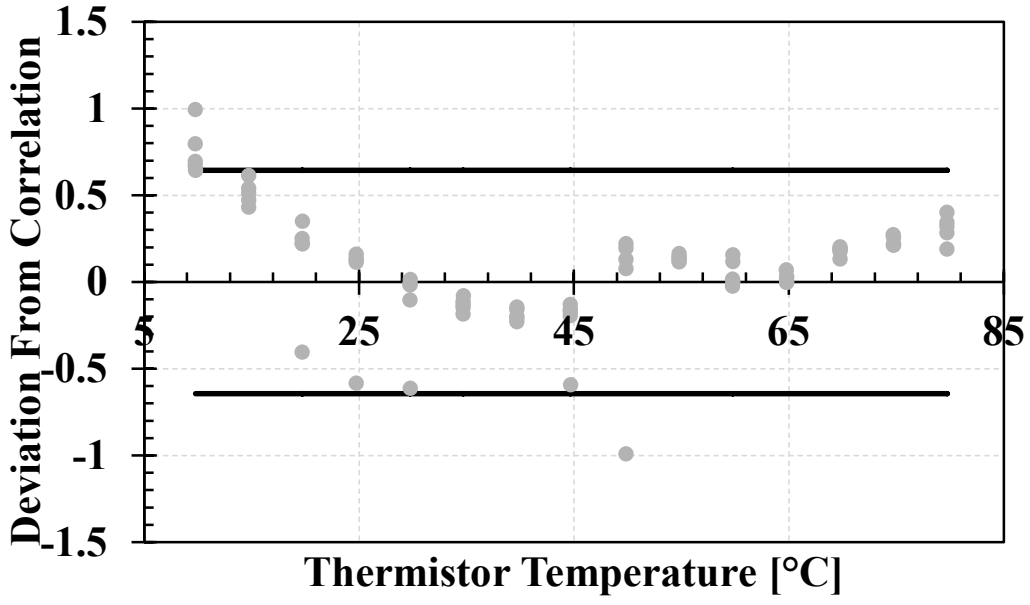

Figure 8.3 - Deviation of Thermistor Temperatures from Linear Regression Equation. Dashed Lines show 95% Interval of Data (±2s)

Uncertainty of Temperature measurements

The total uncertainty in the temperature measurement was estimated by:

$$\delta T = \sqrt{\sum_{i=1} (\delta_i)^2}$$

δ_1: Uncertainty associated with the RTD temperature measurement

δ_2:Uncertainty associated with the position of the RTD

δ_3:Uncertainty associated with the reproducibility of measurements

δ_4:Uncertainty associated with the regression analysis of the calibration data

δ_5:Uncertainty associated with the DAQ

Uncertainty associated with the Steinhart Equation

Uncertainty associated with the thermistor resistance and Arduino resistance

8.2 Uncertainty associated with the RTD temperature measurement

The RTD was used as a reference temperature for the calibration of the thermistors. An Omega DP251 Precision Thermometer (an RTD) was used during this calibration, with a manufacturer's reported accuracy of +/- 0.01°C.

$$\delta_1 = \pm 0.01°C$$

8.3 Uncertainty associated with the position of the RTD

The position of the RTD could be changed between nine different locations within the thermal bath to ensure the constant temperature within the bath. The maximum standard deviation due to the position of the RTD found over the entire temperature setpoints was +/- 0.03°C.

$$\delta_2 = \pm 0.03°C$$

8.4 Uncertainty associated with the reproducibility of measurements

The uncertainty with the reproducibility is estimated twice the standard deviation of the 5 data points at each set temperature. For conservative analysis, the maximum deviation was used for the analysis, which occurred at the highest temperature set point of 80°C. The uncertainty associated with the RTD is +/-0.08C and of the thermistor +/-0.15C.

$$\delta_3 = \sqrt{(0.08)^2 + (0.15)^2} = \pm 0.17°C$$

8.5 Uncertainty associated with the regression analysis of the calibration data

The deviation of one of the thermistor's measurements from the regression correlation was shown in Figure 8.3. This value is dependent on which thermistor is evaluated. For demonstration purposes, the deviation of the same thermistor evaluated earlier is recorded. This uncertainty is based on a 95% confidence interval. The range of values from all the thermistors is 0.49-0.70°C.

$$\delta_4 = \pm 0.58°C$$

8.6 Uncertainty associated with the DAQ

The in-house made DAQ system is composed of different components that each are associated with their uncertainty. The following explains the individual uncertainties.

8.6.1 Uncertainty associated with the thermistor resistance

The thermistor resistance is dependent on the resistance of the resistor in series and the voltage reading of the Arduino. The Arduino has a reported uncertainty of +/- 5 mV by the manufacturer, which corresponds to +/-10 bits. The Arduino also takes a total of 100 samples and uses the average value. Twice the uncertainty for the sample of 100 is +/- 16 bits. The total uncertainty due to the Arduino therefore is,

$$\delta T_3 = \delta T_i + \delta T_{ii}$$

$$\delta T_3 = \sqrt{\delta T_i{}^2 + \delta T_{ii}{}^2}$$

$$\delta T_3 = \sqrt{10^2 + 16^2} = 18.9\ bits, rounded\ 19\ bits$$

Then the thermistor resistance:

$$R_{ther} = \frac{R_{series}}{[\frac{1023}{bits} - 1]}$$

For the analysis shown, the number of bits used is 803, which is the average value of the sample of 100.

Let u = $\frac{1023}{bits}$,

$$\delta u = |u| \frac{\delta_{bits}}{bits} = \left(\frac{1023}{803}\right) \times \left(\frac{19}{803}\right) = 0.03$$

$$\delta R_{therm} = \frac{4700}{[u - 1]} \times \frac{\delta u}{u}$$

$$\delta R_{therm} = \frac{4700}{[1.27 - 1]} \times \frac{0.03}{1.27} = \pm 411.2\ Ohms$$

8.6.2 Uncertainty associated with the Steinhart Equation

The Steinhart equation depends on the thermistor's resistance, nominal resistance of the thermistor in the series, nominal temperature value, and the beta value of the thermistor. The final three variables are constants provided by the manufacturer.

$$\mathrm{T_{steinhart}} = \frac{1}{\left(\frac{1}{\beta}\right) * \mathrm{LN}\left(\frac{\mathrm{R_{thermistor}}}{\mathrm{R_{series}}}\right) + \frac{1}{\mathrm{T_{o+273.15}}}} - 273.15$$

Let x = $\ln\left(\frac{\mathrm{R_{thermistor}}}{\mathrm{R_{series}}}\right)$ and $u = \frac{\mathrm{R_{thermistor}}}{\mathrm{R_{series}}}$,

$$\delta u = |u| \frac{\delta_{Rthe}}{Rseries} = \frac{411.2}{10000} = 0.0411\ Ohm$$

$$\delta x = \frac{\delta_u}{u} = \frac{0.0411}{\left(\frac{17171}{10000}\right)} = 0.024\ Ohm$$

The total uncertainty in the temperature associated with the DAQ is then;

$$\delta_5 = |T_{stein}| \times \sqrt{\frac{\delta\beta^2}{\beta} + \frac{\delta x^2}{x} + \frac{\delta {T_o}^2}{T_o}} = 13.4 \times \frac{0.024}{0.541} = 0.59°C$$

Therefore, the total uncertainty in the thermistor is calculated as:

$$\delta T = \sqrt{{\delta_1}^2 + {\delta_2}^2 + {\delta_3}^2 + {\delta_4}^2 + {\delta_5}^2}$$

$$\delta T = \sqrt{0.01^2 + 0.03^2 + 0.17^2 + 0.58^2 + 0.59^2}$$

$$\delta T = \pm 0.85°C$$

9 Appendix B – Propagation of Error of Temperature to the Thermal Conductivity

The TRT consists of a constant heat injection rate circulating water through a borehole string. The following goes through the uncertainty associated with the calculation of the effective thermal conductivity following a TRT.

9.1 Uncertainty associated with the Temperature

Data was collected in 1 minute or 30-second intervals, depending on the test. The error found in the thermocouples of the inlet and outlet of the GeoCube has an uncertainty of ±0.1°C. The uncertainty in the average temperature is calculated as:

$$\delta_{T_{avve}} = \sqrt{2(0.1)^2} = \pm 0.141℃$$

9.2 Uncertainty associated with the Mass Flow Rate

The mass flow rate was measured using the Coriolis mass flow meter. The flow meter has an accuracy of ±0.2% of the reading. During the TRT, the maximum flow rate was used as a conservative approach to finding the uncertainty in the mass flow reading. Therefore, the uncertainty in the mass flow rate during the P2_1 test is:

$$\delta_{\dot{m}} = (0.002)(\dot{m}_{max}) = 0.002 \times 0.3\frac{kg}{s} = \pm\ 6E-4\frac{kg}{s}$$

9.3 Uncertainty associated with the Specific Heat Capacity

The range of temperature of the water for this TRT is 15-40°C. The uncertainty associated with the specific heat capacity within this temperature range, based on tabular values, is ±0.0043 J/kgK.

9.4 Uncertainty associated with the Heat Injection Rate

The heat injection rate is calculated using:

$$\dot{Q} = \dot{m} c_p \Delta T$$

The uncertainty associated with the heat injection rate is calculated using:

$$\delta_{Q(t)} = \sqrt{\left(\delta c_p\right)^2 + \left(\frac{\delta \dot{m}}{\dot{m}(t)}\right)^2 + \left(\frac{2\delta T}{T_{in}(t) - T_{out}(t)}\right)^2}$$

The uncertainty in the heat injection rate is a time-dependent parameter and is calculated for each time step. The heat injection rate error did not vary by a large amount throughout the test, simply because the temperature difference of the two streams and mass flow rate did not change greatly during the test.

9.5 Uncertainty associated with the slope

Once the average temperature is plotted on a log-time scale, the Monte-Carlo method and Bootstrap analysis are used to determine the slope of the linear trend. The uncertainty associated with the slope from all of the Monte Carlo samples with the Bootstrap method applied is ±0.1881. The total uncertainty with regards to the slope from the linear regression from the sample is, therefore:

$$\delta_{slope} = \pm 0.19$$

The relationship between the slope and the thermal conductivity is shown:

$$k = \frac{Q}{4\pi L m}$$

The uncertainty can then be calculated as:

$$\frac{\delta k}{k} = \left[\left(\frac{\delta Q}{Q}\right)^2 + \left(\frac{\delta m}{m}\right)^2\right]^{\frac{1}{2}}$$

The total error associated with the thermal conductivity from each TRT conducted is displayed in Table 9.2.

Table 9.2 - Error in Effective Thermal Conductivities

TRT	**k [W/mK]**
P2	2.29 ± 0.16
P2_2	2.14 ± 0.16
P2_3	2.07 ± 0.10
P2_4	2.27 ± 0.17
P10	1.73 ± 0.13
P10_2	2.01 ± 0.09
P10_3	2.00 ± 0.11
P4	1.71 ± 0.09
P5	1.74 ± 0.11
C7	1.87 ± 0.11

10 Appendix C - Specific Heat Capacity Sensitivity Testing

Specific heat capacity testing was conducted by varying the value for the simulations. The values extend past the acceptable range for the specific soil type that exists at the borehole field location. Figure 10.1 shows the decreasing RMSE with increasing specific heat capacity. A value of 2526 kJ/m^3/K was used for the simulations conducted in this thesis. The impact of increasing the specific heat capacity to a value greater than 3000 is minimal. The exact value of the soil's specific heat capacity at the borehole field location could be experimentally determined in future work.

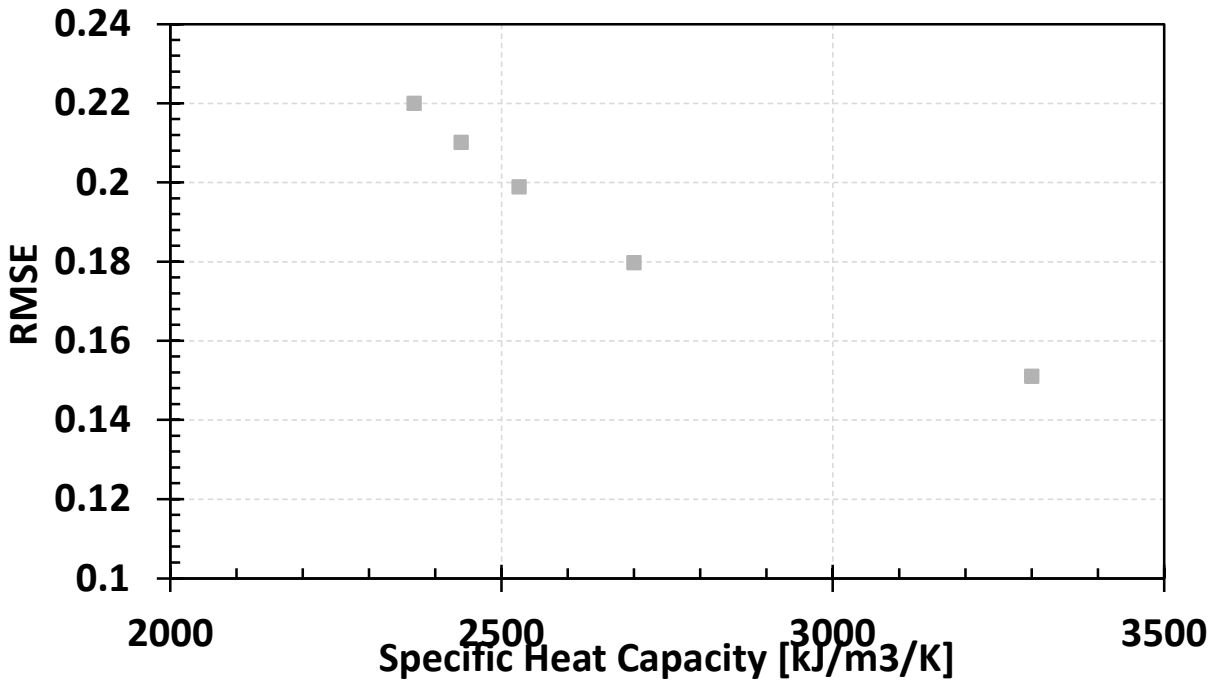

Figure 10.1 - Specific Heat Capacity Sensitivity Testing

11 Appendix D - TRNSYS Simulation Parameters

During the TRNSYS simulations, the parameters varied included the initial fluid temperature, length of the horizontal portion, and the soil thermal conductivity. All parameters, including the varied parameters, are included in Table 11.1.

Table 11.1 - TRNSYS Parameters

Borehole Parameters	**Unit**	**Value**
Storage Volume	m^3	724.1
Borehole Depth	m	24.4
Header Depth	m	3.5
Number of Boreholes	-	3
Borehole Radius	m	0.075
Number of Boreholes in Series	-	3
Number of Radial Regions	-	3
Number of Vertical Regions	-	10
Storage Thermal Conductivity	W/m.K	1.3
Storage Heat Capacity	kJ/ m^3/K	2526.4
Negative of U-Tubes/Bore	-	-1
Outer Radius of U-Tube Pipe	m	0.01664
Inner Radius of U-Tube Pipe	m	0.01372
Center-to-Center Half Distance	m	0.0254
Fill Thermal Conductivity	W/m.K	2.07
Pipe Thermal Conductivity	W/m.K	0.7
Gap Thermal Conductivity	W/m.K	1.3
Gap Thickness	m	0
Reference Borehole Flowrate	kg/s	0.25
Reference Temperature	°C	35
Pipe-to-Pipe Heat Transfer	-	-1
Fluid Specific Heat	kJ/kg.K	4.18
Fluid Density	kg/ m^3	1000
Insulation Indicator	-	2
Insulation Height Fraction	-	0
Insulation Thickness	m	0.2
Insulation Thermal Conductivity	kJ/hr.m.K	0.0144
Number of Simulation Years	-	5
Maximum Storage Temperature	°C	62

Initial Surface Temperature of Storage Volume	°C	17.8
Initial Thermal Gradient of Storage Volume	any	0
Number of Preheating Years	-	0
Maximum Preheat Temperature	°C	30
Minimum Preheat Temperature	°C	10
Preheat Phase Delay	day	90
Average Air Temperature - Preheat Years	°C	5
Amplitude of Air Temperature - Preheat Years	deltaC	17
Air Temperature Phase Delay - Preheat Years	day	0
Number of Ground Layers	-	1
Thermal Conductivity of Layer	W/m.K	1.3
Heat Capacity of Layer	kJ/m^3/K	2310
Thickness of Layer	m	30
Twin-Pipe Parameters		
Length of Buried Pipe	m	7.54
Inner Diameter of Pipes	m	0.02744
Outer Diameter of Pipes	m	0.03328
Thermal Conductivity of Pipe Material	W/m.K	0.7
Buried Pipe Depth	m	3.5
Direction of Second Pipe Flow	-	2
Diameter of Casing Material	m	1.5
Thermal Conductivity of Fill Insulation	W/m.K	1.3
Center-to-Center Pipe Spacing	m	1
Thermal Conductivity of Gap Material	W/m.K	1.3
Specific Heat of Fluid	kJ/kg.K	4.18
Viscosity of Fluid	kg/m.s	0.0005
Initial Fluid Temperature - Pipe 1	°C	17.8
Initial Fluid Temperature - Pipe 2	°C	17.8
Thermal Conductivity of Soil	W/m.K	1.3
Density of Soil	kg/m^3	1600
Specific Heat of Soil	kJ/kg.K	1.579
Average Surface Temperature	°C	10
Amplitude of Surface Temperature	ΔC	0
Day of Minimum Surface Temperature	day	91
Number of Fluid Nodes	-	100
Number of Radial Soil Nodes	-	8
Number of Axial Soil Nodes	-	10
Number of Circumferential Soil Nodes	-	4
Radial Distance of Node -1	m	0.15

Radial Distance of Node -2	m	0.15
Radial Distance of Node -3	m	0.15
Radial Distance of Node -4	m	0.15
Radial Distance of Node -5	m	0.15
Radial Distance of Node -6	m	0.15
Radial Distance of Node -7	m	0.15
Radial Distance of Node -8	m	0.15

12 Appendix E - Grid Dependency Testing

The grid dependency testing was completed by increasing the number of both the vertical and the radial nodes. The effect of increasing the number of regions was evaluated independently. To do so, all other parameters were held constant while changing the number of radial or vertical regions.

The maximum number of radial regions is limited by the number of boreholes connected in series. The number of radial regions must be less than or equal to the total number of boreholes of the string. This limit on the number of radial regions gives a value of 3, however, a total number of 200 radial regions was tested in order to observe the effect on the RMSE. The RMSE was calculated using the experimental outlet temperature and the simulation outlet temperature. The results are shown in Figure 12.1.

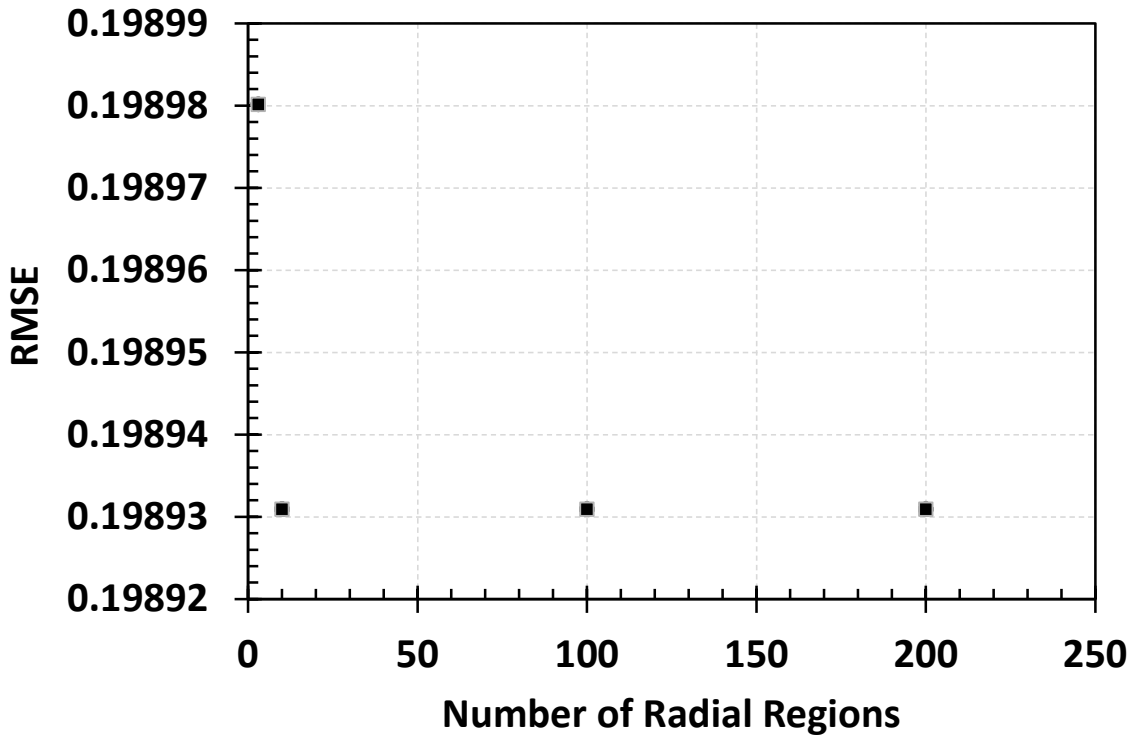

Figure 12.1 - Radial Grid Sensitivity Testing Results

The number of radial regions used for the simulations was 3, as this is the TRNSYS program's limit. The RMSE has shown a difference of only 0.025% when the number of regions is increased to 10 from 3.

The number of vertical subregions must be less than 40 for the case of 3 radial regions. The RMSE was plotted for an increasing number of vertical subregions in Figure 12.2. A total of 20 subregions was used for simulations due to the unchanging RMSE when increasing greater than 20, and since it is less than the maximum of 40.

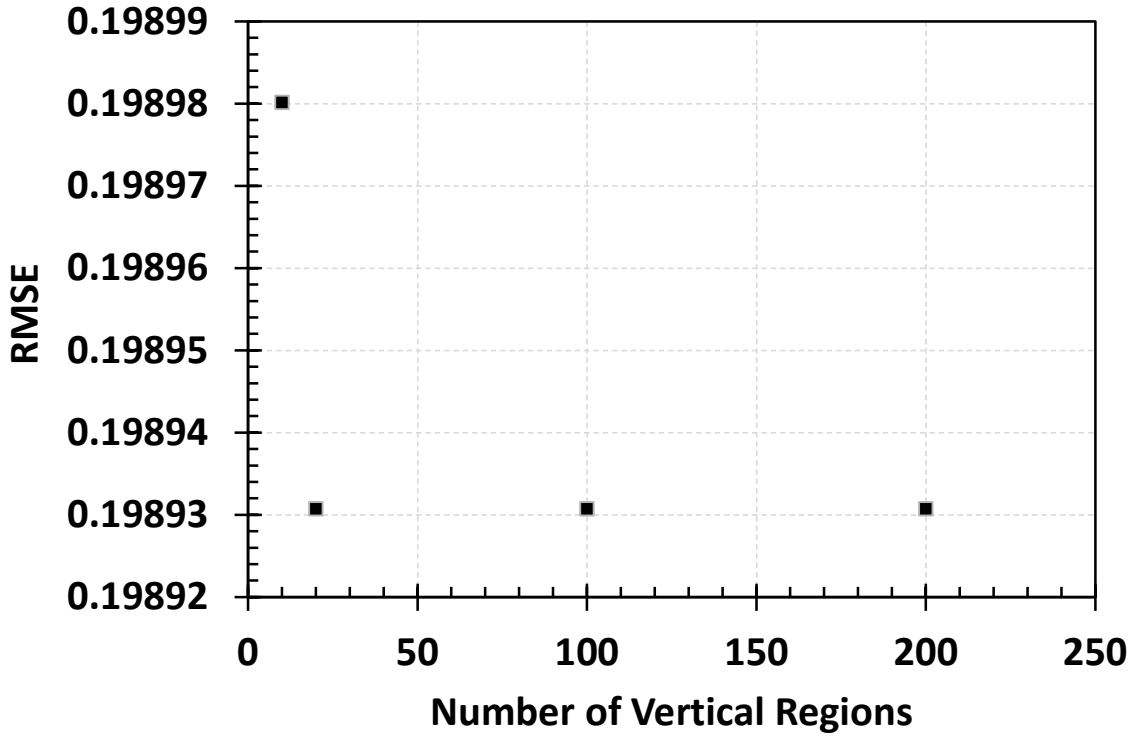

Figure 12.2 – Vertical Grid Sensitivity Testing Results